T 2040

A MAGNETOTELLURIC SURVEY IN THE GERLACH-HUALAPAI FLAT AREA, NEVADA

by

Timothy D. Zeisloft

ProQuest LLC.
789 East Eisenhower Parkway
P.O. Box 1346
Ann Arbor, MI 48106 – 1346

T 2040

A Thesis submitted to the Faculty and Board of Trustees of the Colorado School of Mines in partial fulfillment of the requirements for the degree of Master of Science in Geophysics.

Signed: Timothy D. Bichler
Student

Golden, Colorado

Date: Dec. 8, 1978

Approved: George V. Keller
Thesis Advisor

George V. Keller
Head of Department

Golden, Colorado

Date: Dec. 8, 1978

ABSTRACT

Nineteen MT stations were recorded in the Gerlach-Hualapai Flat area with the purpose of determining a mechanism for the geothermal processes observed in the area. Subsequent analysis indicated a deep conductor on the order of 20-22 km in Hualapai Flat and 25 km south of Gerlach. There is no indication of a shallow magmatic heat source. The deep conductor can be explained in light of the observed heat flows in the area.

TABLE OF CONTENTS

LIST OF FIGURES

ACKNOWLEDGEMENTS

The author would like to thank his committee for their guidance and support: Dr. George Keller, both for his patience and his helpful suggestions; Dr. David Butler, for his moral support; and Dr. Charles Stoyer, who's invaluable suggestions vastly improved the quality of this manuscript. The author would also like to acknowledge the field crew who acquired the data: Dr. Keller, John Jordan, and Koji Tsubota. The author would also like to thank Patricia Hughes for digitizing and Carrie Zwerg for typing.

1.0 INTRODUCTION

The Gerlach-Hualapai Flat area of Nevada has been subject to investigation as an example of a typical Basin and Range geothermal area. Crewdson (1976) has correlated a number of surveys in the area to give a broad geophysical overview of the Basin and Range geothermal system. Crewdson concludes that heat sources are due to elevated heat flow in the crust overlain by a thermally insulating alluvium layer rather than by a magma chamber at depth.

Because of its ability to probe deep earth structures, a magnetotelluric (MT) survey was conducted with the purpose of proving or disproving the existence of a magmatic heat source. MT work was done in a similar area, the Carson Desert, showing a broad area of low resistivity at depths of 2.5 - 7.0 km (Stanley, et. al. 1976). The broad extent of this low resistivity anomaly leads to the belief that the heat mechanism in the area is due to crustal thinning rather than magma.

The survey in the Gerlach area consists of 19 stations with recording periods ranging from 20 sec periods at the high end to 200 - 500 sec periods at the low end. The recording periods are sufficient to provide penetration to the mantle in areas where the resistivity is 100 ohm meters or greater. When the surface resis-

tivities are less than 100 ohm meters the recording periods will allow penetration to the deep crust.

Data are analysed in two manners: first, the polarization ellipses of the electric and magnetic fields were examined to determine preferred directions of current flow. The data were then rotated in the time domain so the measurement axes coincided with the direction of maximum current flow. MT soundings were then calculated for the directions perpendicular and parallel to electric structure, using a fast fourier transform. Cross and auto power spectra were averaged to provide 10 estimates of resistivity per decade. Interpretation was accomplished by comparison with one dimensional theoretical MT models.

Interpretation of magnetotelluric soundings in the Gerlach-Hualapai Flat area is the subject of this thesis. Because the processing of MT data is not a matter of simple algebra, the author also examines this aspect of the MT method.

2.0 STUDY AREA

The study area centers around the Hualapai Flat-Gerlach area in the Basin and Range geologic province of northwestern Nevada (Figure 1). Gerlach is approximately 160 Km north of Reno, Nevada. The study area was crossed by two magnetotelluric profiles, the first following Highway 34 and the second extending northeast from Gerlach.

To the south of Gerlach the southern Black Rock Desert blends into the San Emidio Desert which is bounded on the east by the Selenite Range (Plate 1). To the northeast of Gerlach the Black Rock Desert extends approximately 160 Km Northeast of Gerlach. Hualapai Flat forms a structural basin separating the Granite Range and the Calico Range. These two ranges join at the north end of Hualapai Flat. The Black Rock Desert is separated from Hualapai Flat by a topographic ridge known as Steamboat Ridge.

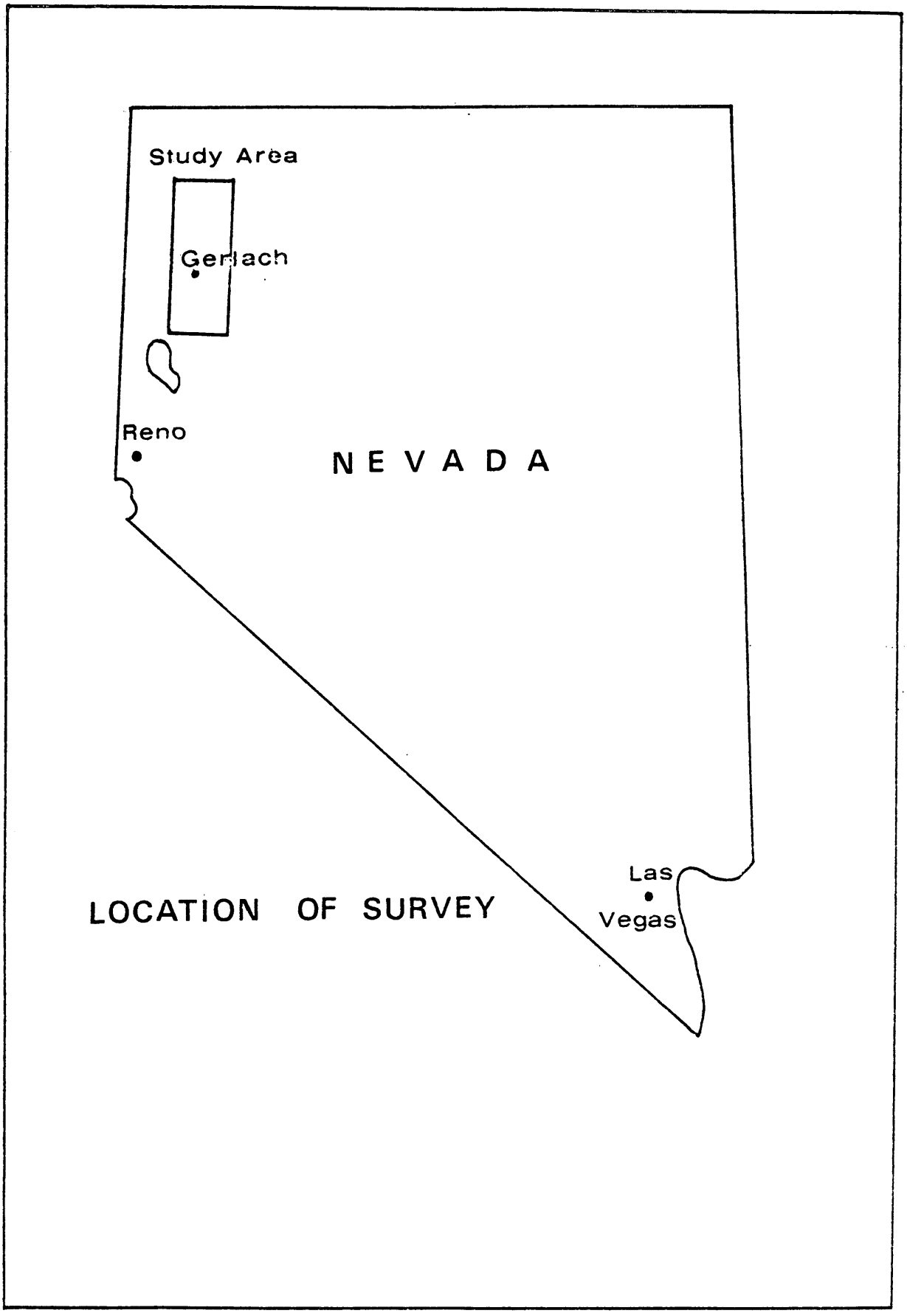
Study Area
Gerlach
Reno
NEVADA
Las
Vegas
LOCATION OF SURVEY

Figure 1

2.1 STATION LOCATIONS

Nineteen MT stations were recorded, mainly along Highway 34, running north-south through Gerlach (Figure 2). Stations 16-19 were recorded north of Gerlach. Station 13 was recorded on playa northeast of Gerlach, station 14 was recorded approximately 10 km north of Gerlach on an alluvial fan, and station 15 was recorded at the intersection of Highway 34 and Route 81.

The majority of stations fall in a north-south profile 75 km long ranging from 26 km south of Gerlach to 48 km north of Gerlach. An additional five station line extends 24 km north and east of Gerlach. Stations are spaced 6 km apart south of Gerlach and approximately 3 to 4 km apart to the north of Gerlach.

Because the near-surface geology is well known in the Hualapai Flat area, it was possible to locate stations on bedrock or areas of thin alluvium which decreased the amount of recording time necessary to achieve a given penetration.

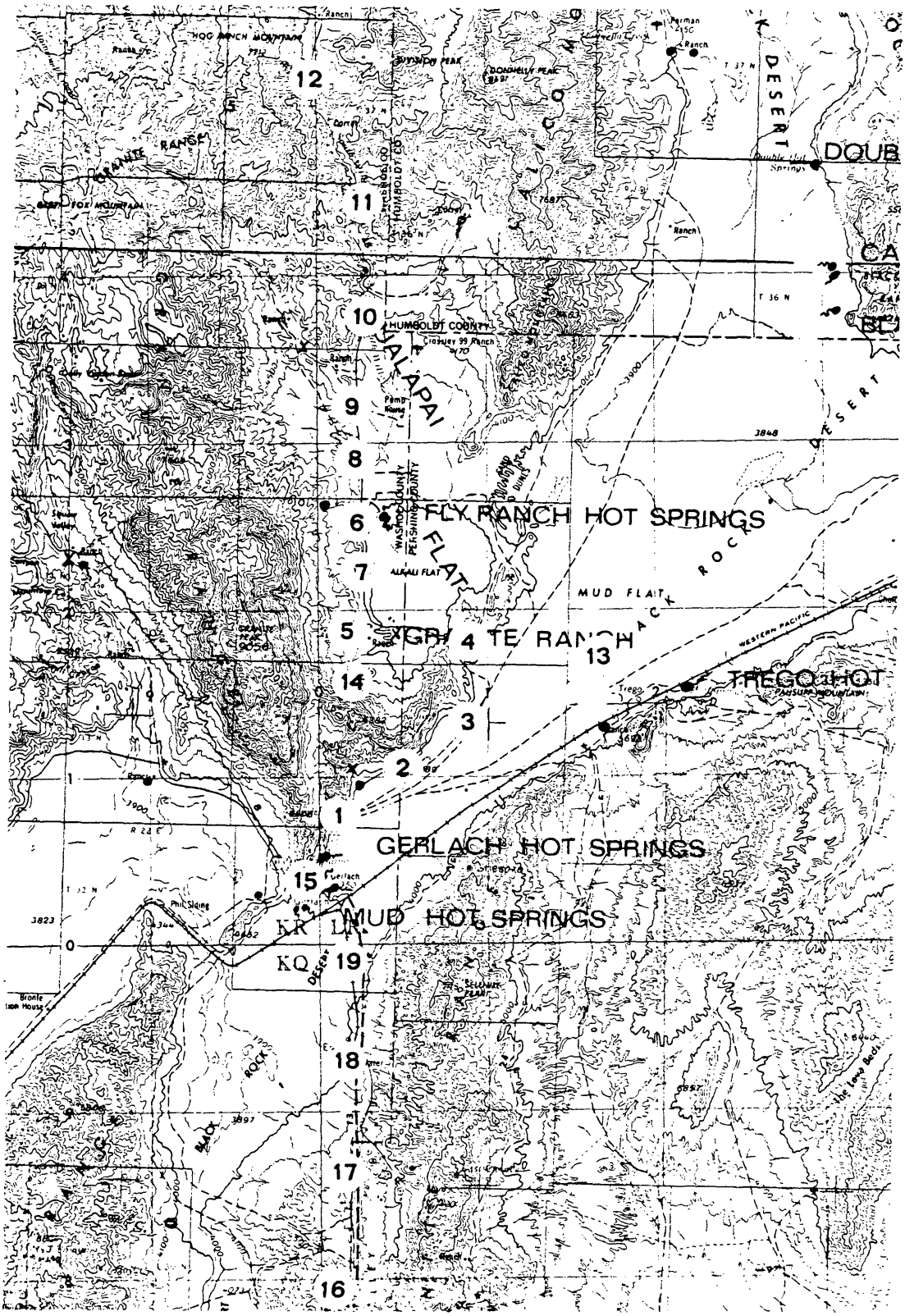

Figure 2 Station Locations

2. 2 GEOLOGY

Mapping by Sperandio (see Keller and Grose, 1975) in the Hualapai Flat area shows the southern part of the Granite Range consists of Cretaceous granodiorite with outcrops extending out along Steamboat Ridge (Plate 1). Northwest of Hualapai Flat the Granite Range consists mainly of granites, with Tertiary basalts, tuffs, metasediments and metavolcanic flows, flow breccias and volcanoclastics. Composition of the southern Calico Mountains consists of chert, sandstone, shale, mudstone and limestone. Hualapai Flat itself consists of Quaternary alluvium, playa, lake beds and eolian dunes. In the northern part of Hualapai flat an outcrop of Tertiary volcanics occurs. Along the western edge of Hualapai flat there are outcrops of volcanics through the alluvial cover. Hualapai Flat is separated from the Black Rock Desert by a line of metavolcanics outcropping from Steamboat Ridge to the southern tip of the Calico Mountains. The western side of Hualapai Flat is bounded by a fault with the Granite Range on the upthrown side. A fault also separates Hualapai Flat from the Black Rock Desert.

Mapping by Smith (see Keller and Grose, 1975) shows composition of the Selenite Range to be similar to the Granite Range with granodiorites occuring on the north and east edge and Paleozoic metavolcanics and sediments, Tertiary basalts, and sedimentary units comprising the western part.

PLATE I

FORMATIONS

QUATERNARY
- Qp - PLAYA SEDIMENTS
- Q - COLLUVIUM, ALLUVIUM, DUNES

TERTIARY
- Tb - BASALT FLOWS
- Ts - SILICIC FLOWS, PYROCLASTICS, VOLCANIC SED. ROCK
- To - ANDESITIC FLOWS AND BRECCIAS

CRETACEOUS
- Kg - GRANODIORITE
- Kd - QUARTZ DIORITE

PERMO-TRIASSIC
- PTRvs - METAVOLCANIC, METASEDIMENTARY ROCKS
- PTRv - METAVOLCANIC ROCKS
- Po - AMPHIBOLITE, LOCALLY GNEISSIC

EXPLANATION

- FORMATION CONTACT, DASHED WHERE APPROXIMATELY LOCATED, DEGREES OF DIP SHOWN WHERE MEASURED
- FAULT, DASHED WHERE APPROXIMATELY LOCATED, DOTTED WHERE CONCEALED, BARB SHOWS DIP DIRECTION & DEGREES OF DIP WHERE MEASURED, BALL ON DOWNTHROWN SIDE
- STRIKE & DIP OF BEDDING
- VERTICAL BEDDING
- THERMAL SPRINGS

CALICO MTS.
HUMBOLDT CO
PERSHING CO
TECTONIC CRACKS
HUALAPAI FLAT
FLY RANCH H.S.
HOT SPG. 2 MILES
EAST MARGIN OF MODOC PLATEAU
GRANITE RA.
TREGO H.S.
BLACK ROCK DESERT
SMOKE CREEK DESERT
GERLACH H.S.
MUD H.S.
GERLACH
SELENITE RA.
FOX RA.
SAN EMIDIO DESERT
EMPIRE
NEVADA
SCALE 1:125,000
TOPOGRAPHIC CONTOUR INTERVAL 1,000 FEET

GEOLOGIC MAP OF THE GERLACH-HUALAPAI FLAT AREA
by: L.T. GROSE & R.J. SPERANDIO

INTERPRETED GEOLOGIC CROSS SECTIONS OF GERLACH-HUALAPAI FLAT AREA
by: L.T. GROSE

SCALE: H = V

SYMBOLS AS ABOVE ON GEOLOGIC MAP, BUT IN ADDITION:
- PROMINENT REFLECTING HORIZON
- Tv TERTIARY VOLCANIC ROCK UNDIFF.
- FAULT WITH RELATIVE DISPLACEMENT

D' (E) — CALICO MOUNTAINS — BLACK ROCK DESERT — HUALAPAI FLAT

D (W) — HUALAPAI FLAT — SURFACE RIFTS

C' (E) — BLACK ROCK DESERT — HUALAPAI FLAT — FLY RANCH H.S. — GRANITE RANGE

C (W) — GRANITE RANGE — HUALAPAI FLAT

B' (E) — BLACK ROCK DESERT — HUALAPAI FLAT — TREGO H.S. — GRANITE RANGE

B (W) — GRANITE RANGE — HUALAPAI FLAT

A' (ESE) — SELENITE RANGE — BLACK ROCK DESERT — GERLACH H.S. — GRANITE RANGE

A (WNW) — GRANITE RANGE — SMOKE CREEK DESERT

The Granite Creek and northern San Emidio Deserts consist of Quaternary alluvium, playa and lake deposits. The Black Rock is separated from the Smoke Creek Desert by outcrops of basalt and granodiorite stretching in a line from Gerlach to the northern tip of the Fox Range.

The depth to the mantle is estimated at 28 km for the basin and Range province (Pakiser and Hill, 1963). The worldwide average for the continental crust is estimated at 35 km (Takeuchi, et. al. 1967).

2.3 PREVIOUS GEOPHYSICS

Several geophysical surveys have been conducted in the area that are of direct interest as modelling aids. Electrical surveys have been carried out my Morris (1976), Ofrey (1975), and Crewdson (1976). Morris conducted a Quadripole mapping survey over the area of Hualapai Flat and north of Gerlach. Ofrey did time domain electromagnetic soundings (TDEMS). Crewdson covered Hualapai Flat and portions of the Black Rock Desert with TDEMS. In addition to the electrical surveys, a gravity survey was conducted by Crewdson (1976) covering the Gerlach Hualapai Flat area and the southern Black Rock Desert. A reflection seismic profile was carried out by Callaway from the Granite range in Hualapai Flat to Trego in the Black Rock Desert (see Keller and Grose, 1978).

The importance of Quadripole mapping results to MT interpretation is the definition of near surface resistivity zones for use in formulating MT models. Quadripole mapping showed apparent resistivities of 5 ohm meters for the Black Rock Desert, 20 ohm meters for southern Hualapai Flat and 5 ohm meters for northern Haulapai Flat (Figure 3). The Black Rock Desert is separated from the Hualapai Flat by a 100 ohm meter high corresponding to Steamboat Ridge. The resistivity structure in Hualapai Flat is caused by basement depth rather than variations in the resistivity of the alluvium. The high resistivities in the western part of Hualapai Flat and along Steamboat Ridge correspond to thin or

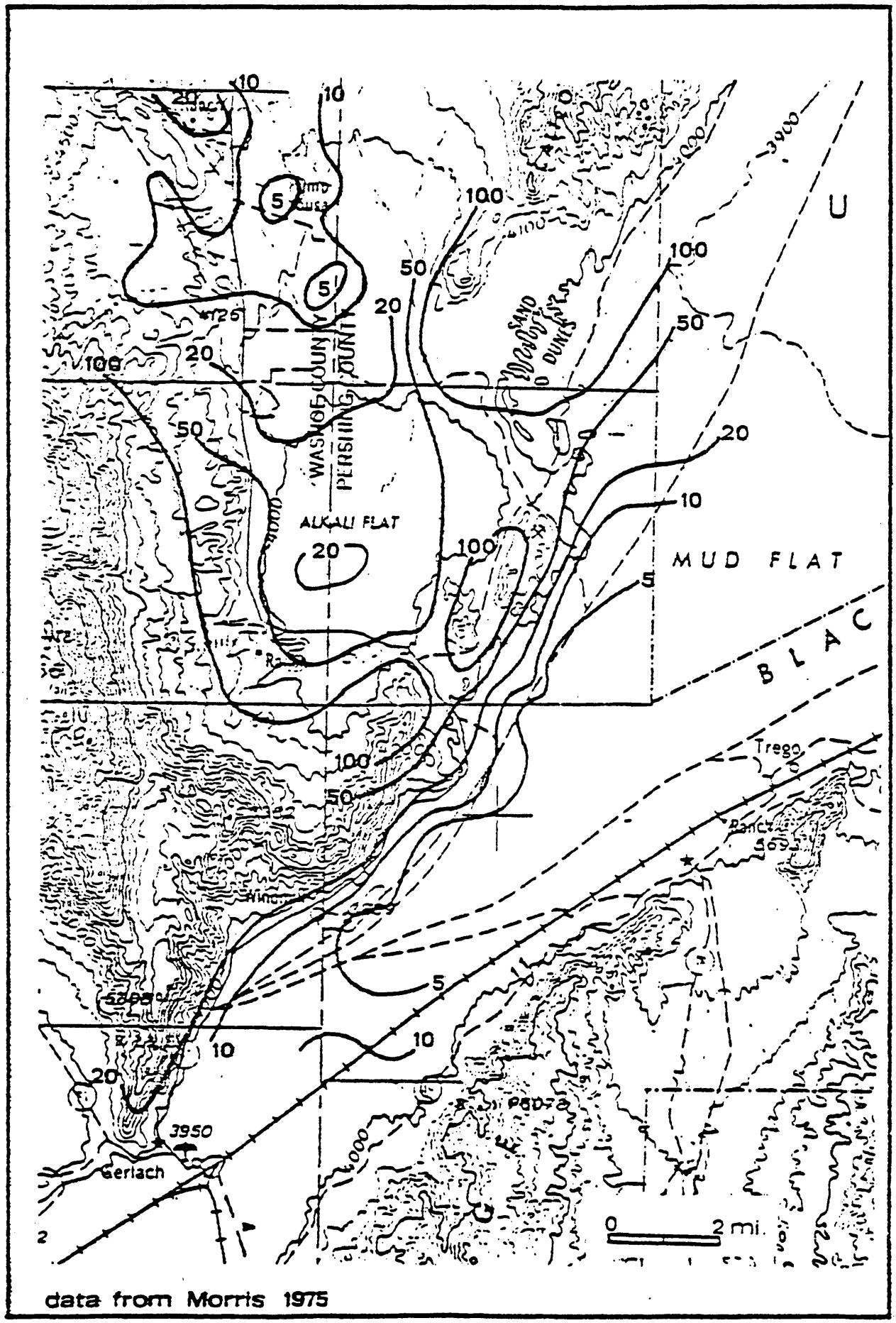

Figure 3 D.C. Resistivity Map (Ohm-M) From Crewdson, 1976

From Crewdson, 1976

non-existant alluvial cover. Crewdson (1976) feels the 5 ohm meter lows in the north of Hualapai Flat cannot be completely accounted for by lithology alone and suggests the presence of hot water at depth. Low resistivities in the Black Rock Desert are thought to be due to lithology rather than presence of geothermal waters.

TDEMS is a method of determining earth resistivity by measuring a secondary magnetic field induced in the earth by a varying primary magnetic field. The primary magnetic field is caused by the abrupt reversal of current in a grounded wire, forming a current dipole. Because the TDEMS method measures the vertical magnetic field, the resistivity measured can be considered to be a depth sounding rather than just yielding one value of resistivity per station, as in DC methods. The TDEMS method measures resistivity as a function of time, yielding information about resistivity structure as a function of depth. TDEMS therefore details resistivity structure rather than giving an average resistivity estimate. The maximum resistivity TDEMS map compiled by Crewdson (Figure 4) corresponds closely to the DC resistivity map. Soundings interpreted by Crewdson (1976) in northern Hualapai Flat indicate resistive layers overlying conductive layers. The maximum resistivity in this area is 3 ohm meters or less. Crewdson interprets depth to the top of the conductor to be 430 to 610 meters. This conductor at depth is believed to be due to the presence of a geothermal reservoir.

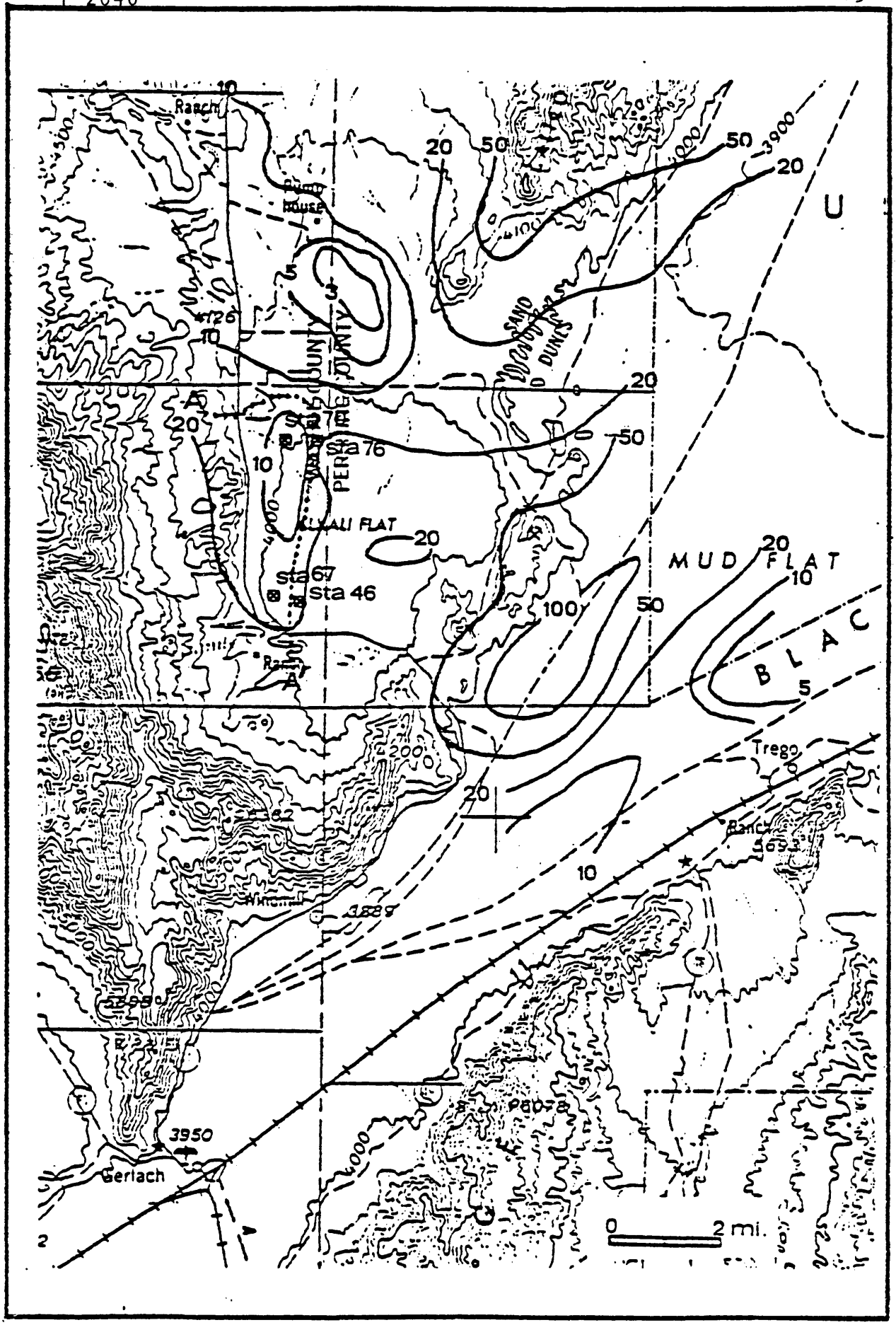

Figure 4 TDEM maximum resistivity map. From Crewdson, 1976

TDEMS by Ofrey (1975) in the Gerlach area indicates a 3 layer structure. The first layer resistivity is 1 ohm meter, the second layer averages about 10 ohm meters and the bottom layer averages about 250 ohm meters. Whereas the average resistivity of the second layer is about 10 ohm meters, in places it is as low as 1 ohm meter. The low values of second layer resistivity generally correspond to larger second and first layer thicknesses indicating deeper basement in these areas. Ofrey shows depths to the top of the second layer as being about 200 meters. These low resistivity areas in the second layer are interpreted to be due to presence of geothermal waters.

Gravity surveys measure gravitational attraction at a point. Because density can be related to gravitational attraction, when rock densities can be estimated, the thickness of units with differing densities can be determined. Gravity surveys usually give a good indication of the thickness of alluvial cover in an area. Gravity data are of interest to the MT modeller because they provide a look at depths to resistive basement. Gravity data usually gives a more accurate estimate of depth to basement than electrical methods.

The gravity survey showed depths to bedrock of between 0 and 5000 feet. Figure 5 is a depth to bedrock map compiled by Crewdson from the gravity profiles. The greater the depth to bedrock on the gravity map, the lower the resistivities on the DC and TDEMS maps. Depth to bedrock is shown as 0 - 1000 feet in southern Hualapai Flat

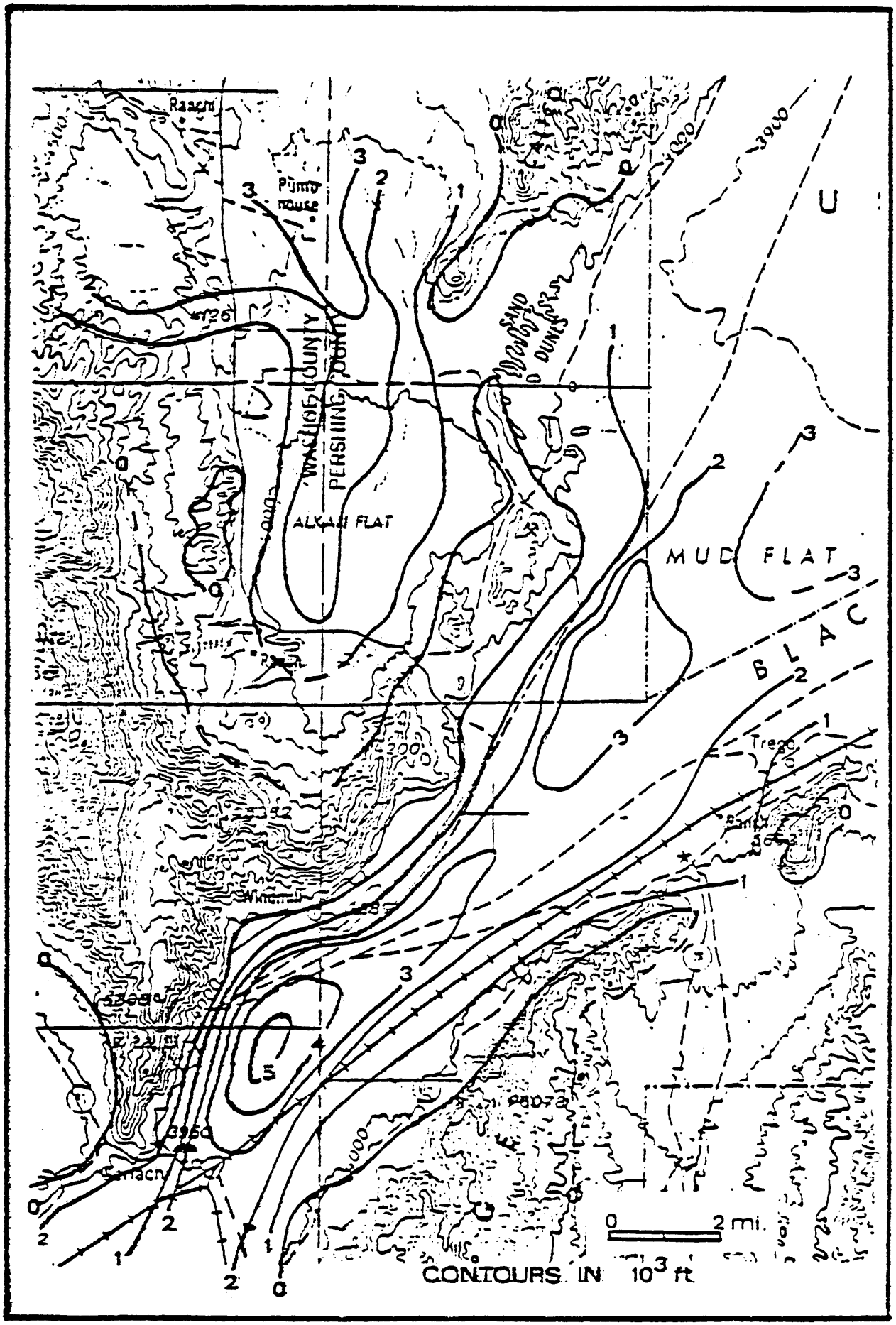

Figure 5 Depth to bedrock. From Crewdson, 1976

falling as low as 3000 feet in the north end of Hualapai Flat. In the Black Rock Desert, the depths to basement are 5000 feet north of Gerlach rising to 3000 feet in the more northeastern areas of the desert.

The seismic reflection profile distinguished three reflecting horizons in the Black Rock Desert. The first horizon is a low velocity layer (1 km/sec) interpreted as lake deposits and range in thickness from 150 meters to 350 meters (Crewdson, 1976). The second layer is interpreted as volcanic and sedimentary rocks, ranging in thickness from 0 - 500 meters. The third layer is a high velocity horizon, possibly granodiorite (Callaway, see Keller and Grose, 1978). In addition, Crewdson reports a deep reflector at about 11 km, believed due to a change in the character of the earth's crust (Crewdson, 1976). Although the data quality was not as good in Hualapai Flat, Crewdson interprets two horizons as correlating with the reflectors in the Black Rock Desert.

The geophysical investigations cited above point to two areas of interest as geothermal reservoirs. One area is northern Hualapai Flat and the other area is about 3 km northeast of Gerlach. Both the areas of interest are in the deeper part of the basins which is the logical place for geothermal waters to accumulate. In addition, the areas of maximum depth to bedrock are also the areas of maximum insulation and so would trap more heat for the heating of water.

3.0 THE METHOD

MT sounding is a method of measuring earth resistivity by observing natural electric and magnetic fields in the earth. These natural electromagnetic (EM) fields are due to electromagnetic currents in the upper atmosphere caused by solar activity (Vozoff, 1972). Other sources of EM energy in the earth are due to lightning and manmade EM disturbances, especially in the frequency ranges above 8 hz. For the purposes of MT soundings, the natural EM fields are assumed to consist of planar waves. The MT sounding method gives a resistivity distribution as a function of frequency. The depth of penetration of an EM wave is dependent on the frequency of the wave and the earth's resistivity and permeability. Skin depth is a measure of the penetration of EM waves. Skin depth is defined as the depth at which the amplitude of an EM wave drops to 1/e of its initial amplitude. The expression for skin depth in a homogeneous, isotropic media is:

$$\delta = \sqrt{\frac{2}{\omega\mu\sigma}}$$

where: δ = skin depth, in meters

ω = frequency, in radians/sec.

μ = permeability, in henrys/meter

σ = conductivity, in mhos/meter

Holding conductivity and permeability constant, one can see that skin depth increases with decreasing frequency. The only limits to how deeply MT soundings "see" is the patience of the person acquiring the data and the planar earth model. MT soundings possess this advantage over the other electrical methods: It may yield information about very deep earth structure. For example, at a period of 18 minutes and a resistivity of 100 ohm meters, the skin depth is 50 km. At 1 ohm meter and 18 minute period, the skin depth is 5 km. This indicates that the presence of a low resistivity surface layer can greatly effect the estimation of thickness of structure.

Cagniard (1953) defined apparent resistivity for MT soundings in a plane layered earth from the electric and magnetic fields as:

$$\rho a = 0.2\ T(E/H)^2$$

In this case E and H are the electric and magnetic fields respectively and are measured perpendicular to each other, and T is period, in seconds. Notice that for the plane layered case, it does not matter what the orientation of the measuring axes are, as long as they are perpendicular with respect to each other. When lateral boundaries occur in the earth, or the earth is anisotropic, resistivities vary with orientation. The maximum and minimum values of resistivity always occur when the orientation of the measurement axes are coincident with the structural axes of the earth, for a two dimensional case. This is because when the earth is non-uniform, electric current tends

to flow in the path of least resistance. When the earth is channeling current directions, an impedance tensor is used to define apparent resistivity. The tensor Zxy replaces the simple expression E/H. The tensor Zxy is defined as the solution of the equations:

$$E_x = Z_{xx}H_x + Z_{xy}H_y$$

$$E_y = Z_{yx}H_x + Z_{yy}H_y$$

where the subscripts x and y denote perpendicular measurement axes. There are several methods for the solution of the above equations. Sims (1971) and Hermance (1973) show that if two independent data sets are used, solutions for Zxy can be found. If more than two independent data sets exist, Zxy can be solved for using least squares techniques. Two data sets are considered independent when their H field polarizations are different. Sims also suggested the use of cross power spectra to solve for Zxy:

$$E_xH_y^* = Z_{xx}H_xH_y^* + Z_{xy}H_yH_y^*$$

$$E_xE_x^* = Z_{xx}H_xE_x^* + Z_{xy}H_yE_x^*$$

where * denotes the complex conjugate. The above equations can be solved for Zxx and Zxy and similar equations can be used for the solution of Zyy and Zyx. Once the impedances are solved, the axes are rotated to directions that maximize Zxy or Zyx and tensor resistivities can be defined:

$$\rho_{xy} = 0.2T\ (Z_{xy})^2$$

Another method exists for the evaluation of tensor impedances. Porstendorfer (1975) shows that when the measurement axes are aligned with structural axes, the inline impedances Zxx and Zyy become small and theoretically should disappear for a two dimensional earth. The equations for defining impedance are then simplified to:

$$E_x = Z_{xy} H_y$$

When the above conditions can be met, the problem of determining impedance is greatly simplified. Porstendorfer has stated that the maximum directions of the electric field polarization coincides with the maximum resistivity directions. When one component of the electric field is plotted against the other component in the time domain, any preference in current flow is clearly shown (Figure 6). Once the preferential direction is determined, a simple rotation of axes can be performed according to the formulas:

$$x' = x\cos\theta - y\sin\theta$$

$$y' = x\sin\theta + y\cos\theta$$

for clockwise rotation and:

$$x' = x\cos\theta + y\sin\theta$$

$$y' = -x\sin\theta + y\cos\theta$$

When the data is represented in the principle axes, the data are fourier transformed and the impedance is determined with the formula:

$$Z_{xy} = E_x H_y^* / H_y H_y^*$$

$$Z_{yx} = E_y H_x^* / H_x H_x^*$$

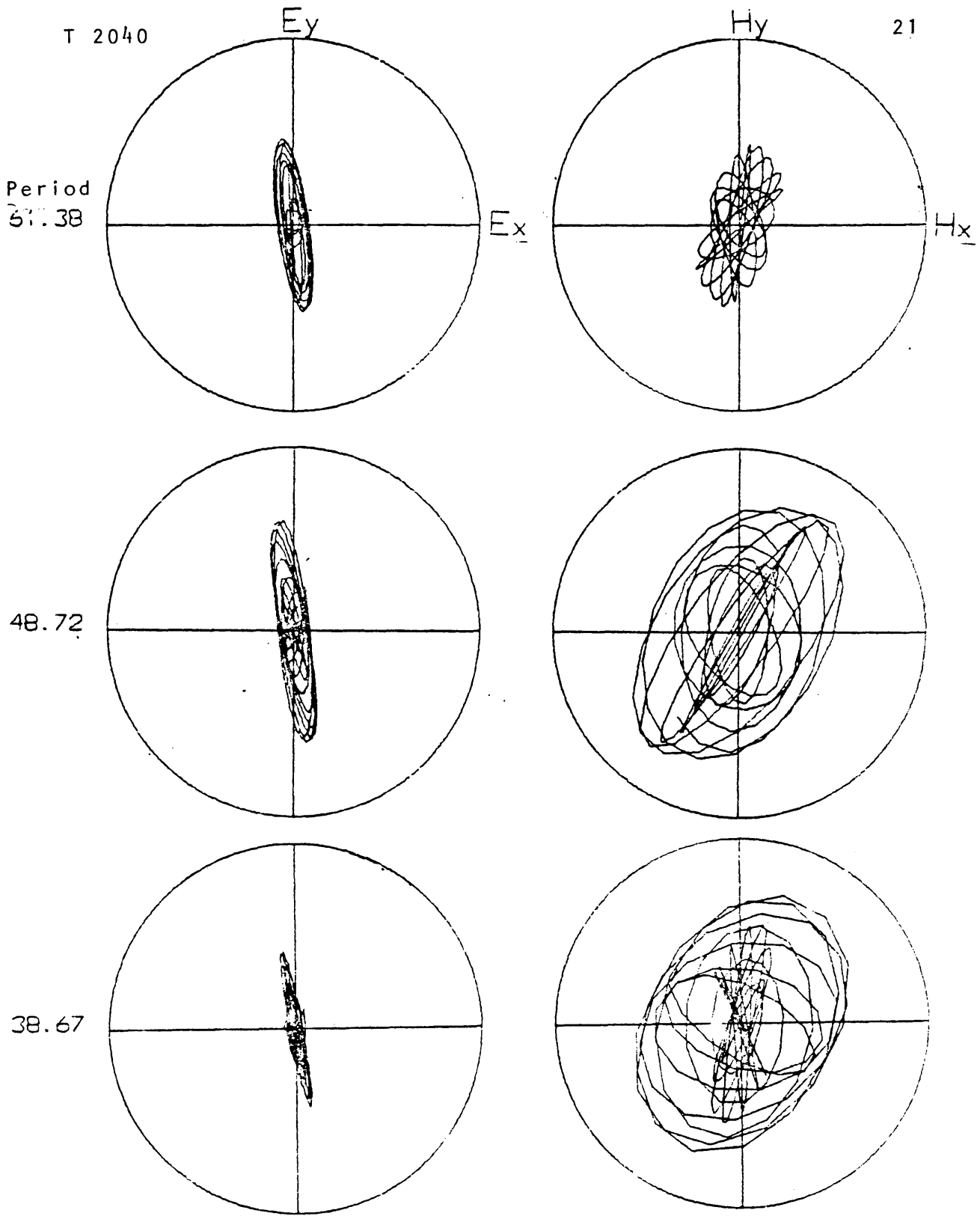

Figure 6. Preferred current directions at station 1

where $E_x H_y$ is the complex cross power spectrum and $H_y H_y^*$ is the auto-power spectrum.

Data quality is determined by its coefficient of coherence. The coefficient of coherence between two series A and B would be defined as:

$$C_{AB} = \frac{\langle AB^* \rangle}{\sqrt{\langle AA^* \rangle \langle BB^* \rangle}}$$

where $\langle AB^* \rangle$ is the magnitude of the cross power spectrum of A and B (Madden, 1964). Coherence is a measure of how well two series correlate, or how alike they look. If two series are identical, their coherency is 1. If two series are totally dissimilar, their coherence will be small compared to 1. In this survey coherencies of .8 were used with coherencies of as low as .65 being used in poor quality curves.

4.0 DATA REDUCTION

There are probably as many permutations on the MT processing scheme as there are MT processors. The method preferred by the author includes inspection of the analog records, digitization, scaling, determining preferred directions, rotation, and spectral analysis. Final quality of resistivity values is checked using the coefficient of coherence.

Analog data are visually separated into 3 categories: 5 component soundings, 4 component soundings and 2 component soundings. A 5 component sounding is typified by activity on 2 perpendicular horizontal E-field traces and activity on 3 mutually perpendicular H-field traces. A 4 component sounding is active on all traces except the vertical H-field. Two component soundings are active on only an E-field and its perpendicular H-field. An active Hz component indicates a violation of the requirement of planar incidence. Four and five component records were digitized for processing of tensor fields. Two component soundings were discarded. The raw data were also inspected for noise bursts, spikes, and large offsets due to use of the cryogenic magnetometer. Noise bursts were not digitized, spikes were manually smoothed prior to digitization and offsets were manually corrected in digitization and also were removed digitally.

Once the data are digitized they are scaled to the units mv/km for the electric field and gammas for the magnetic field. All data files were handled in formatless binary mode to facilitate speed in input-output and to retain full significant figures.

At this stage an attempt was made to remove offsets caused by use of a cryogenic magnetometer either resetting or flux jumping. Resetting occurs when the output voltage from the magnetometer gets too large, saturating a capacitor which discharges resetting the output voltage to zero. This causes an offset to occur on the output record. Flux jumping is a complex phenomenon associated with cryogenic temperatures and quantum mechanics. Flux jumping can cause both spikes and offsets to occur on the output record. The problem of offsets and spikes is compounded when filters are used in the output stage of the amplifier. Filters cause otherwise sharp cornered offsets to be more rounded off and may cause oscillations in the output record. This filtering of offsets can cause confusion as to what is signal and what is noise, particularly in portions of the record that has high signal levels. Slow rates of greater than 33 mv or 33 gammas per second were considered to be due to voltage offsets rather than signal and were removed.

The data were then bandpass filtered at three frequencies for the purpose of making polarization plots. Polarization plots are Lissajou type figures created when the two components of the electric

field traces are plotted against each other, with a similar arrangement for the H field traces. When there is a preferred direction of current flow in the earth a similar direction shows up on the polarization plots. Figures 7a and 7b show two polarization plots, one taken near a resistive ridge with the measurement axes not parallel to structure and the other taken near a basin margin fault with the measurement axes parallel to structure. Notice that both plots show a high degree of ellipticity on the E field trace. The ratio of the major and minor axes of the E field trace have the same proportions as the major and minor axes of the apparent resistivity ellipse (Porstendorfer, 1975). When the axes of the electric field ellipse are parallel to the measurement axes, the sounding is in principle directions. If the E field ellipses are not in principle directions, they can be rotated so that they are. Figure 7c shows the sounding in Figure 8b after rotation.

Once the data are in principle directions, the data are fast fourier transformed (FFT). Preparations for the FFT include removal of DC level and drift, and truncation with a hamming operator. The data are band pass filtered to remove all signals below the frequency that would allow 10 full cycles for the length of the data and above .25 of the nyquist frequency. Finally, the data are padded with zeros so the length of the data string is a power of two to facilitate the FFT. The FFT itself is done with a subroutine available in the

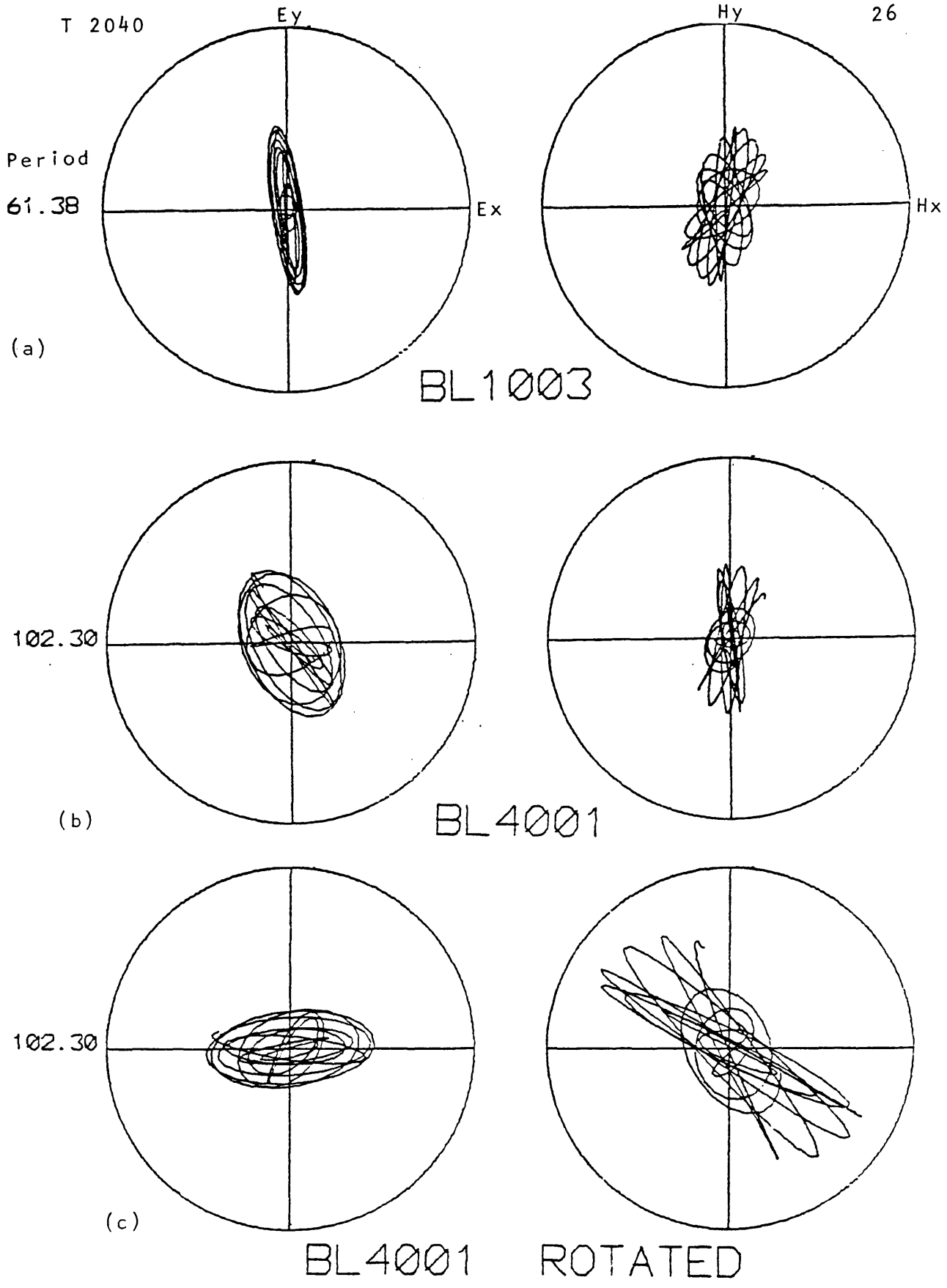
T 2040
Ey
Hy
26
Period
61.38
Ex
Hx
(a)
BL1003
102.30
(b)
BL4001
102.30
(c)
BL4001 ROTATED

Figure 7.

CSM IMSL software library. For an input of N pieces of data, the subroutine returns N/2 useable fourier coefficients. For the data sample M, returned from the subroutine, the frequency associated with M is:

$$f = \frac{M}{N.\Delta T}$$

where ΔT is the sampling rate in seconds. Since M can vary between 1 and N/2 it can be seen that the FFT returns frequencies from

$$\frac{1}{N.\Delta T}$$

to the nyquist frequency.

Once the data are transformed, cross power spectra can be determined by multiplying the fourier coefficient of one component by the complex conjugate of the other component. Auto power spectra can be calculated by multiplying the fourier coefficient of a trace with its own complex conjugate. Frequencies can then be selected to give 10 estimates of resistivity per decade on the frequency scale. The power spectra were then averaged over 50% bands and the averaged power spectra were used to calculate the resistivity and coherency estimates.

5.0 DATA QUALITY

The criterion for acceptance or rejection of data for use in sounding curves is the coefficient of coherence, as described in section 3.0. The coefficient of coherence is a measure of how well two series correlate. Perfect correlation leads to a correlation of 1.0. When uncorrelated noise is present on one channel, the coherencies will vary from 0.0 for no correlation at all to some fraction of one as the noise level decreases. Sources of noise that lead to poor coherence are wind, "cultural noise", digitizing errors, and geologic noise.

Noise due to wind can occur when E field wires are moved by the wind. The noise problem can be aggravated when wires are strung through bushes and can be extreme when the wires are taut, causing movement of the electrode. Vozoff (1972) suggested burying wires to alleviate wind noise. Burying wires is not really feasible in an exploration method because of the time involved. Care in the placement of wires seems to be the best compromise between speed in setting up and minimizing wind noise. The magnetometer is very sensitive to motion so movement of vegetation can cause noise on the magnetic channel. Shielding the magnetometer from wind and isolating it from vegetation will lessen magnetometer noise. Noise due to wind is generally of higher frequency than that of interest in this survey. In extreme cases, however, wind noise can be so

great as to effectively mask the frequencies of interest.

Cultural noise is noise associated with man, most often power-lines and vehicles. The survey area is in a primitive area so power-line noise is easily avoided. 60 cycle noise associated with the generating system used in the survey can be minimized by locating the generator and the magnetometer on opposite sides of the recording vehicle. Noise due to vehicles is dependant on the distance of the moving vehicle from the recording site, speed of the vehicle and the weight of the vehicle. The faster the vehicle is traveling, the higher the frequency of the noise and the amplitude of the noise. The frequency of noise due to vehicles can be right in the middle of the range of interest. Noise from vehicles is most severe on the magnetic channel. Like most of the noise sources discussed so far, vehicular noise is best alleviated by distance.

Digitizing errors are errors caused by the person or equipment digitizing the data. A digitizing error may consist of a wrong value for a point or an extra point added or omitted. Wrong values show up as spikes or offsets. When spikes and offsets become severe, they are removed by computer software. Duplicate or missing points cause two data files digitized over the same time span to have differing lengths. The addition or subtraction of data points will tend to distort any phase information in the sounding curve. The effect of duplicate points on coherency varys,

according to where the point is introduced. Introduction of a data point at the beginning of a file will tend to have little effect on coherency but will have the maximum damaging effect on phase. Addition of a point in the middle of a data file will have the worst effect on the coherency because the first half of the data will correlate differently than the second half of the data. Addition of a data point at the end of a data file has little effect on either coherency or phase. The lower the frequency involved, the less the effect of an added point. Since all the soundings had length discrepancies to some extent, it was assumed that phase information was distorted and so was not shown.

The best way to prevent digitizing errors is to use a digital recording system. Due to fatigue and boredom, the author believes that manual digitization of long chart records can never be completely error free.

Geologic noise occurs when skin depths become great enough so that a significant portion of the signal is due to lateral discontinuities. Effects due to lateral geology sometimes manifest themselves in the vertical magnetic component. Signals on the vertical component are evidence that lateral geology is affecting the sounding. Lateral effects will tend to distort information pertaining to vertical depth soundings. Examination of Figure 8 indicates that distortion due to vertical faulting is minimum when considering the E-perpendicular mode on the resistive side of the fault. If deep penetrations are desired, preplanning of station locations can minimize lateral effects.

The author was not present when the MT data were acquired and so does not have first hand knowledge as to the problems caused by wind and cultural noise. However, inspection of the records does not reveal any indication of severe wind noise. Vertical components were active on many of the soundings, indicating some lateral effects. The parallel component generally is less affected by lateral inhomogenieties and when available, was used in modelling.

6.0 INTERPRETATION

Interpretation is the art of coalescing physical data about the earth into a reasonable geologic model. MT data can be interpreted in two ways: with an interest in lateral geology and with an interest to vertical geology. Lateral geology can be interpreted by examining polarization ellipses and comparing them to theoretical profiles across vertical faults. Vertical geology can be interpreted by examining MT sounding curves and comparing them to theoretical 1-D sounding curves.

When E fields are measured within a skin depth of a lateral geologic feature, the E fields tend to polarize either parallel or perpendicular to the feature. Figure 8 shows a single frequency profile across a vertical fault as shown in Vozoff, 1972. Also shown in Figure 9 are the major and minor axes of the apparent resistivity ellipses at four distances from the fault. At a great distance from the fault on either side, the apparent resistivities between the parallel and perpendicular components are approximately equal and the polarization ellipses become circular. The apparent resistivities approach the proper scalar value of resistivity for the media. This situation is shown in cases A and D in Figure 8.

When the fault is approached from the conductive side, the E perpendicular mode of apparent resistivity decreases with respect to the true resistivity and the E parallel mode increases with respect

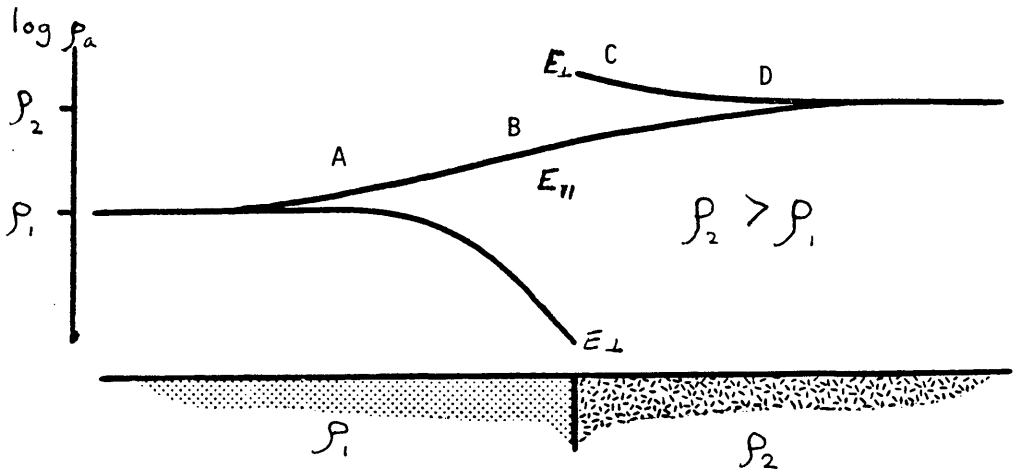

Resistivity profile across a vertical fault.

(after Vozoff, 1972)

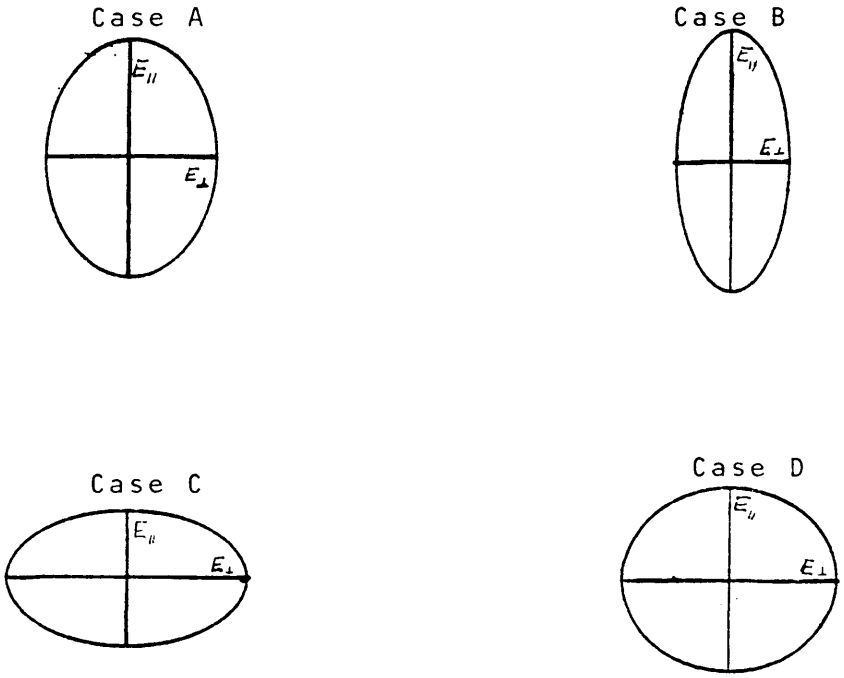

Apparent resistivity ellipses for various distances from fault.

Figure 8.

to true resistivity. This makes the E parallel mode the major axis of the apparent resistivity ellipse. Since the E field ellipse is related directly to the resistivity ellipse, when a sounding is recorded on the conductive side of a fault, the E field polarization ellipse should point in the direction parallel to the structure. This situation is shown as case B in Figure 8.

When the fault is approached from the resistive side, the E perpendicular mode tends to show a higher apparent resistivity than the E parallel mode. So in the case where the recording is done on the resistive side of a fault, the major axis of the E field ellipse will be the E perpendicular component and the ellipse will point perpendicular to strike. This situation is shown as case C in Figure 8. In general, the closer to a fault, the greater the ellipticity becomes.

Figure 9 shows polarization directions plotted on a topographic map. Only stations showing preferential directions are shown on the map. The stations showing preferential directions were stations 1-4, 6-8, 11, 13, 15 and 19. The polarizations shown in Hualapai Flat are all more perpendicular than parallel to mapped structure as shown in Plate 1. This indicates that stations 6, 7, 8, and 4 were all recorded on the resistive side of faulting. Gravity profiles by Crewdson (Fly Ranch profile, 1976) indicate a basement fault with the east side downthrown to the east of the recording stations

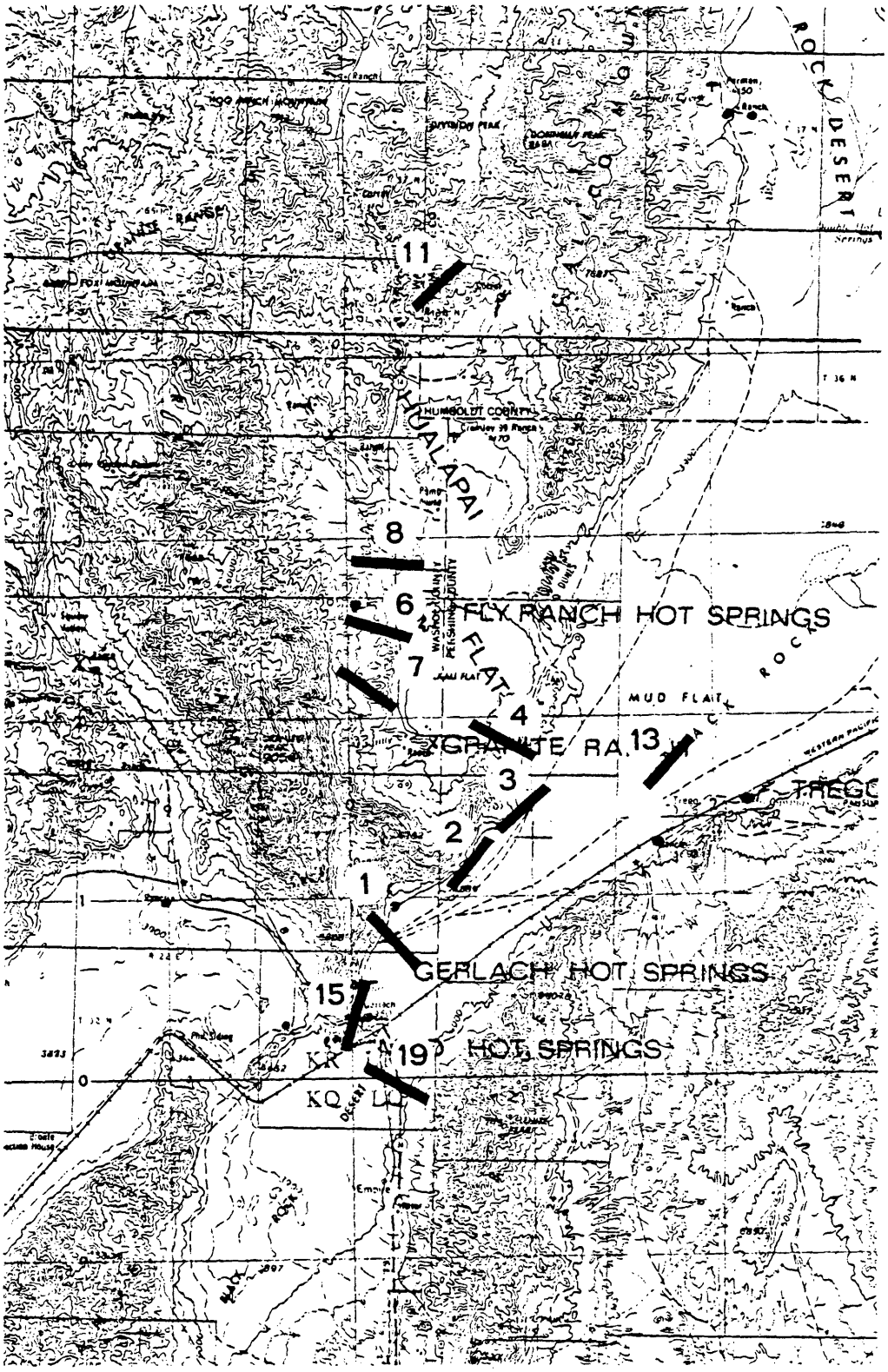

Figure 9. Directions of preferred current flow.

near the road, supporting the contention that the MT stations were recorded on the resistive side of a fault. Station 4 is recorded on a structure shown by Crewdson as being basement outcrop (Figure 5).

Structure in the Black Rock Desert generally coincides with the major topographic changes. Stations 15, 2, and 3 are taken near abrupt topographic changes and their polarization ellipses are parallel to these topographic changes. The stations are assumed to be recorded on the conductive side of the basin margin fault. Station 1, however, has polarization directions perpendicular to the topographic trends. Station 1 is located in a topographic embayment of the desert into the Granite Range. The polarization direction of station 1 indicates the possibility of a resistive shelf extending under the desert and the recording site and dropping off to the south and east of the recording site.

Station 19 south of Gerlach also indicates the presence of a resistive shelf underlying the desert at the recording point stretching from the Selenite Range and dropping off to the north and west of the recording site.

Station 13 is located in the Black Rock Desert, four to five km from the nearest mountains. The polarization direction of station 13 is consistent with that of stations 2 and 3, the nearest stations in the Black Rock. Investigation of the polarization vs. period shows

that the polarization increases with period (Figure 10). The ellipticity at 81 sec period is 2.2 and the ellipticity at 102 sec. period is 6.6 indicating that the skin depth to the feature occurs when the period is between 80 and 100 sec. Assuming a thick sequence of low resistivity material (1 ohm meter) overlaying a basement fault, the skin depth indicates the feature is about 4 to 4.5 km from the recording site. The direction of polarization indicates the recording is taken on the conductive side of a fault so the feature could conceivably be the basin margin fault near Trego.

The MT sounding is the major tool of the MT method. When modelling sounding curves, the 1-D model is the only model that can be quickly calculated for a large number of cases. 2-D modelling tends to either be prohibitively expensive or uselessly simple. Quantitative interpretation of MT soundings can be accomplished by matching theoretical curves to the field data.

For the purposes of this survey 1-D theoretical soundings were matched to the data by considering the limiting case. For the limiting case if the data are not seen to roll over the question is asked, "What happens if the curve rolls over right at the point the data stops?" In this manner the minimum depth to the layer that causes the roll over can be found. In general, gravity and TDEMS show a sequence of alluvial material up to 2 km thick. TDEMS also show a low resistivity top layer of about .2 to 1 ohm meter that can be 200 to 300 meters

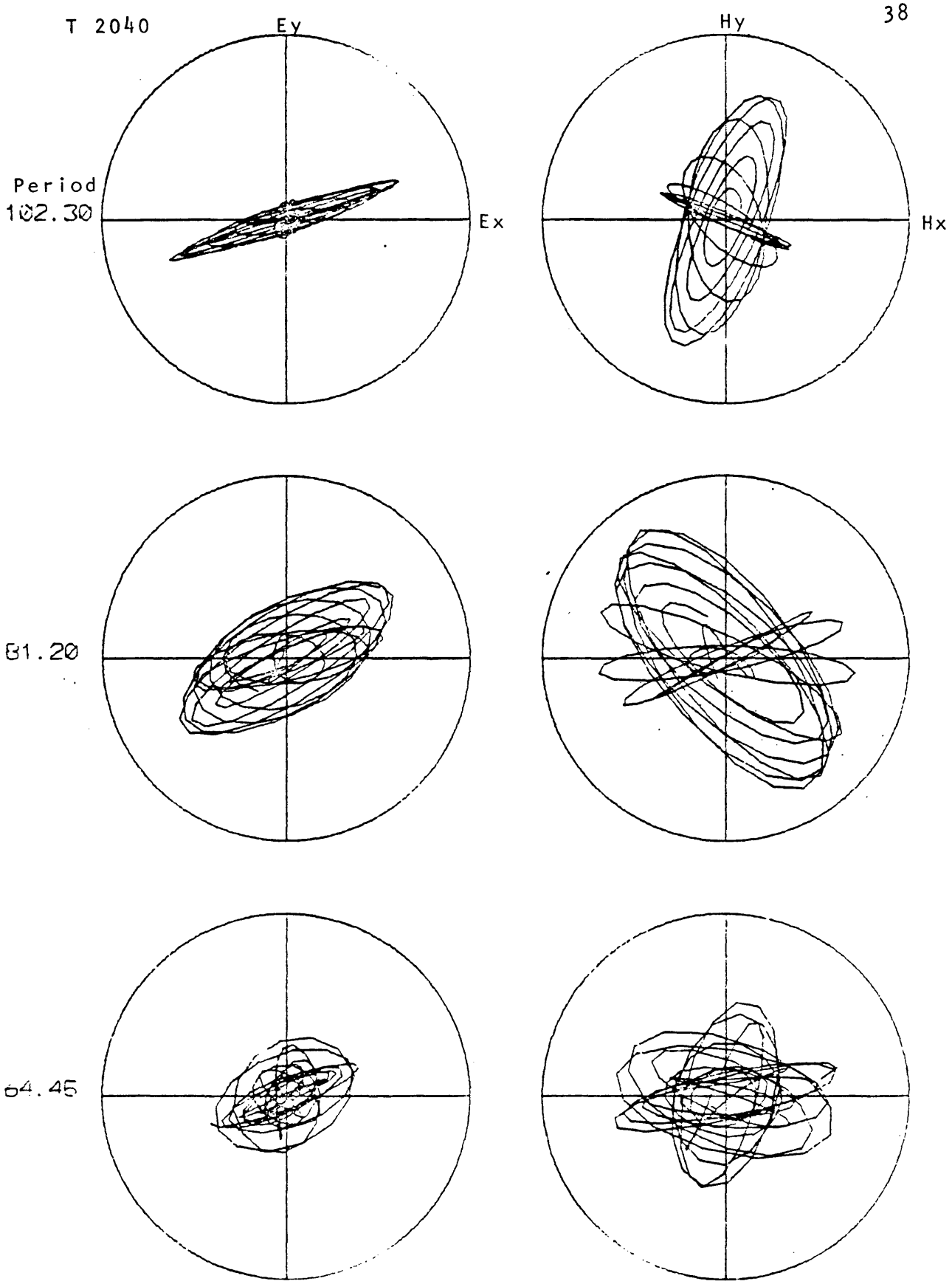

Figure 10. Polarizations for station 13.

thick. Underlaying this low resistivity layer the TDEMS indicate higher resistivity matter of about 10 ohm meters that can be 500 to 1000 meters thick. The low resistivity layer can have a great effect on the sounding curve because the curve is asymptotic to the first layer resistivity and can only rise at a slope of 1 on a log-log scale. The underlaying 10 ohm meter layer has virtually no effect on the sounding curve. Figure 12 shows a 2 layer conductor over resistor theoretical curve with the first layer resistivity being .5 ohm meters and the second layer resistivity being 100 ohm meters. When an intermediate layer of 10 ohm meters is added two km thick the effect is negligible. The important factors that will effect sounding curves are the resistivity and thickness of the first layer, the resistivity and thickness of the high resistivity basement and the resistivity of the conductor at depth. Four soundings were chosen for modelling. Other soundings were considered unsuitable because of either too much scatter or indications of large scale lateral effects. The soundings chosen were soundings 6, 7, 12, and 16.

Sounding 6 indicates a resistor over conductor type geometry (Figure 13a). The resistor over conductor is typified by a curve that is descending from the resistivity of the first layer to the resistivity of the second layer at a minimum slope of -1 on a log-log scale. The two modes are represented by the two different symbols on the plot. In Figure 13a the two modes are similar in their be-

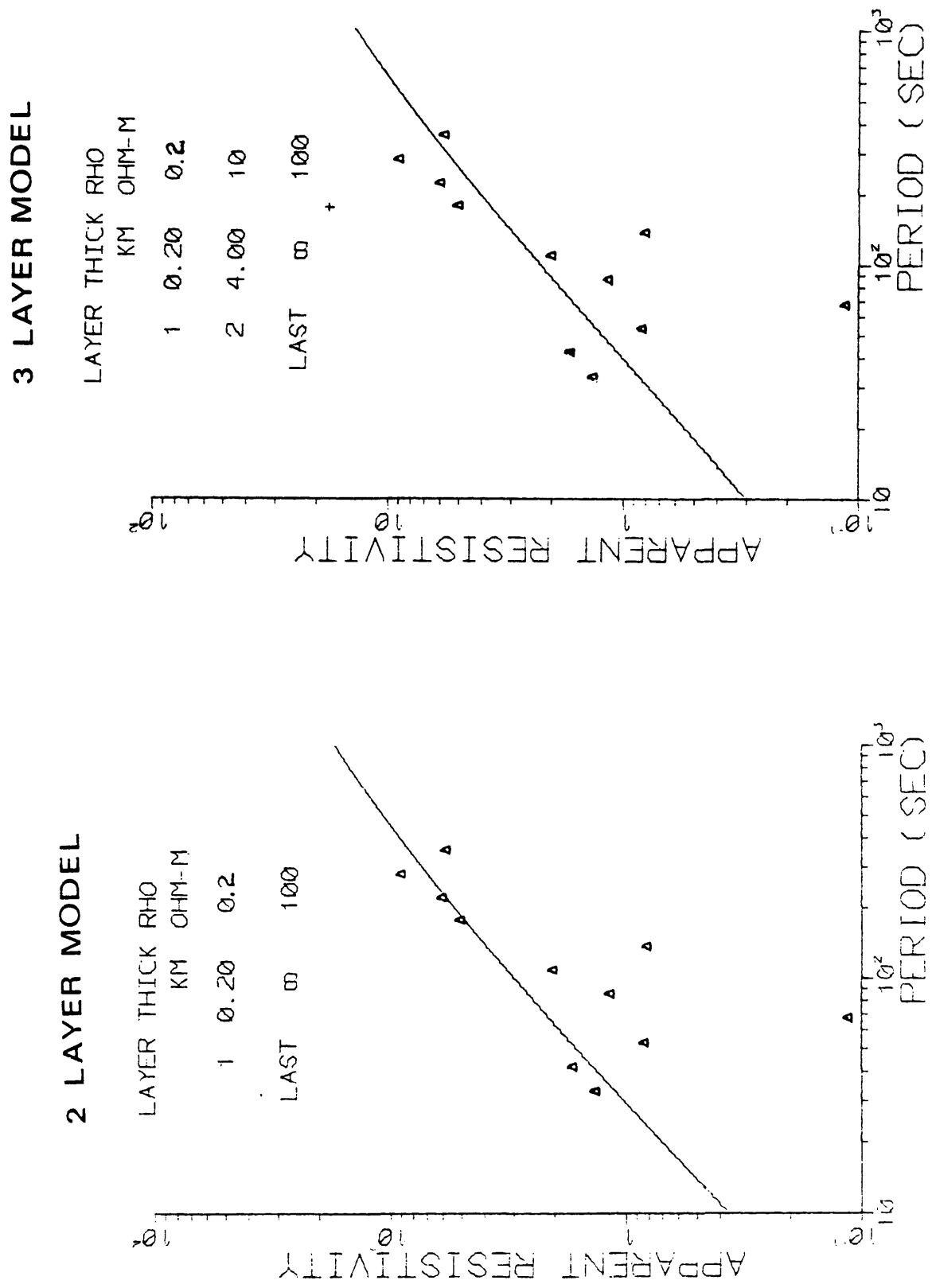

Figure 11. 2 and 3 layer models for station 16.

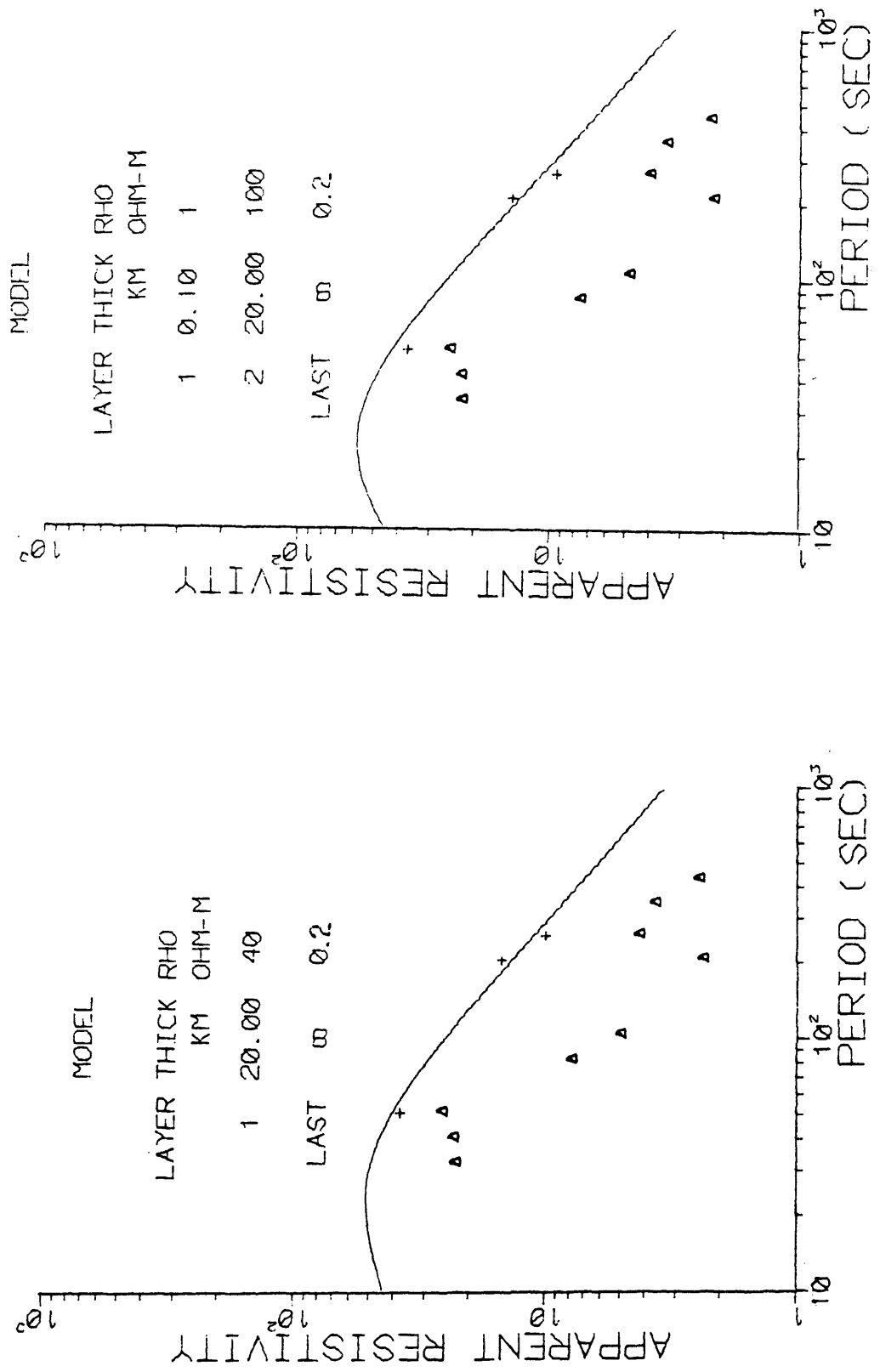

Figure 12. 2 and 3 layer models for sounding 6.

havior. Modelling of the more resistive mode although it only has 3 points gives more realistic results. The modelling was done assuming that the two modes were similar in shape with only the resistivities being different, when the separation between modes is not large.

When a 2-layer theoretical curve is matched to the data with the first layer resistivity constrained to be 40 ohm meters, the first layer thickness is shown to be 20 km (Figure 12b). A low resistivity layer with a thickness of up to 100 meters can be added without effecting the thickness of the second layer although the resistivity of the second layer must be raised to 100 ohm meters. The 3 layer model is more realistic in terms of what is known about the area.

Sounding 16 (Figure 13) has more scatter than sounding 6, but it can be seen that the curve is ascending, indicating a conductor over resistor. The two modes are equal in the level of resistivity so it is indeterminate which mode is the parallel or perpendicular mode. The mode that is displayed with the triangles has the least scatter, so it was the mode used for modelling purposes. A two layer curve was matched to the data with a km of .8 ohm meters material and 50 ohm meters basement. If it is assumed that the curve rolls over at 300 seconds, the minimum thickness of the second layer is 25 km (Figure 13).

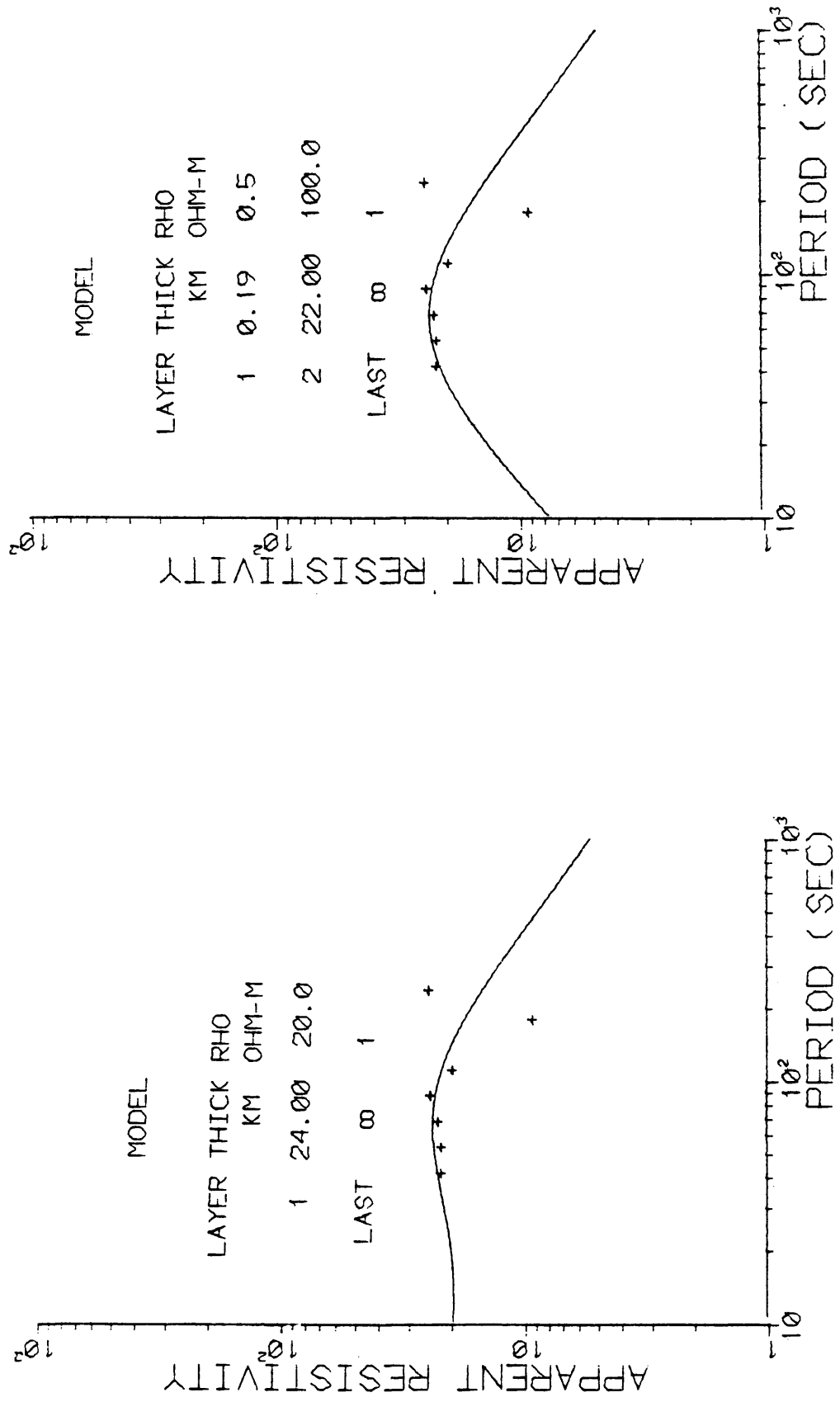

Figure 13. 2 and 3 layer models for sound 16.

Sounding 7 (Figure 14) rolls down at about 70 sec. period. A two layer curve can be fit to the data with a thickness of 25 km at 25 ohm meters. When the limiting 3 layer case is considered, the conductive first layer can be up to 150 meters thick with a second layer of 100 ohm meters material 21 km thick.

Sounding 12 (Figure 15) was modelled using the more resistive component of apparent resistivity. The three layer model showed a first layer 190 meters thick and a second layer thickness of 22 km. It is not certain exactly what the behavior of this curve is. The curve was modelled using the assumption that the data are all at the top point of the curve and the data rolled down on both sides.

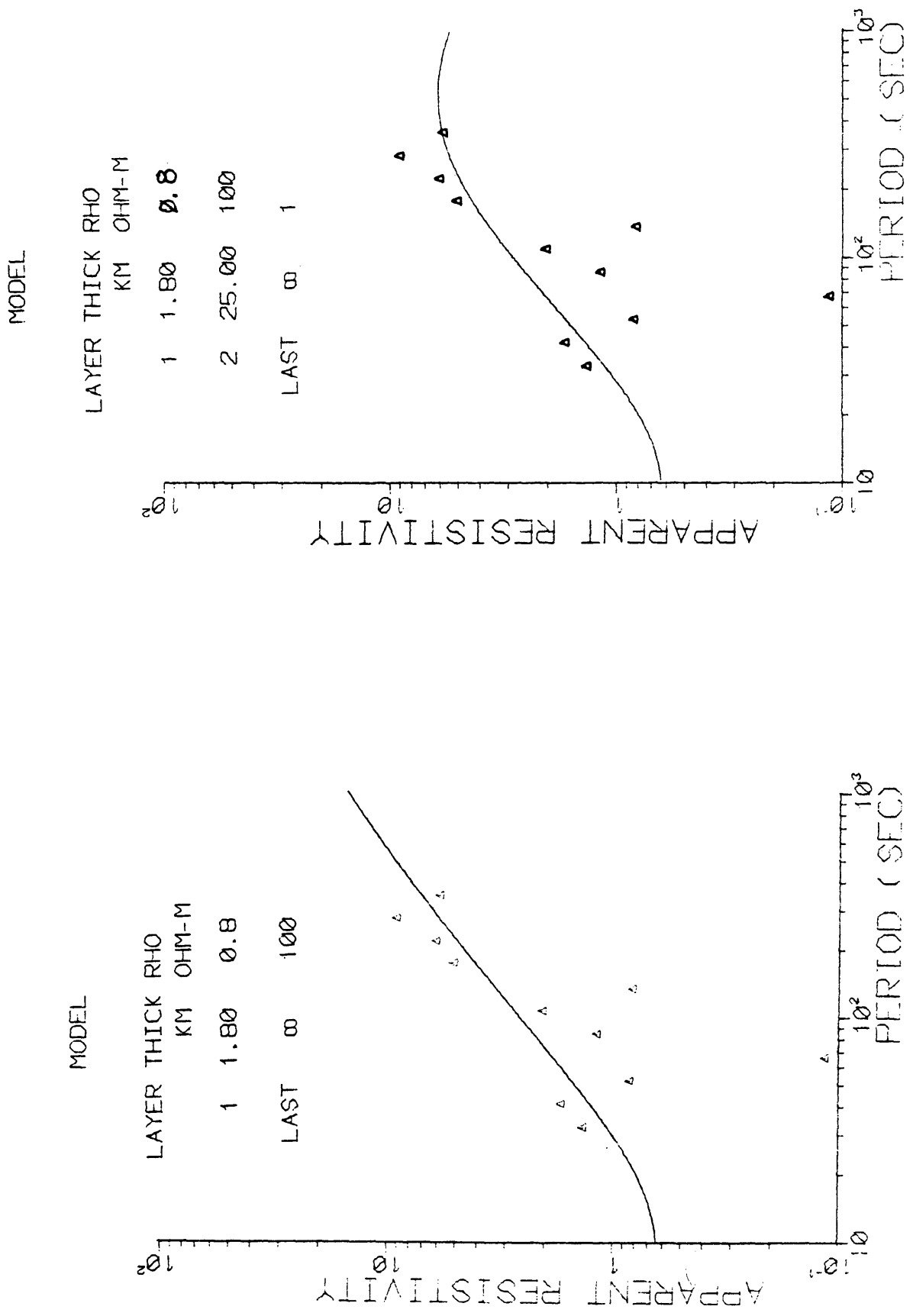

Figure 14. 2 and 3 layer models for sounding 7.

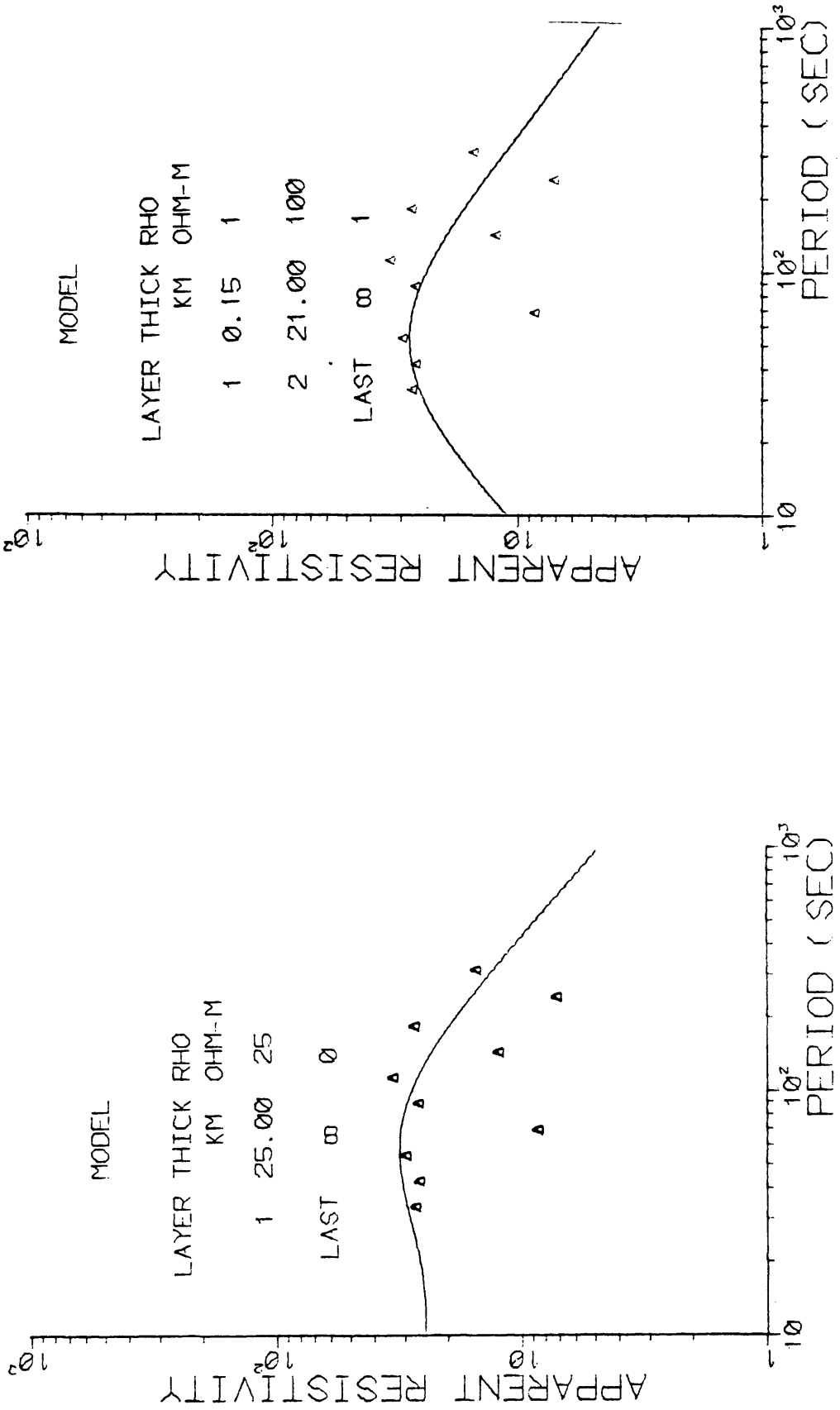

Figure 15. 2 and 3 layer models for sounding 12.

7.0 CONCLUSIONS

MT data have been evaluated in two ways: examination of polarization ellipses and modeling of selected sounding curves.

Polarization ellipses revealed information about surface and near surface structure, mainly faulting. In an area where the geology is not well known or perhaps covered, the polarization ellipses can be an effective reconnaissance tool for locating and determining the strike of faulting. The polarization ellipses tend to yield good quality data about structure even when the MT sounding curves may be poor.

Modeling of MT curves indicate the depth of a deep conductor in the lower crust to be about 25 km in the south end of the survey area and 20 to 22 km in the Hualapai Flat area and north of the Hualapai Flat area. The effect of noise on H field channels due to flux jumping and resets will tend to bias the resistivity curves down from what they would normally indicate in a less noisy sounding. The fact that the soundings may have higher apparent resistivities than indicated would place the depth to a conductor deeper than shown.

Heat flow in the Western United States generally ranges from 1.5 to 2.5 HFU (Sass, et. al., 1971). Within Nevada heat flow values average about 2.0 HFU. Within 50 miles of Gerlach there are observed

observed heat flows of greater than 2.5 HFU (Diment, et. al., 1975). Assuming a thermal conductivity of 6×10^{-3} cal/cm sec ^{o}C, which is the average for igneous rocks (Stacey, 1969) and assuming a modest heat flow of 2.0 HFU, a temperature of about $1000^{o}K$ is reached at a depth of 22 km. Assuming a heat flow of 2.5 HFU the extrapolated temperature is $1200^{o}K$.

The observed regional heat flow of the area not only provides an adequate mechanism for the geothermal process, but also provides an explanation for the observed MT soundings. The MT method has proved to be an effective tool in the delineation of Basin and Range heat source mechanisms. When it is possible to locate MT stations on high resistivity bedrock, much of the effect of lateral discontinuities can be avoided and near surface geologic noise such as alluvial fill can be minimized.

REFERENCES

Callaway, J., 1978, Reflection seismic traverse across Black Rock Desert and Hualapai Flat, Nevada: CSM Quarterly, v. 73, no. 3, p. 65-72.

Cagniard, L., 1953, Basic theory of the magnetotelluric method of geophysical prospecting: Geophysics, v. 18, no. 3, p. 605-635.

Crewdson, R. A., 1976, Geophysical studies in the Black Rock Desert geothermal prospect, Nevada: Thesis T-1866, C.S.M., Golden, CO.

Diment, W. H., Urban, T. C., Sass, D. H., Marshall, B. V., Munroe, R. J., and Lachenbruch, A. H., 1975, Temperatures and heat contents based on conductive transport of heat: in Assessment of Geothermal Resources of the U.S., 1975, USGS Circular 726.

Grose, L. T. and Sperandio, R. J., 1978, Geology of the Gerlach-Hualapai Flat geothermal area, northwest Nevada: CSM Quarterly, v. 73, no. 3, p. 1-10.

Hermance, J. F., 1973, Processing of magnetotelluric data: Physics of the Earth and Planetary Interiors, v. 7, p. 349-364.

Keller, G. V., and Frischknecht, F. C., 1966, Electrical methods in geophysical prospecting: International series of monographs in electromagnetic waves, v. 19, Pergammon Press, Inc., London.

Keller, G. V. and Grose, L. T., 1975, The Colorado School of Mines geothermal study, Progress report no. 4 for period February 1 to October 1, 1975.

Madden, T., 1964, Spectral, cross-spectral and bispectral analysis of low frequency electromagnetic data, in Natural Electromagnetic Phenomena, D. F. Biehl, editor, Plenum Press, NY.

Morris, Drew, 1975, Quadripole mapping near the Fly Ranch geothermal prospect, northwest Nevada: Thesis T-1699, CSM, Golden, CO.

Ofrey, O., 1975, Time domain electromagnetic soundings in the Black Rock Desert, northwest Nevada: Thesis T-1749, CSM, Golden, CO.

Pakiser, L. C., and Hill, D. P., 1963, Crustal structure in Nevada and southern Idaho from nuclear explosions: JGR, v. 68, no. 20, p. 5757-5766.

Porstendorfer, G., 1975, Principles of magnetotelluric prospecting: Geoexploration Monograph Series I, no. 5, 118p., Gebruder Borntraeger, Berlin West and Stuttgart.

Rooney, D., and Hutton, V. R. S., 1977, A magnetotelluric and magnetovariational study of the Gregory Rift Valley, Kenya: Geophysical Journal, Royal Astr. Society, v. 51, p. 91-119.

Sass, J. H., Lachenbruch, A. H., Munroe, R. J., Greene, G. W. and Moses, T. H., Jr., 1971, Heat flow in the western United States: JGR, v. 76, no. 26, p. 6376-6413.

Sims, W. E., Bostich, F. X., Jr., and Smith, H. W., 1971, The estimation of magnetotelluric impedance tensor elements from measured data: Geophysics, v. 36, no. 5, p. 938-944.

Stacey, F. D., 1969, Physics of the earth: John Wiley and Sons, Inc. New York.

Stanley, W. D., Whal, R. R., and Rosenbaum, J. G., 1976, A magneto-telluric study of the Stillwater-Soda Lakes, Nevada geothermal area: USGS open file report no. 76-80.

Swift, C. M., 1967, A magnetotelluric investigation of an electrical conductivity anomaly in the southwestern U.S.: Ph.D. thesis, MIT, Cambridge, MA.

Takeuchi, H., Uyeda, S., Kanamori, H., 1967, Debate about the earth: Freeman, Cooper and Co., San Francisco, CA.

Vozoff, K., 1972, The magnetotelluric method in the exploration of sedimentary basins: Geophysics, v. 37, no. 1, p. 98-141.

APPENDIX A

BLACK ROCK MT 1 #2

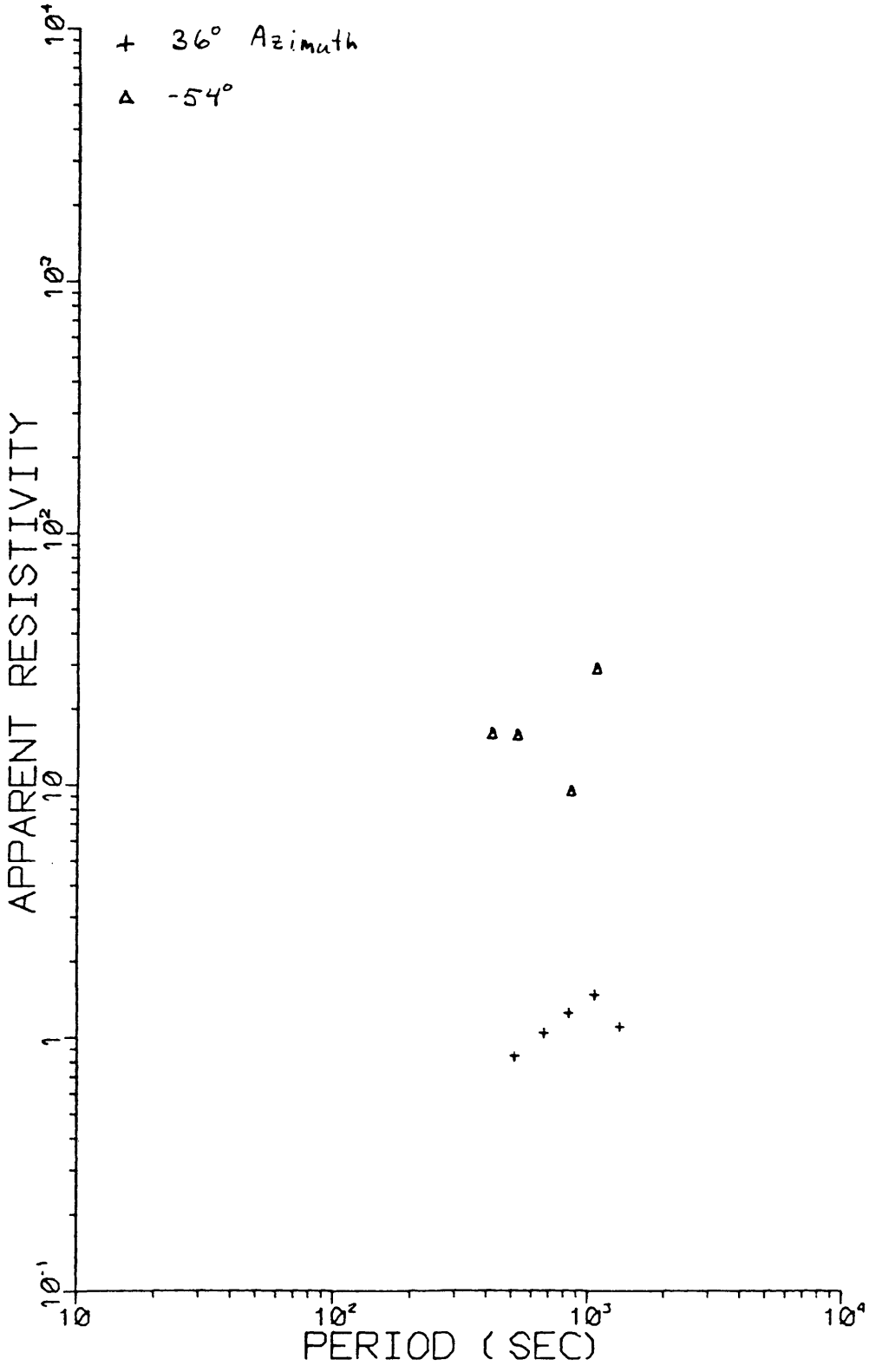

BLACK ROCK MT 1 PART 3

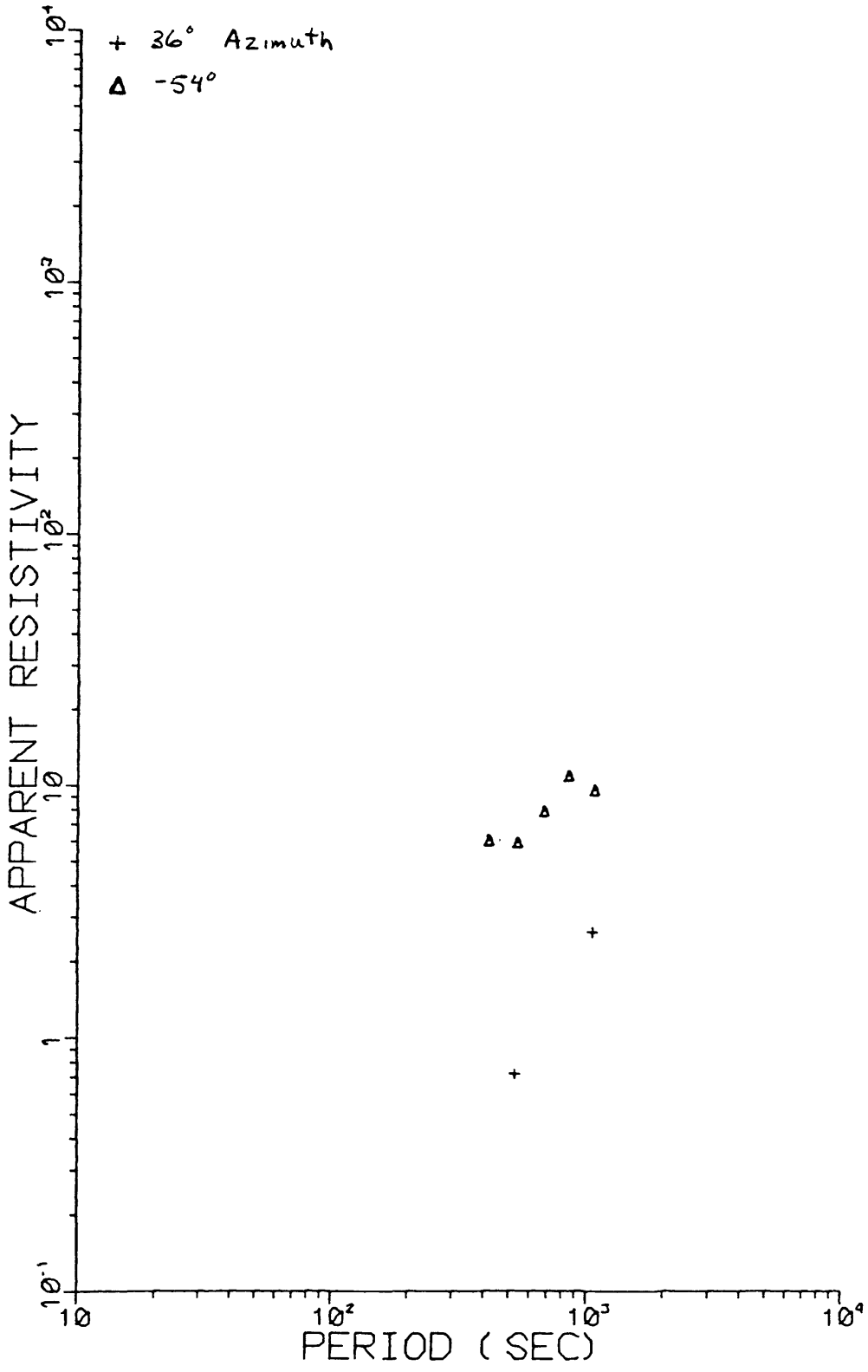

BLACK ROCK DESERT SOUNDING 5

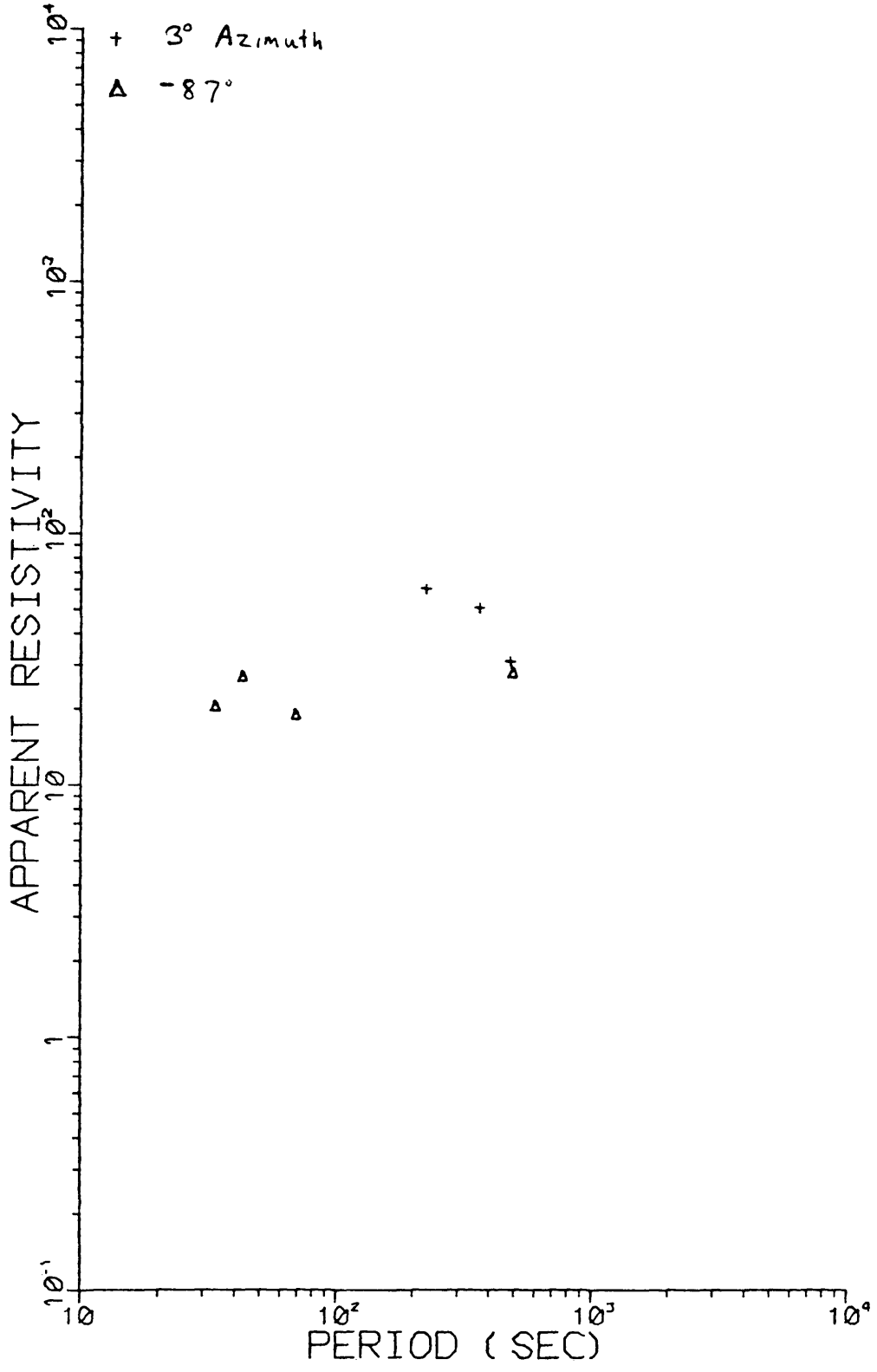

BLACK ROCK MT 6

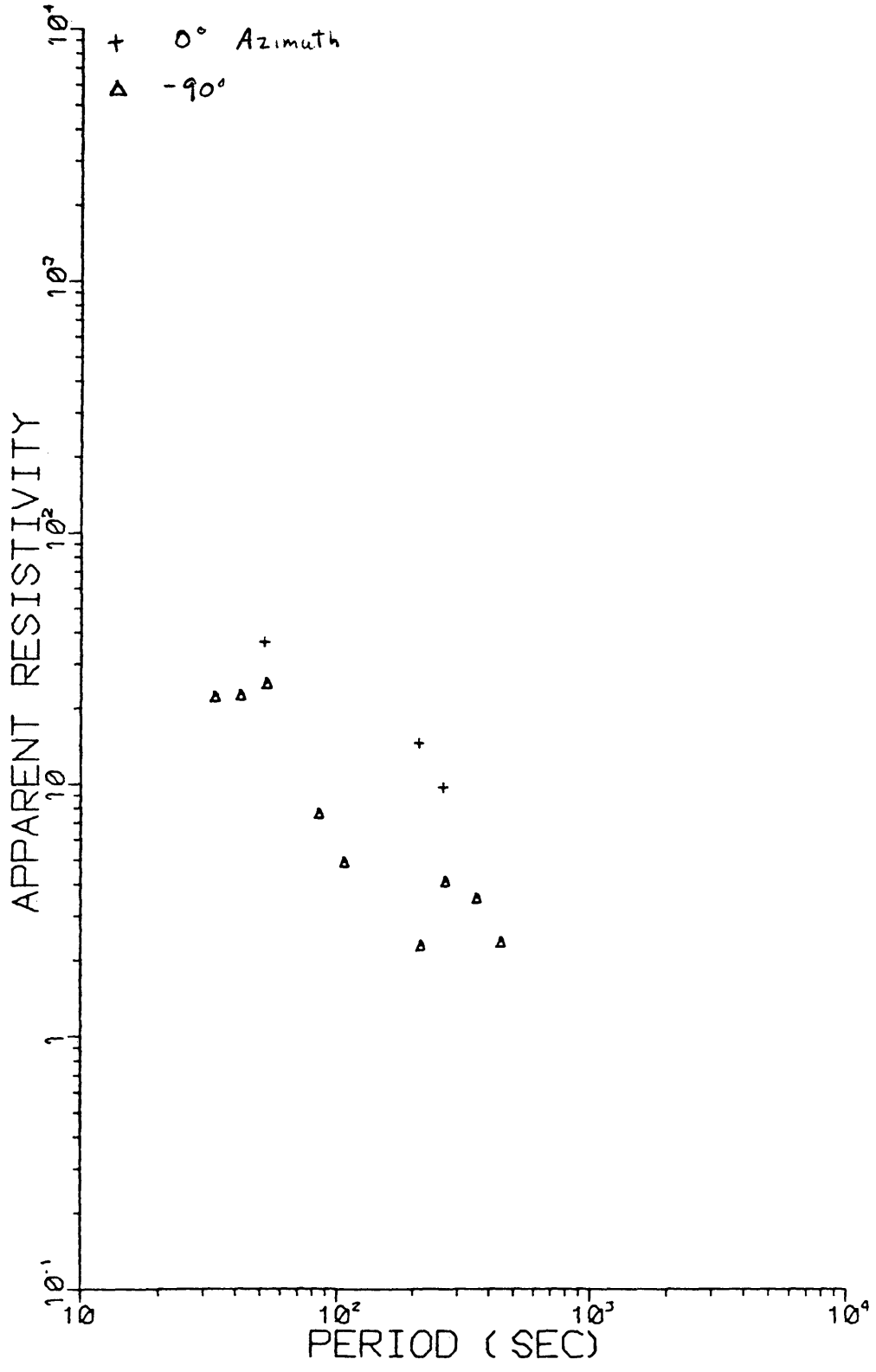

BLACK ROCK MT 7 PART 1

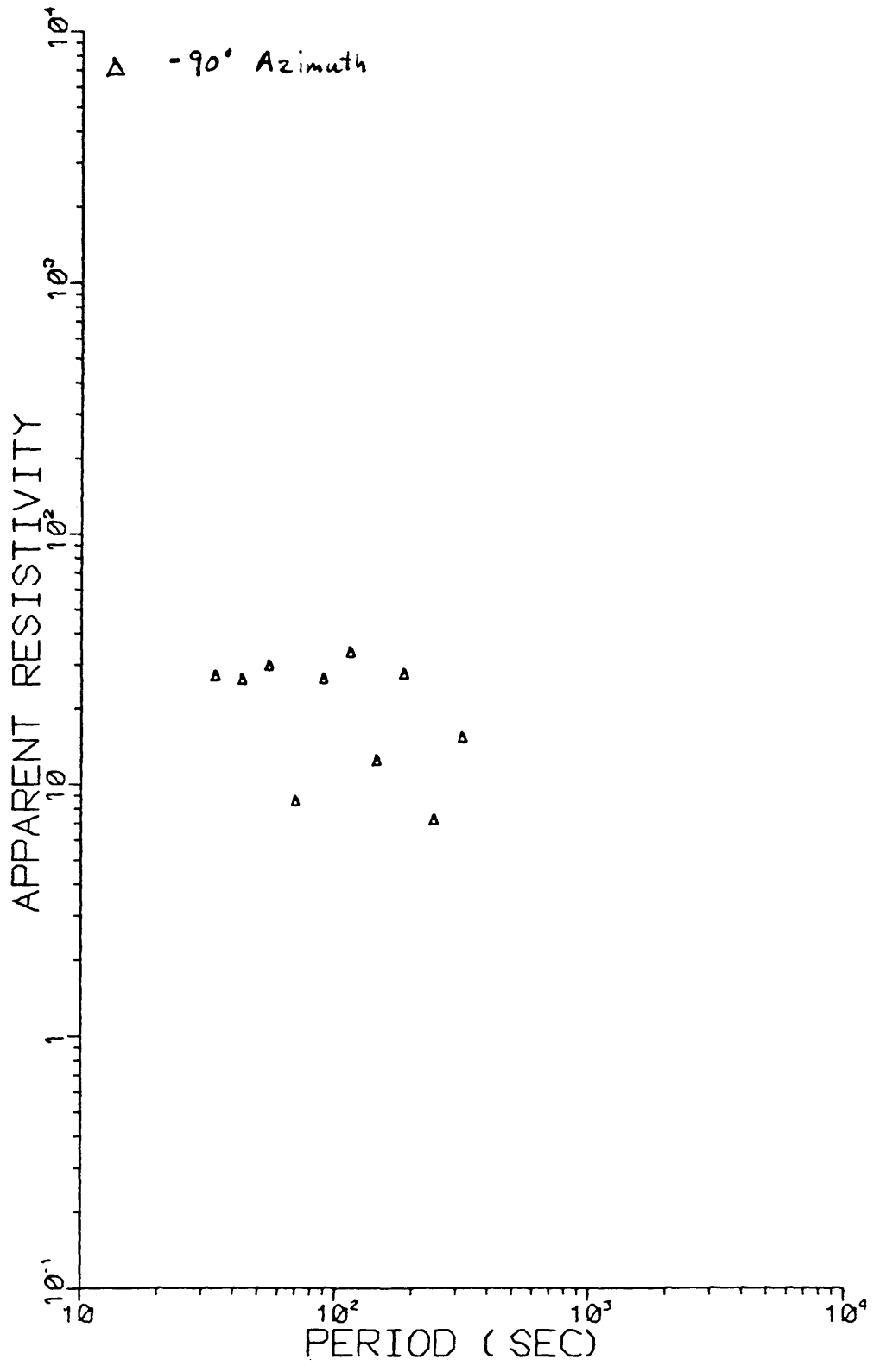

BLACK ROCK MT 8 #1

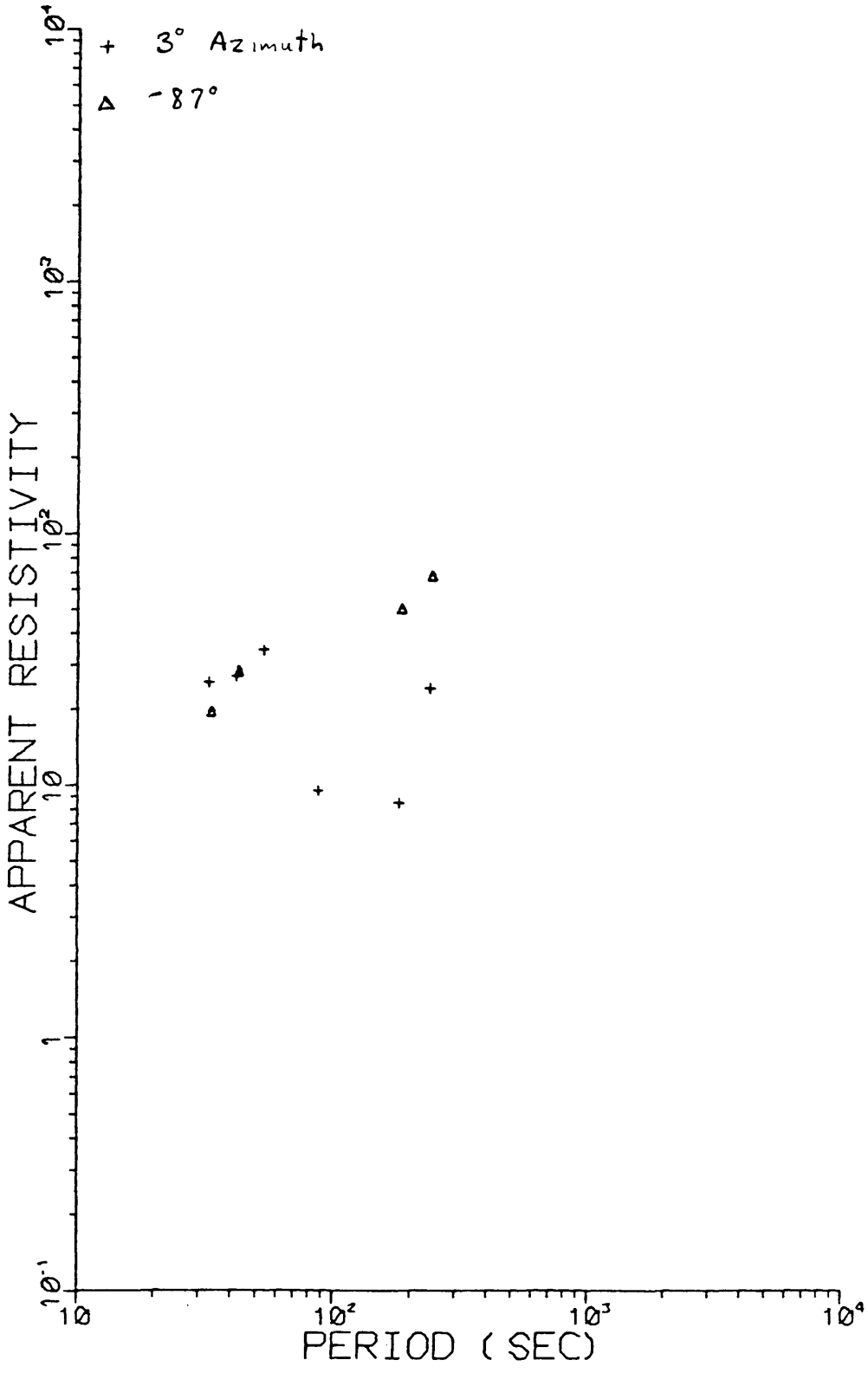

BLACK ROCK MT 9

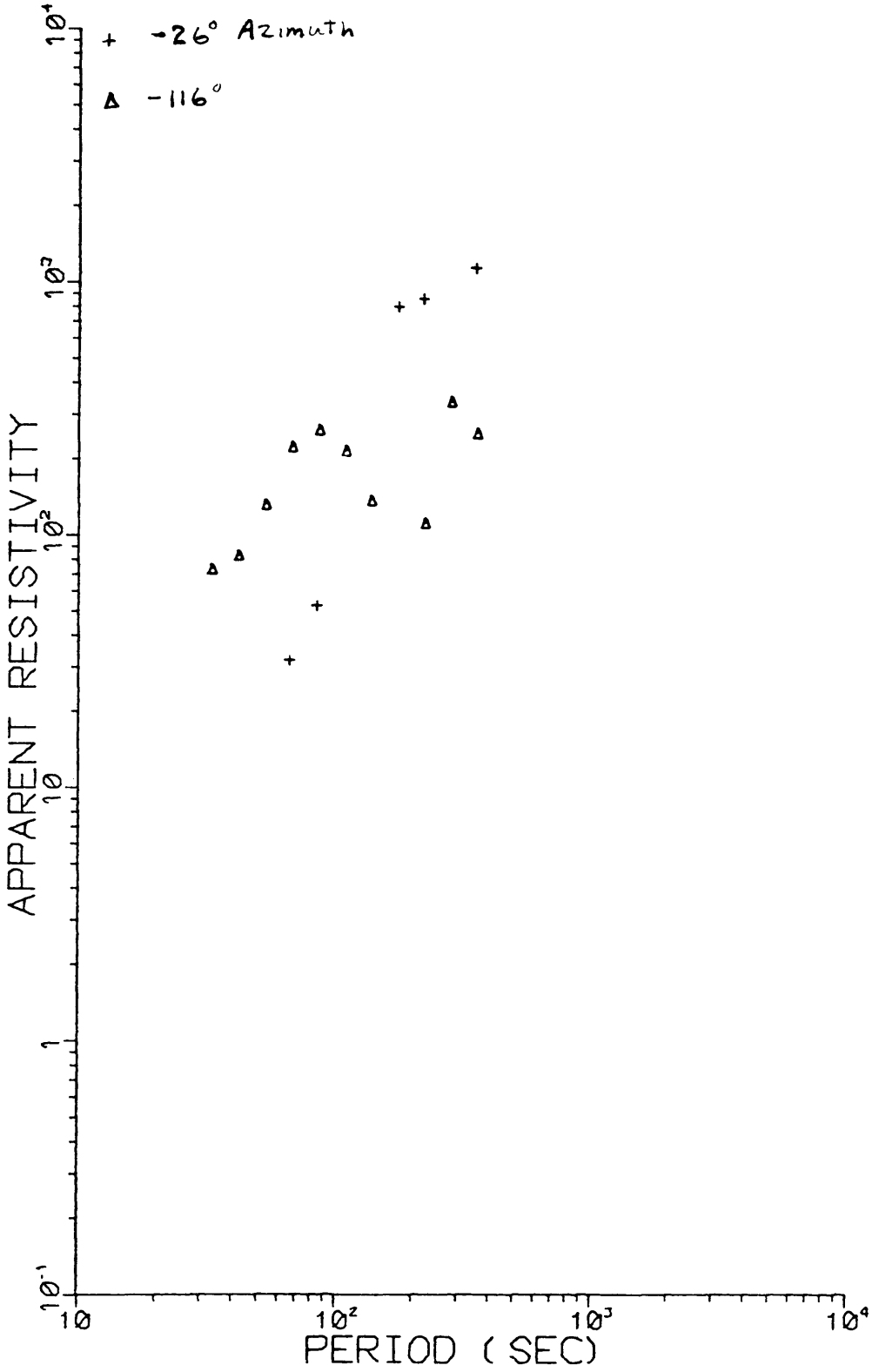

BLACK ROCK DESERT SOUNDING 12

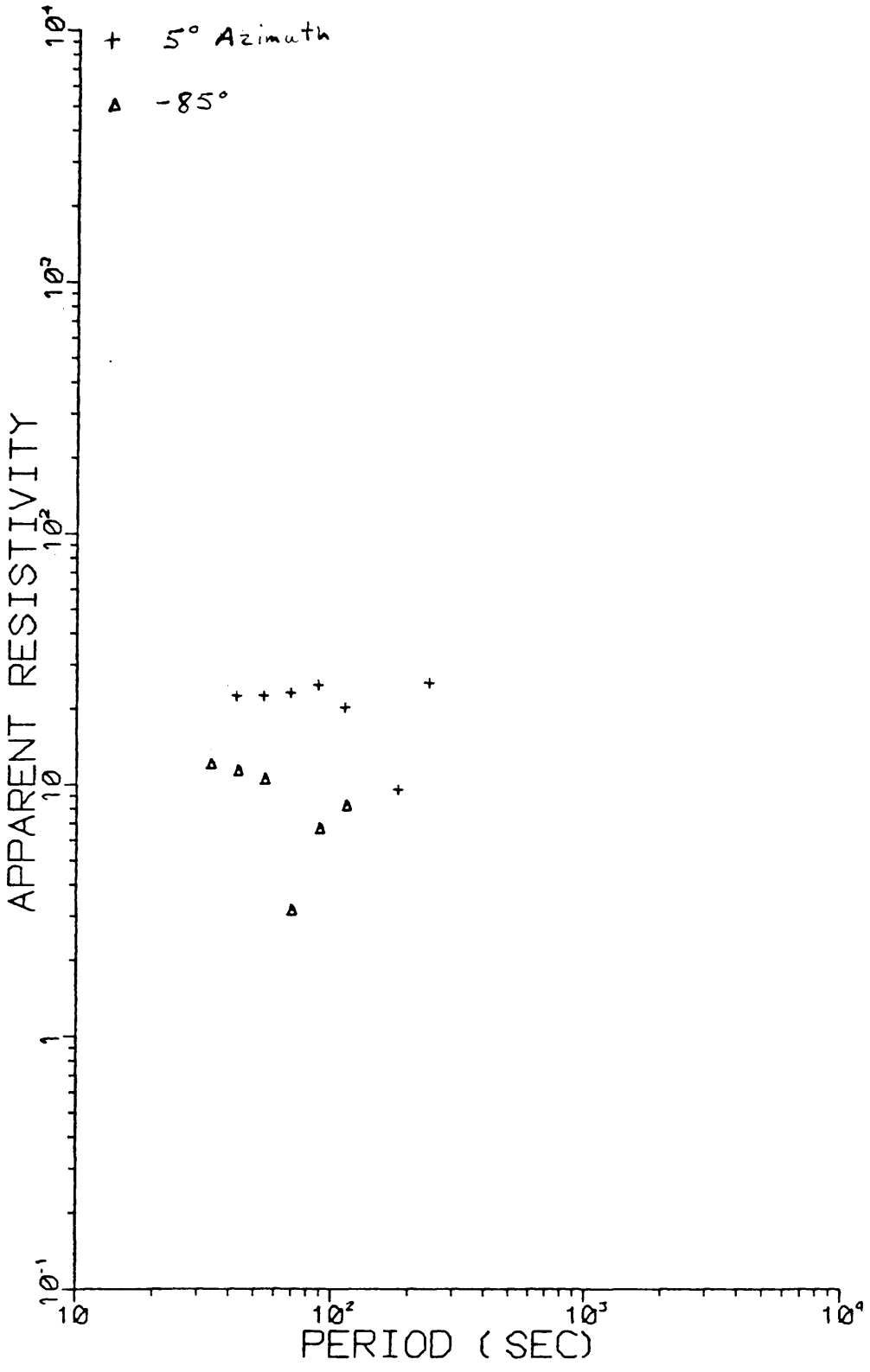

BLACK ROCK MT 13

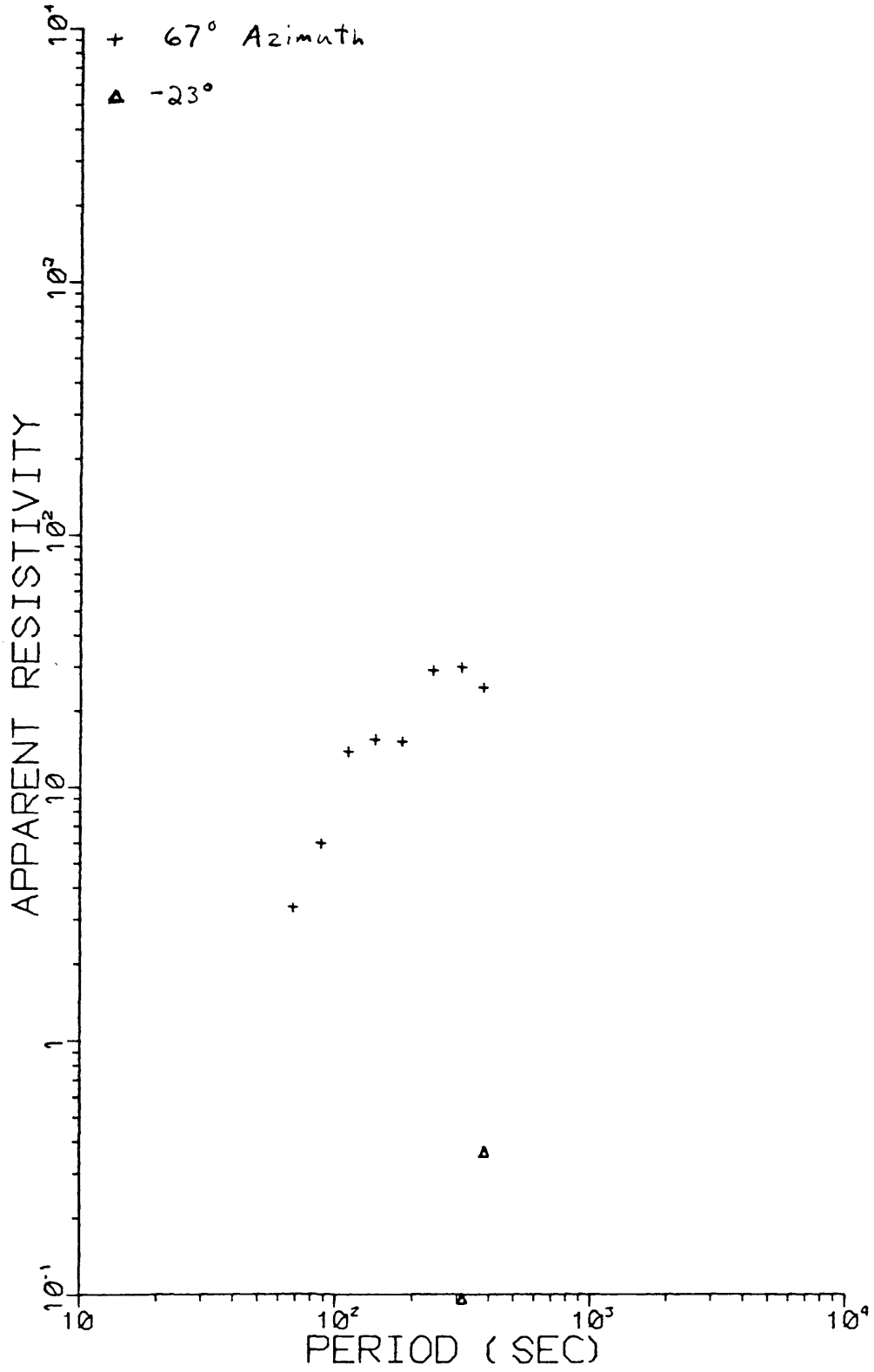

BLACK ROCK DESERT SOUNDING 16

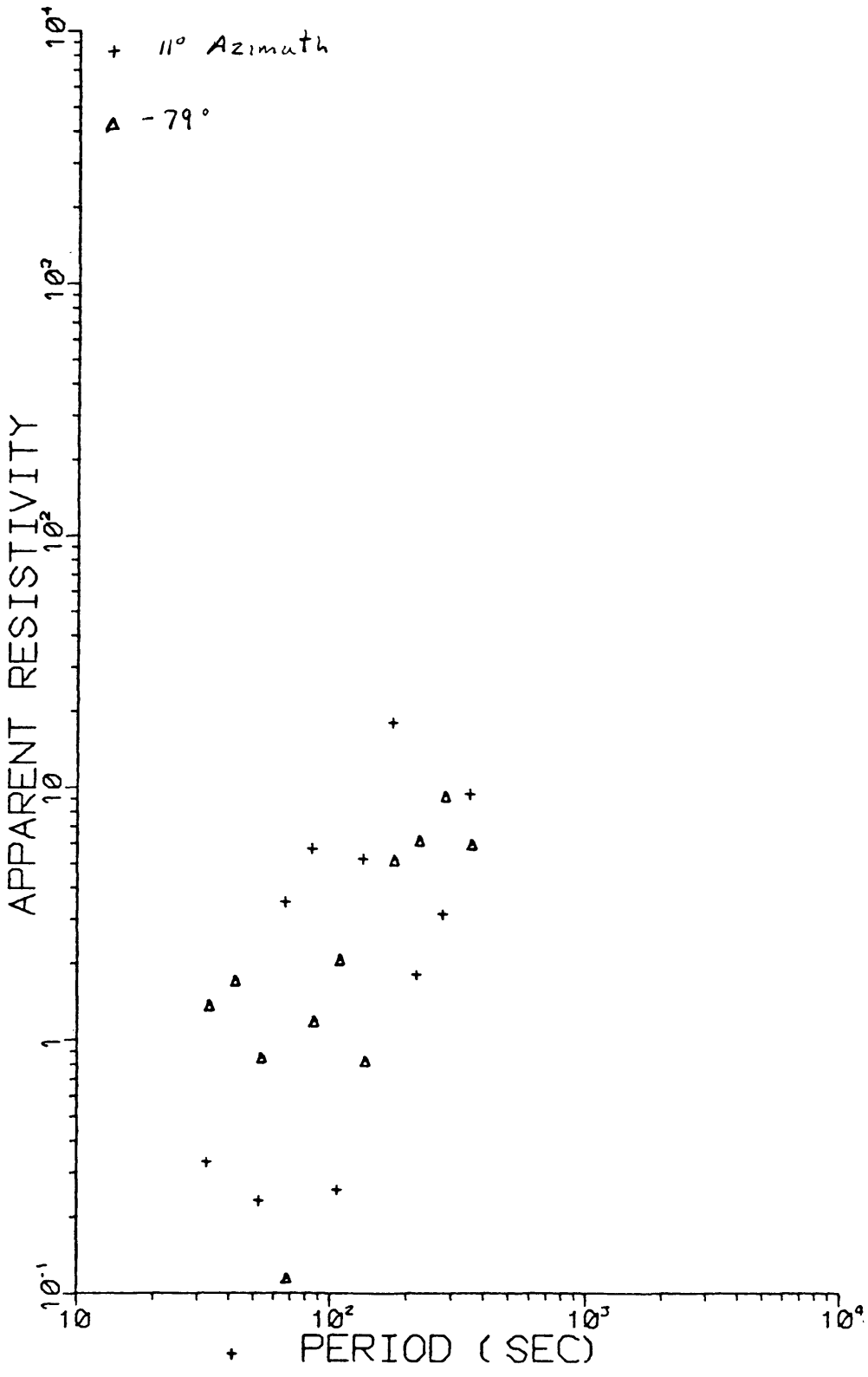

BLACK ROCK MT 19

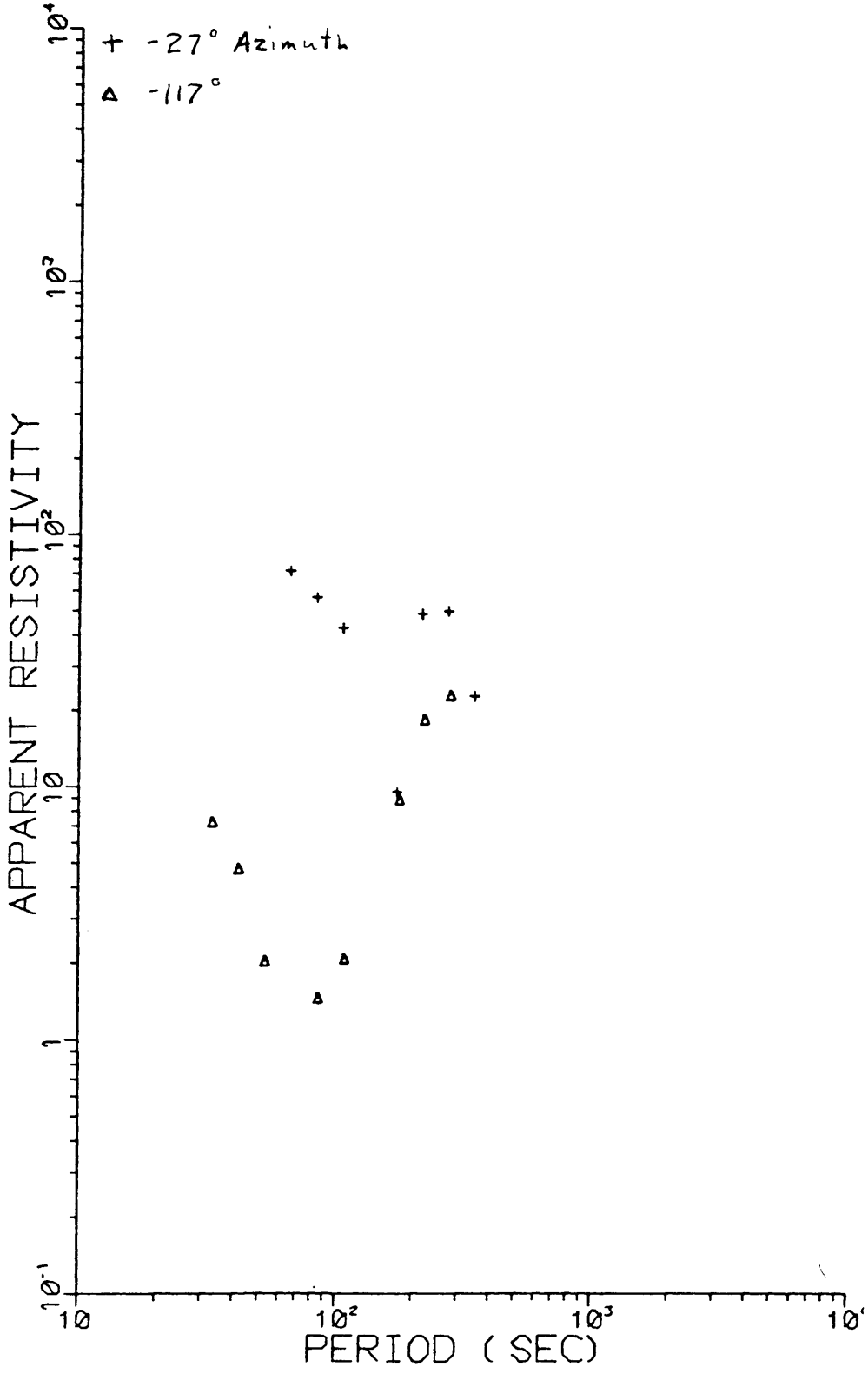

APPENDIX B

BL1002

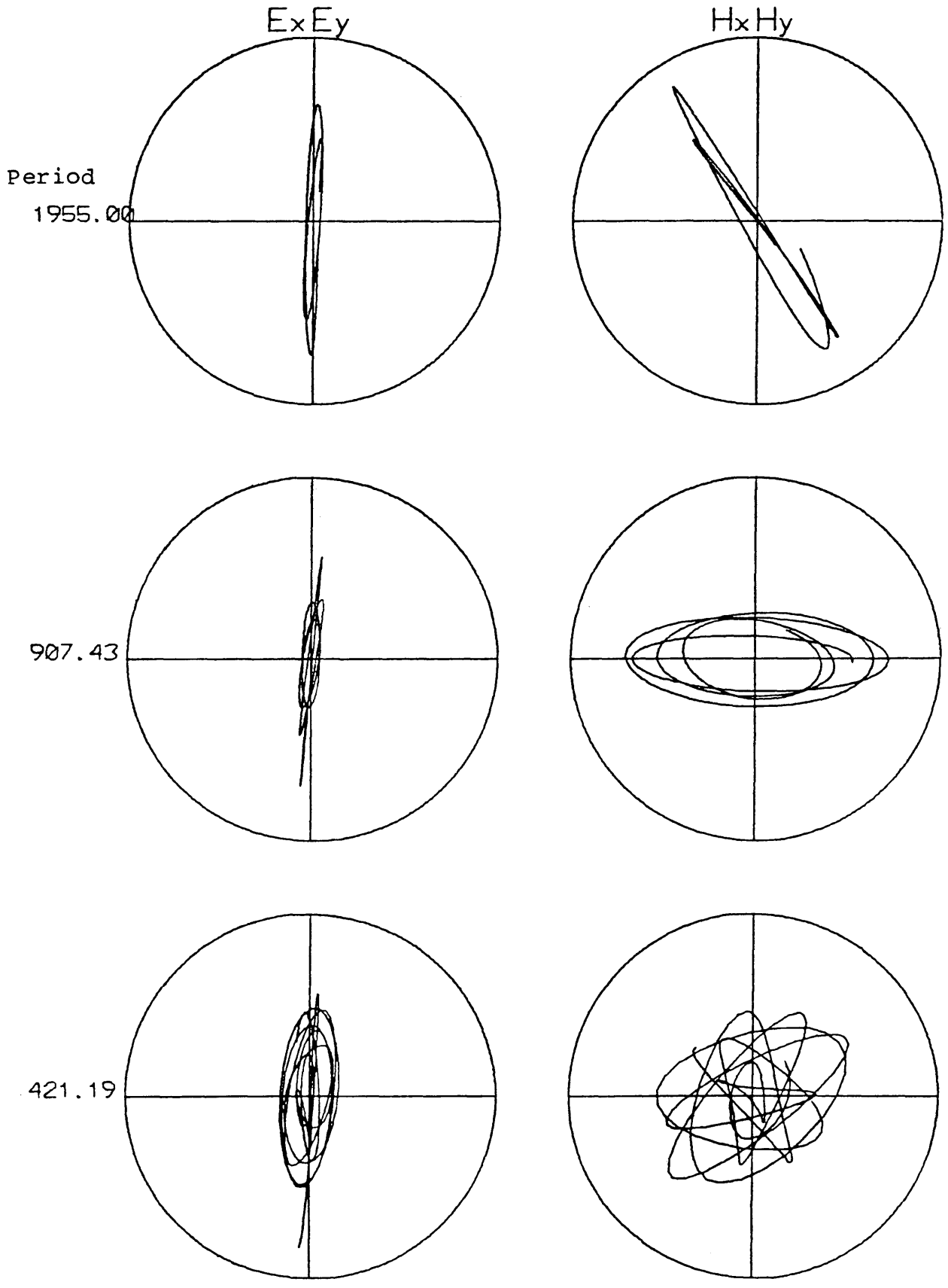

Station 1

BL1003

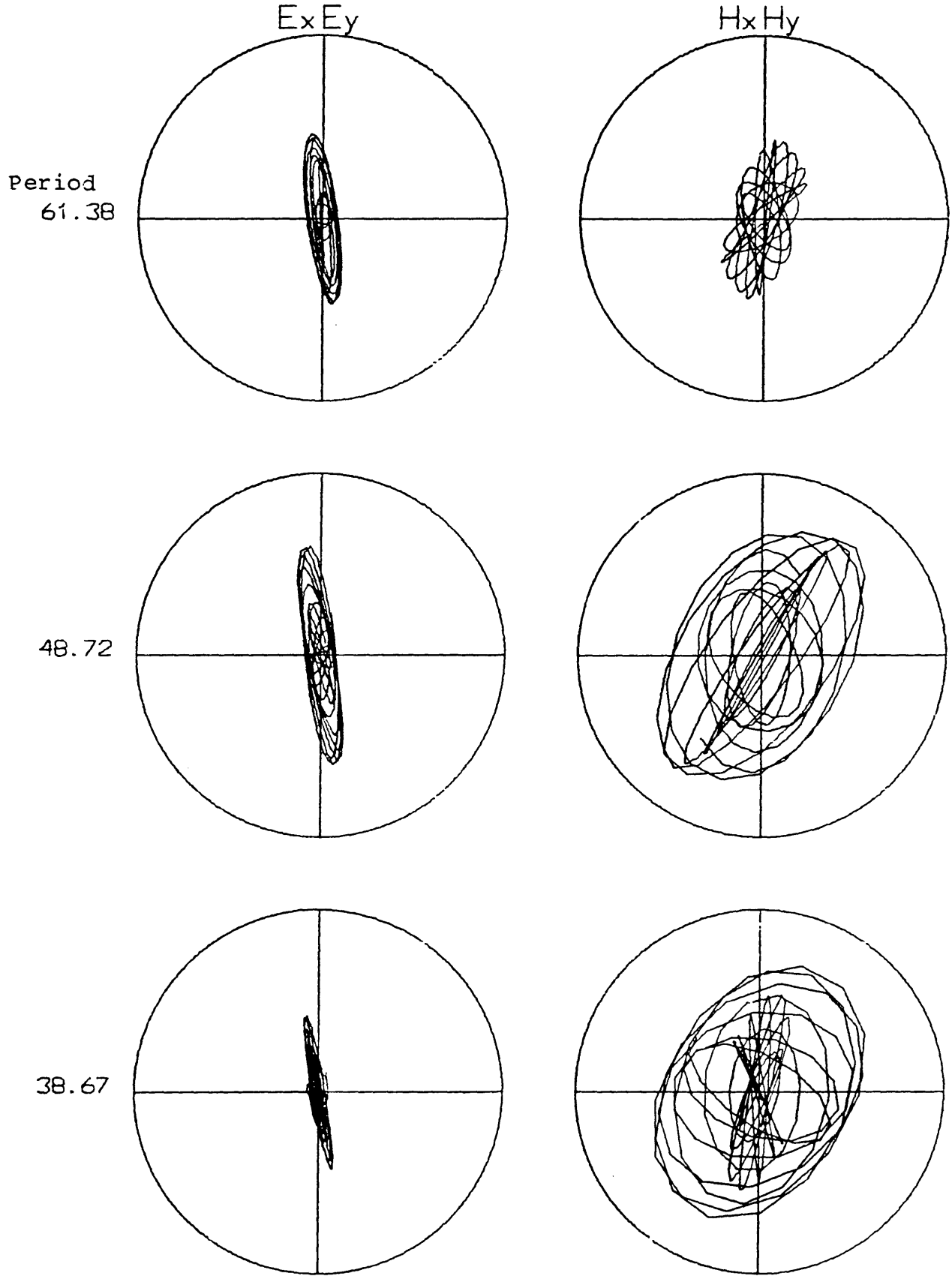

Station 1

BL2000

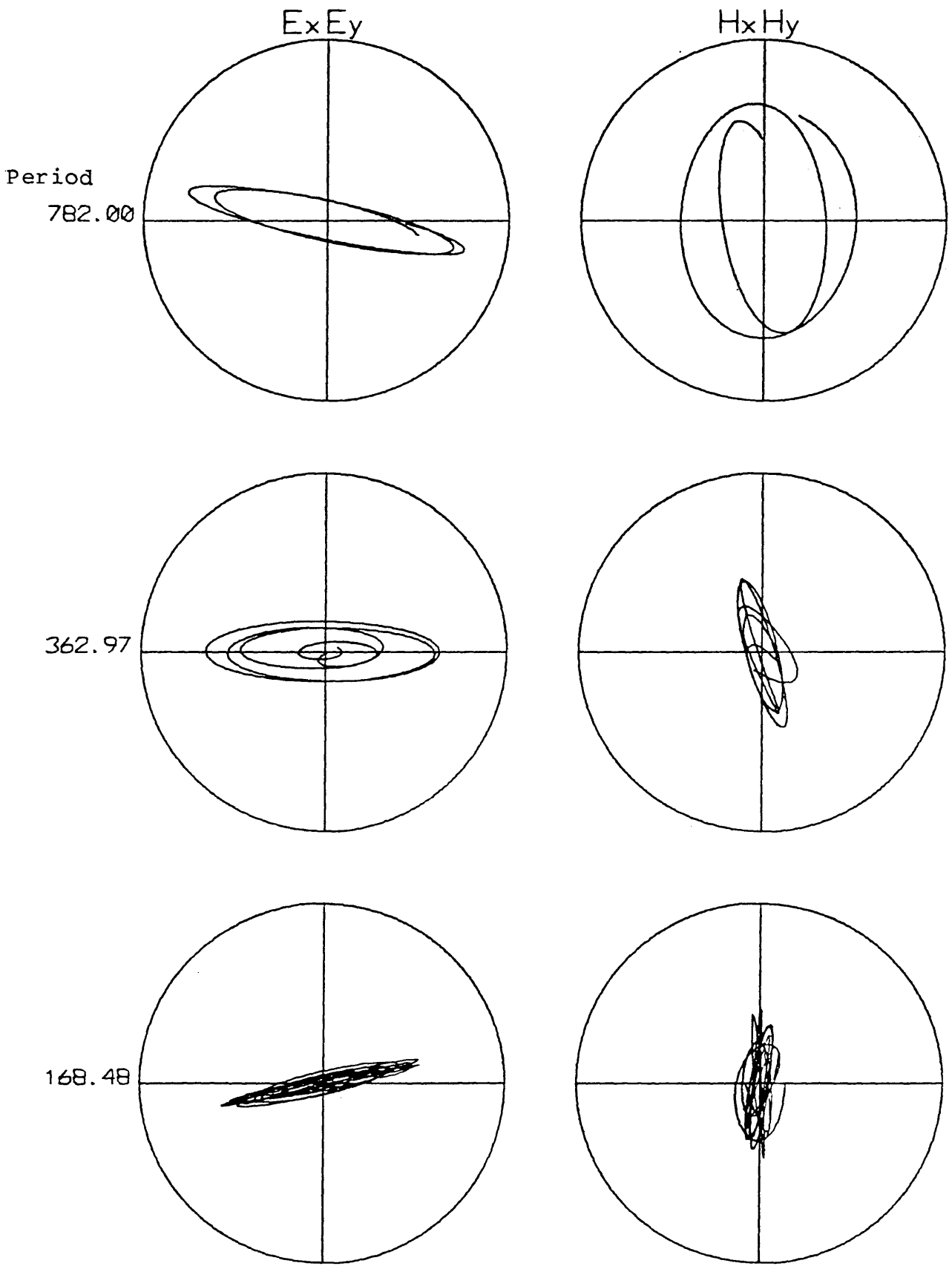

Station 2

BL3000

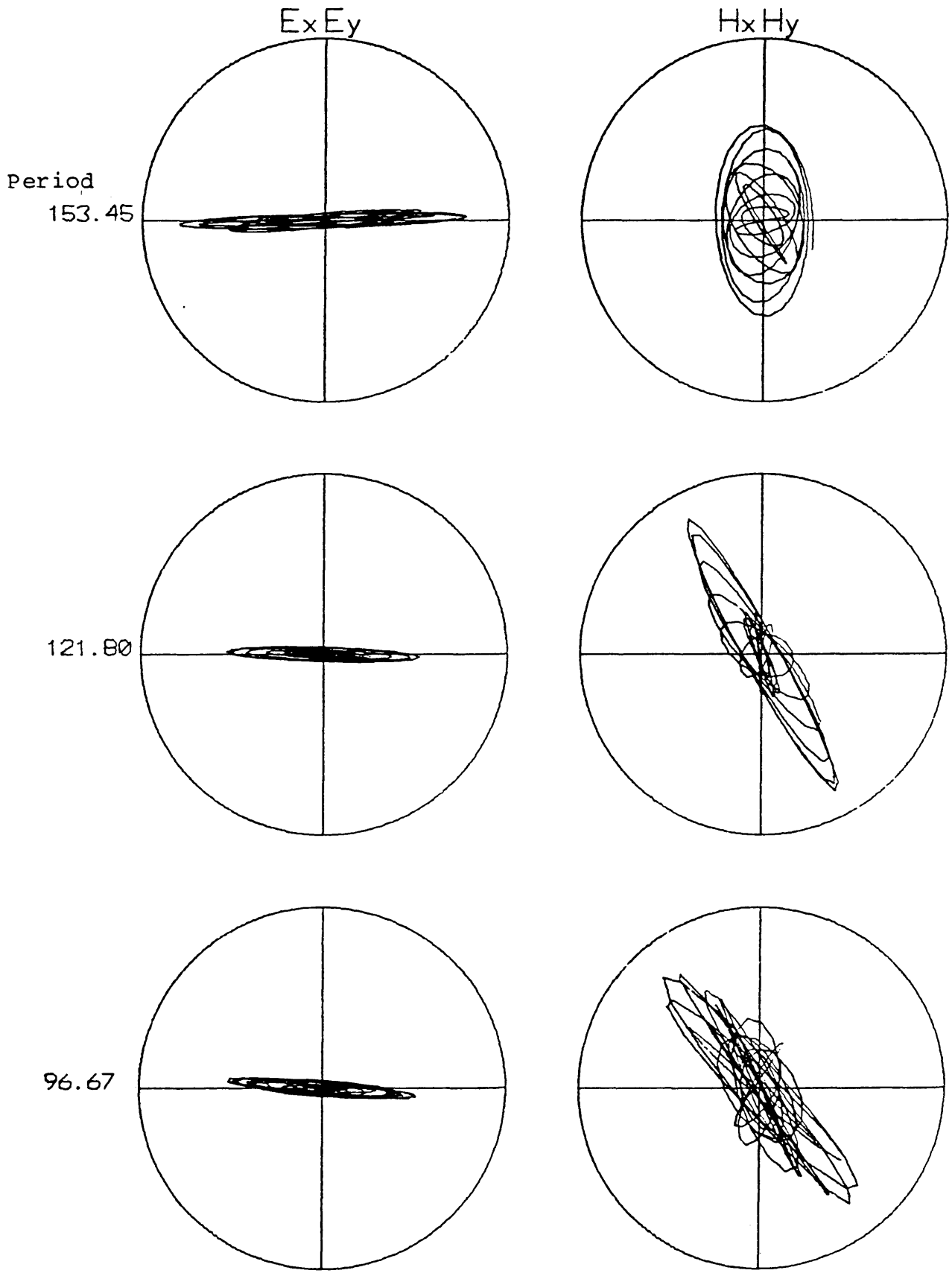

Station 3

BL4001

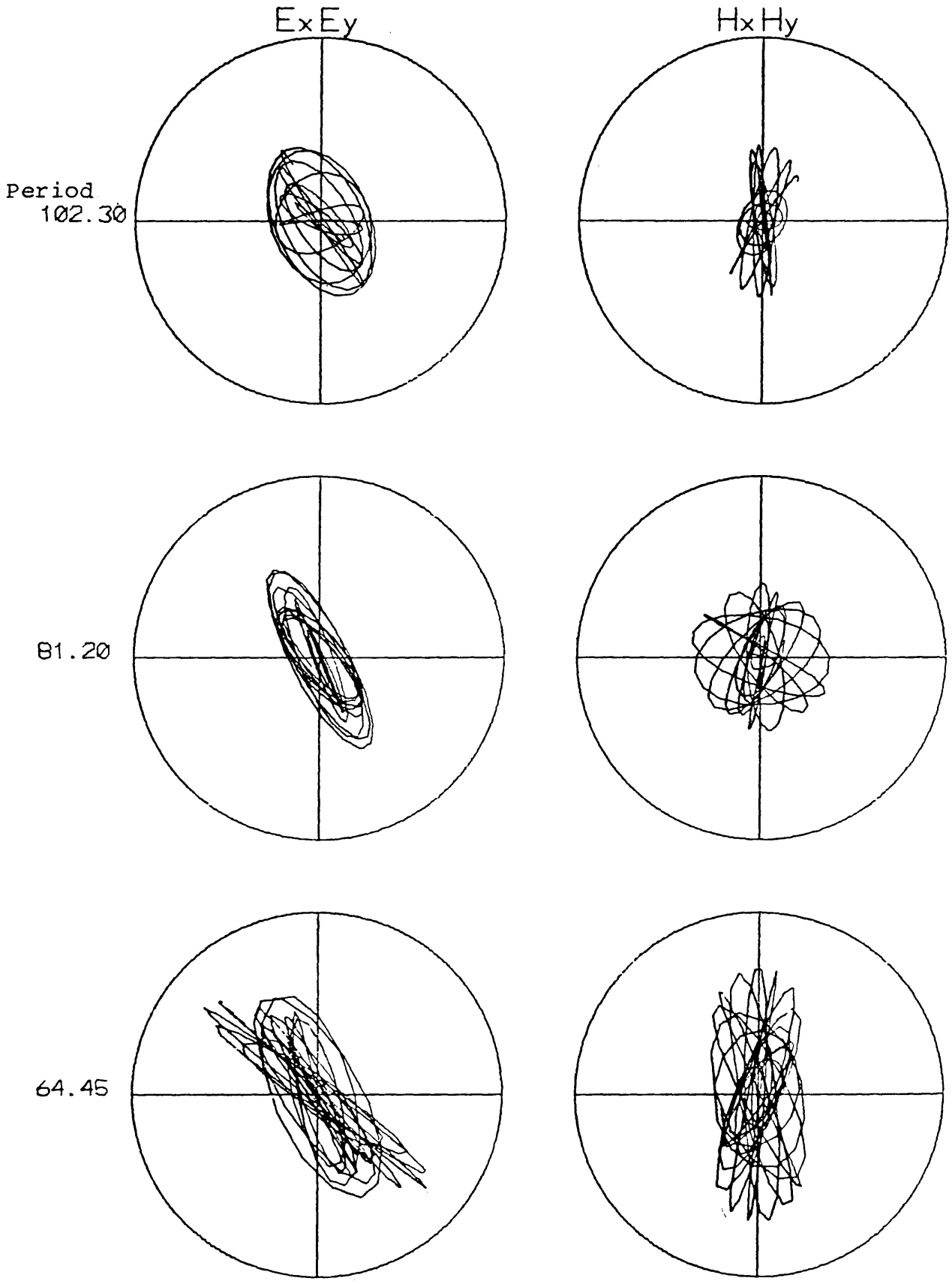

Station 4

BL4002

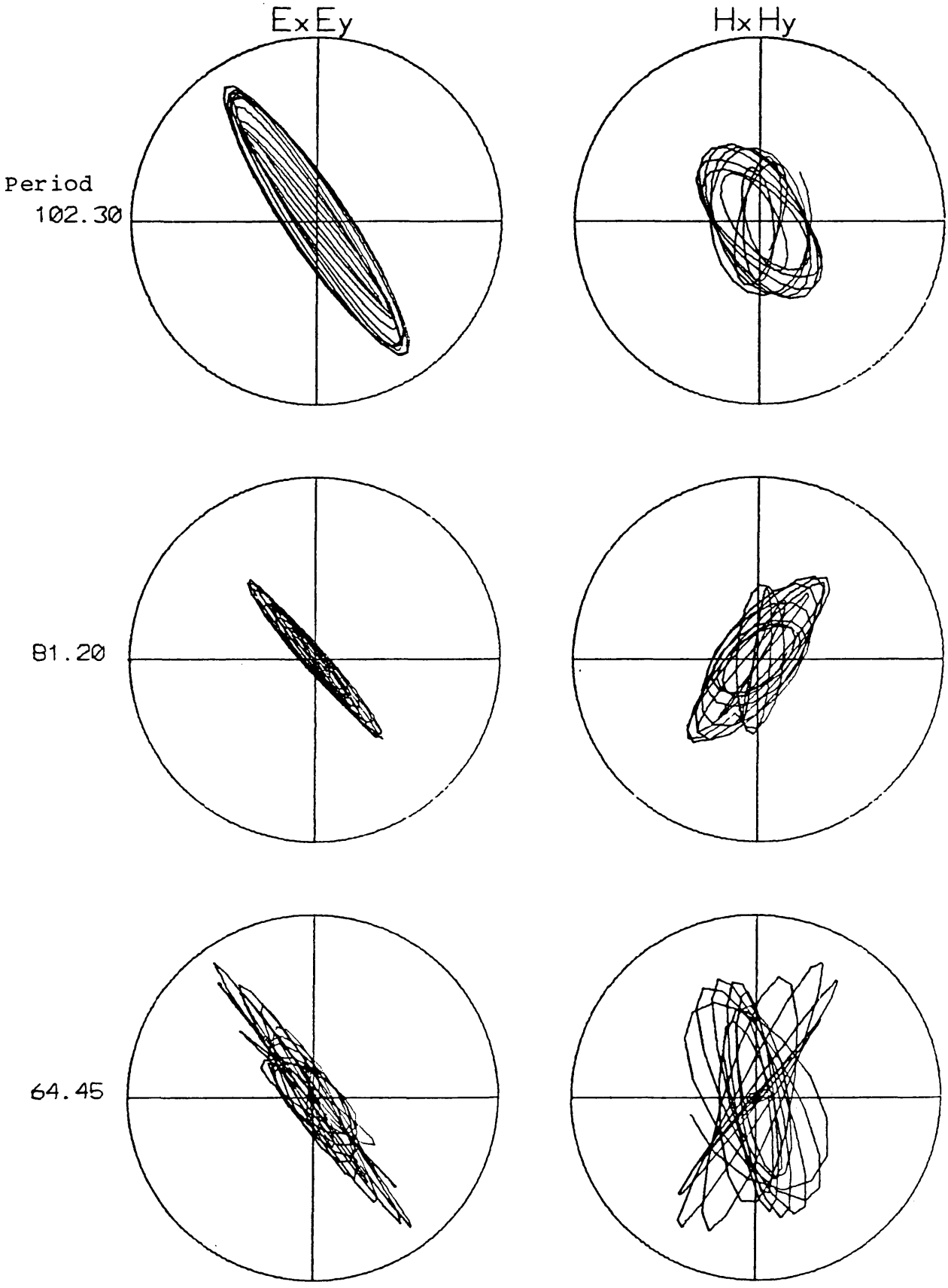

Station 4

BL5000

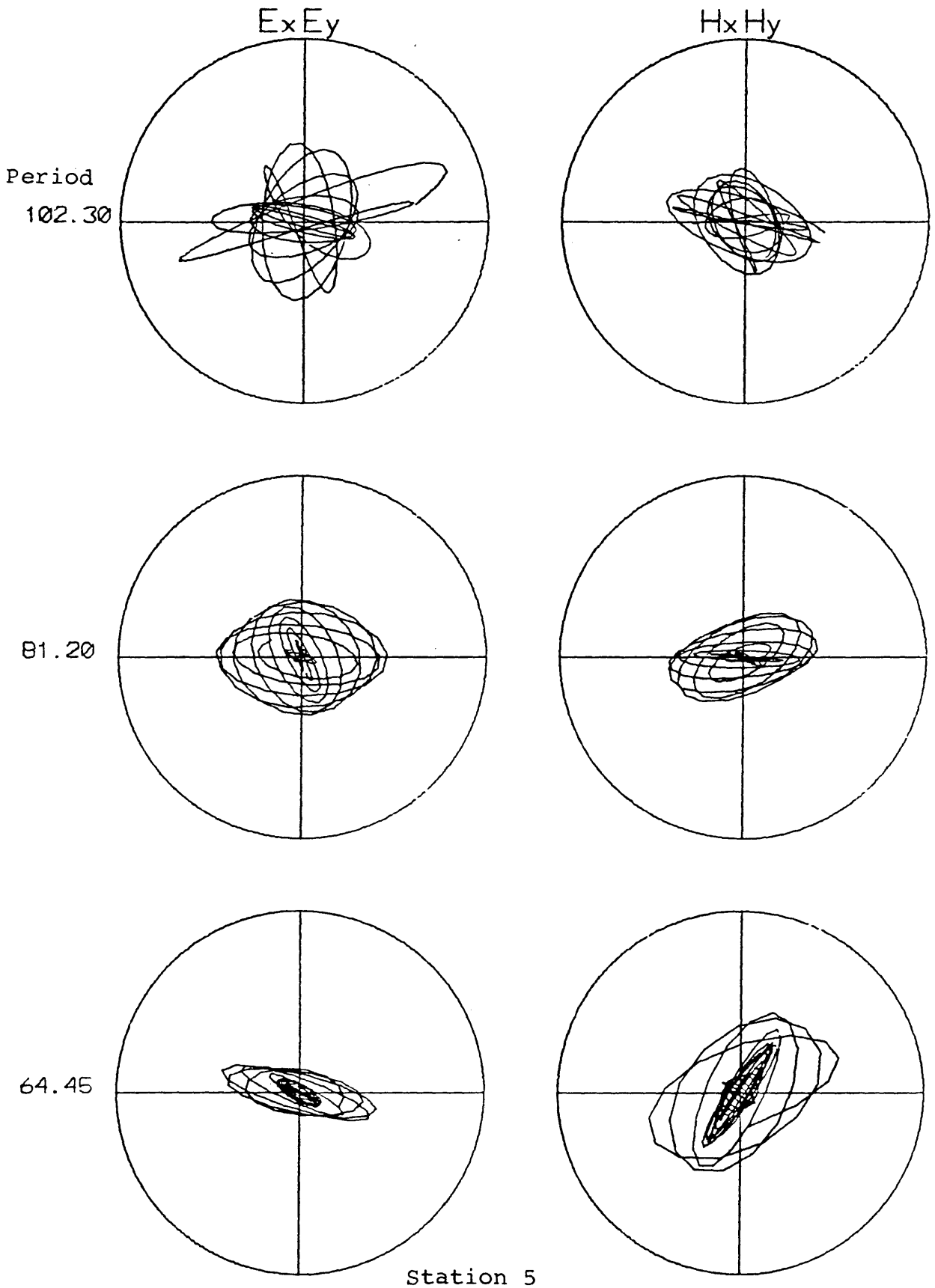

Station 5

BL6000

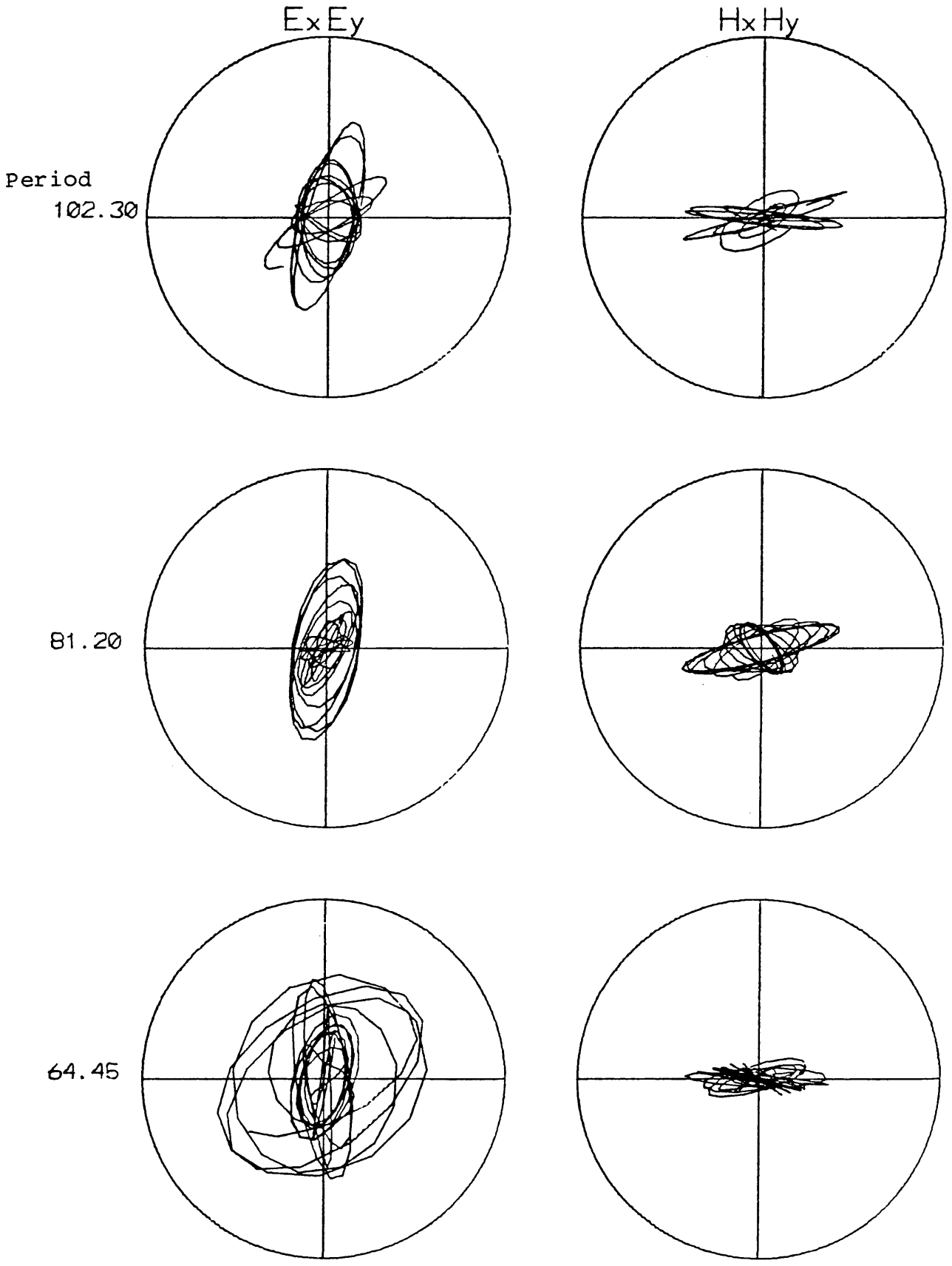

Station 6

BL7001

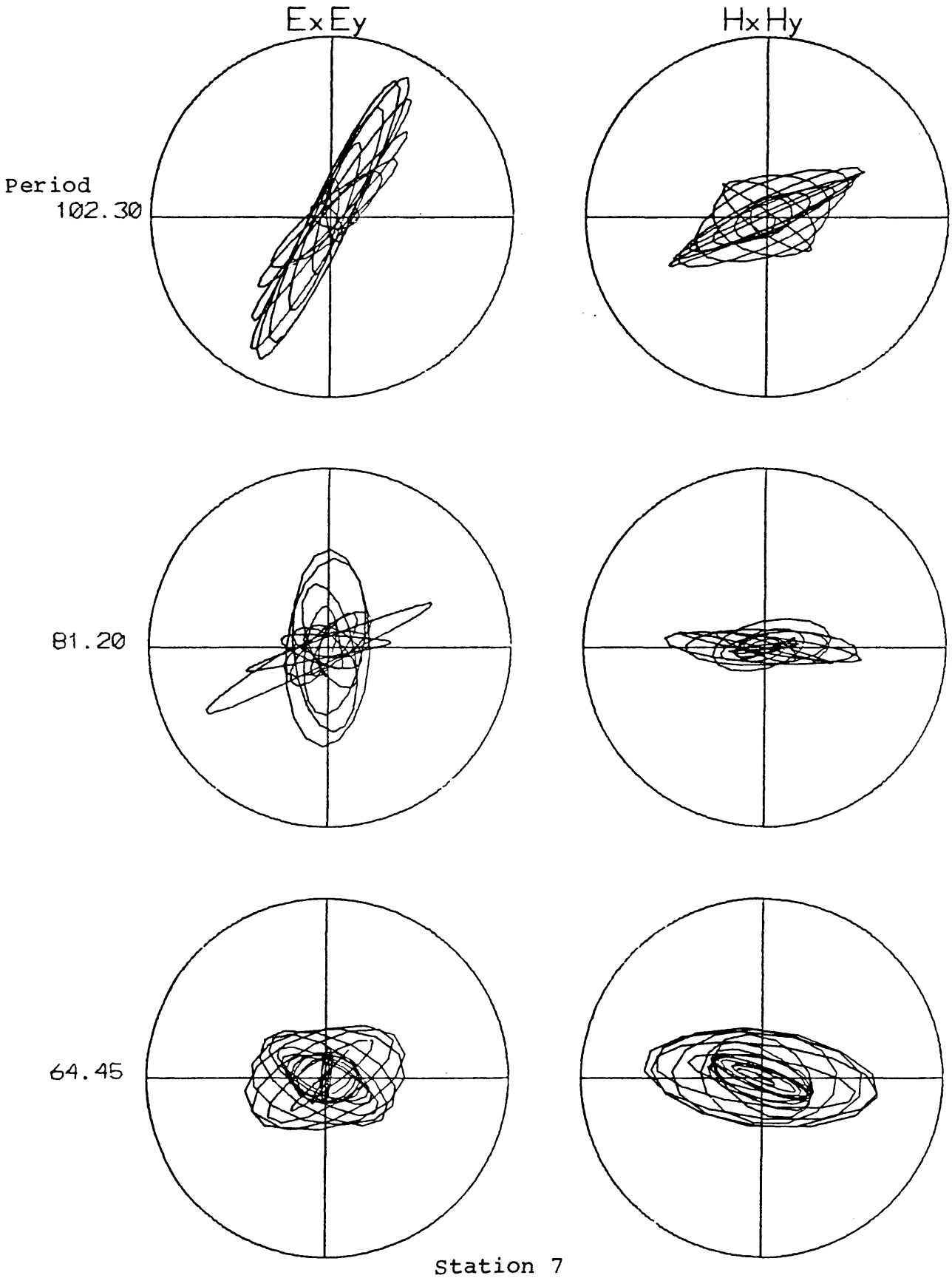

Station 7

BL8001

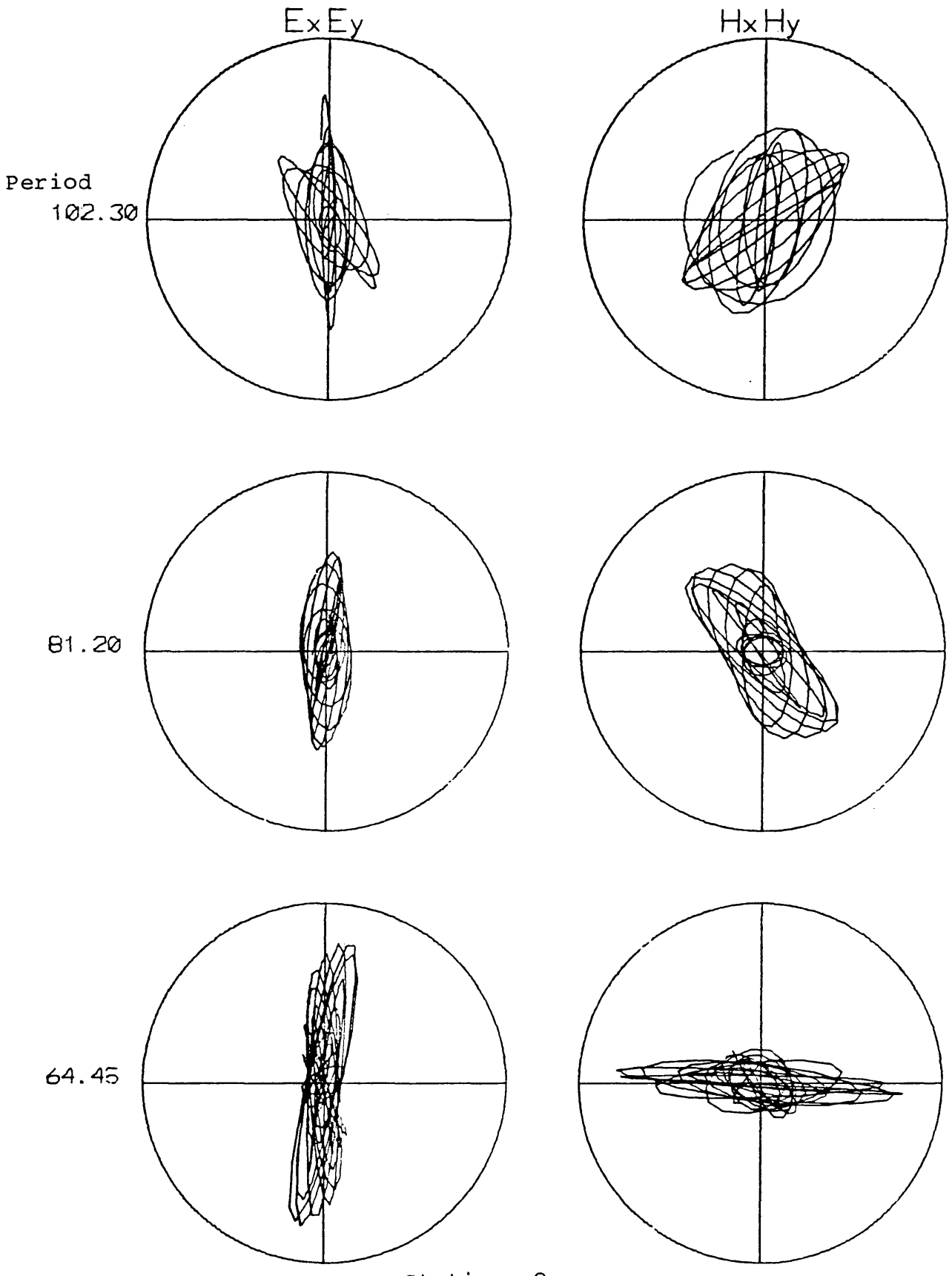

Station 8

BL9000

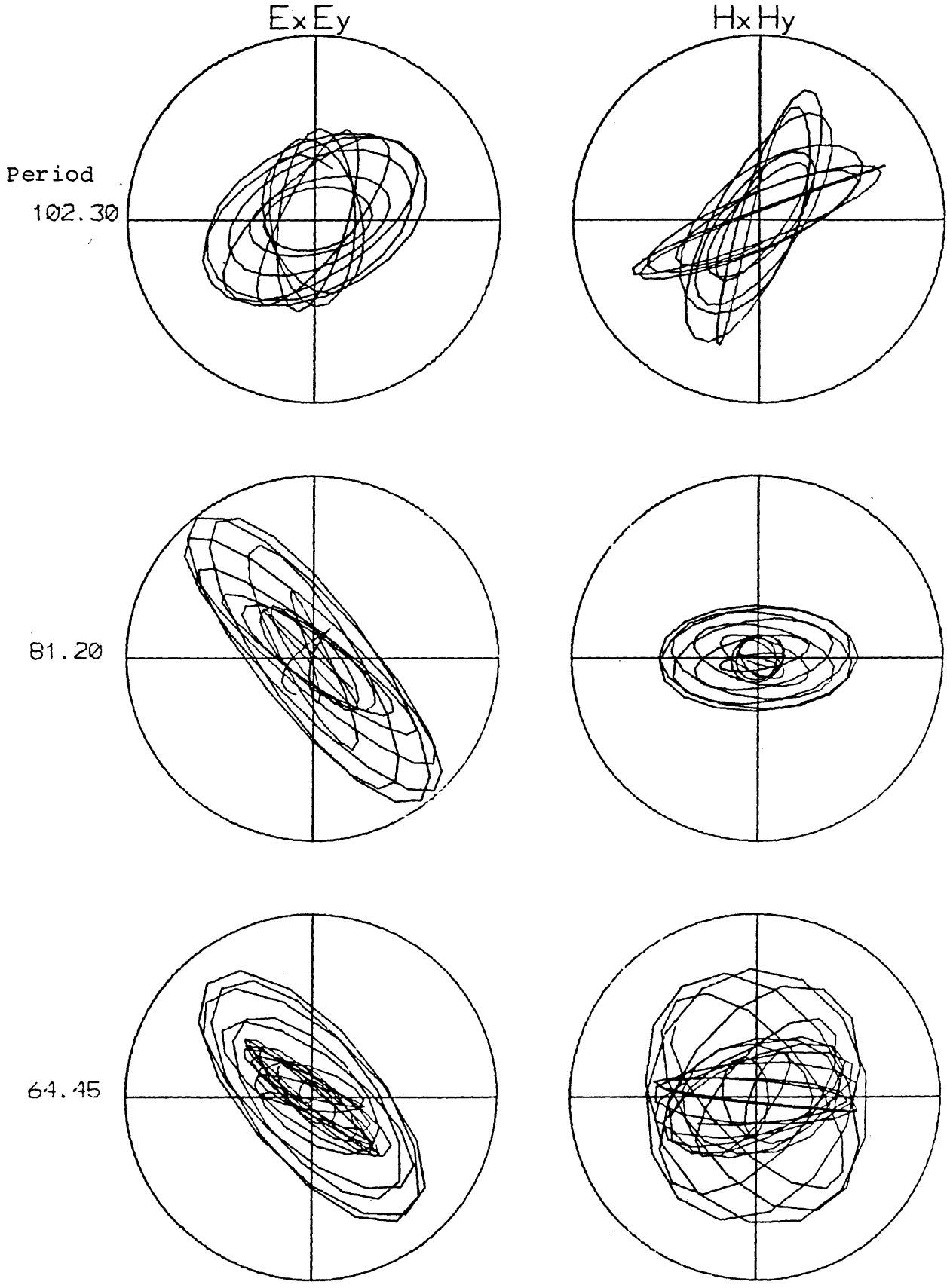

Station 9

BL1100

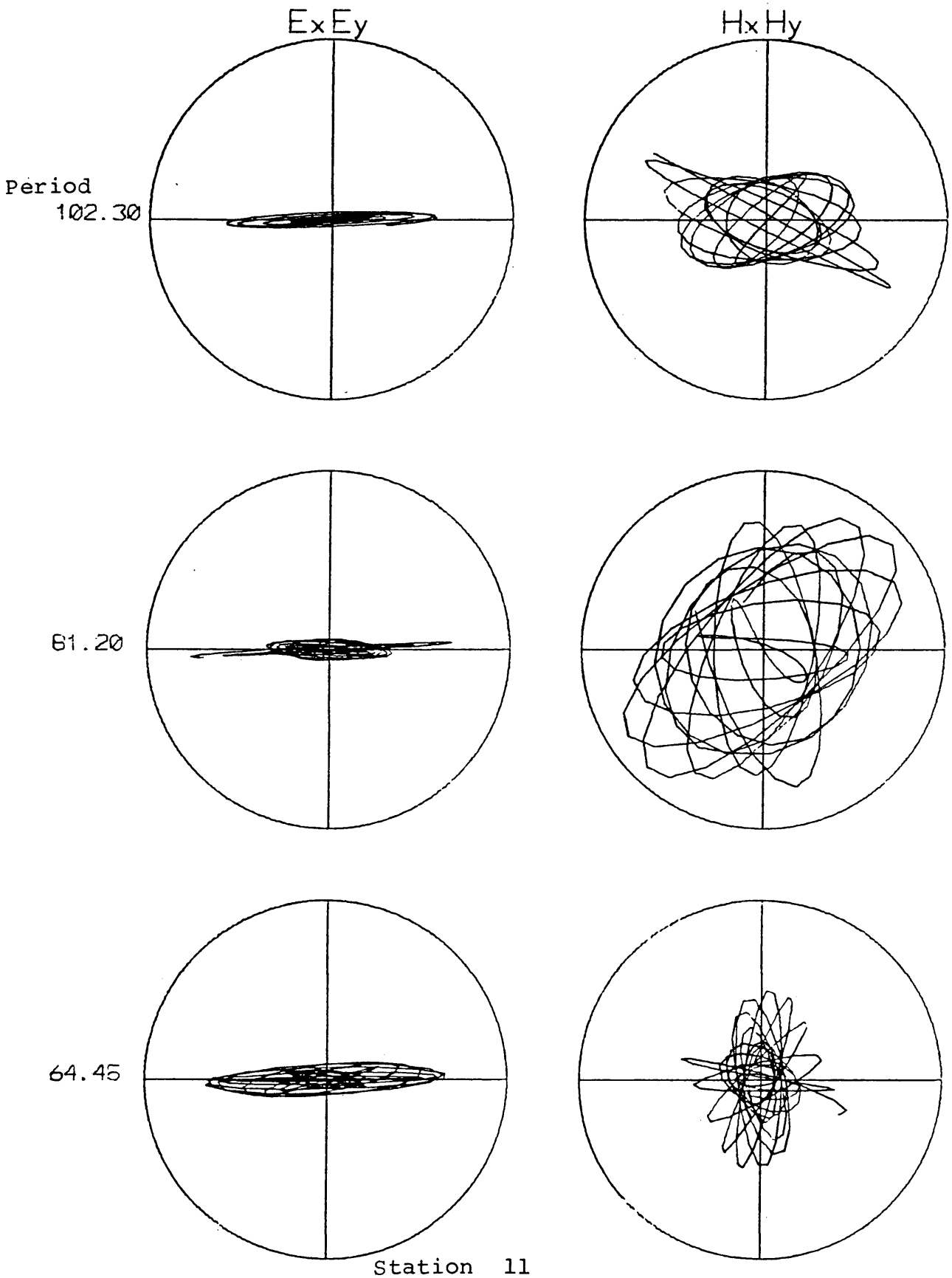

BL1200

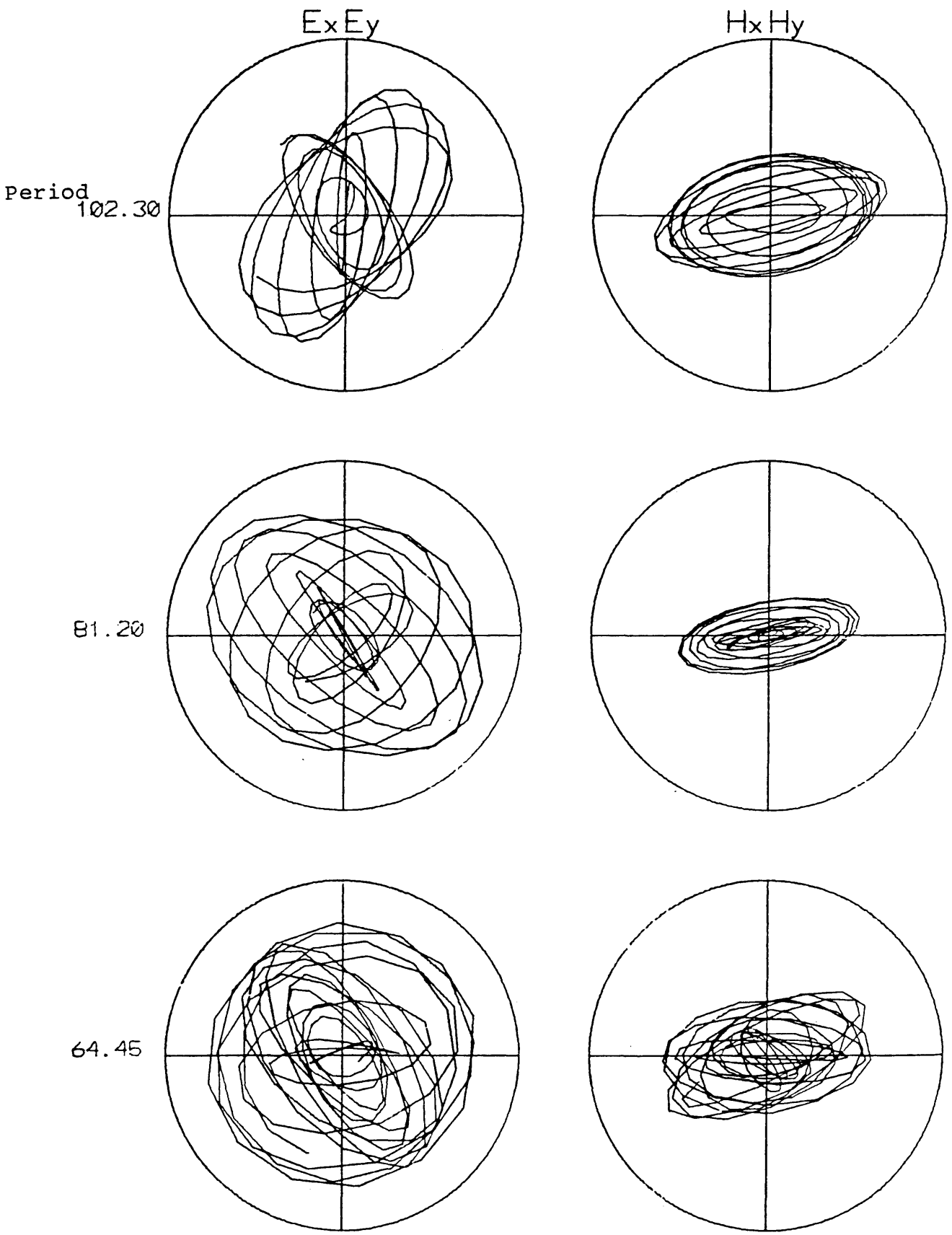

Station 12

BL1300

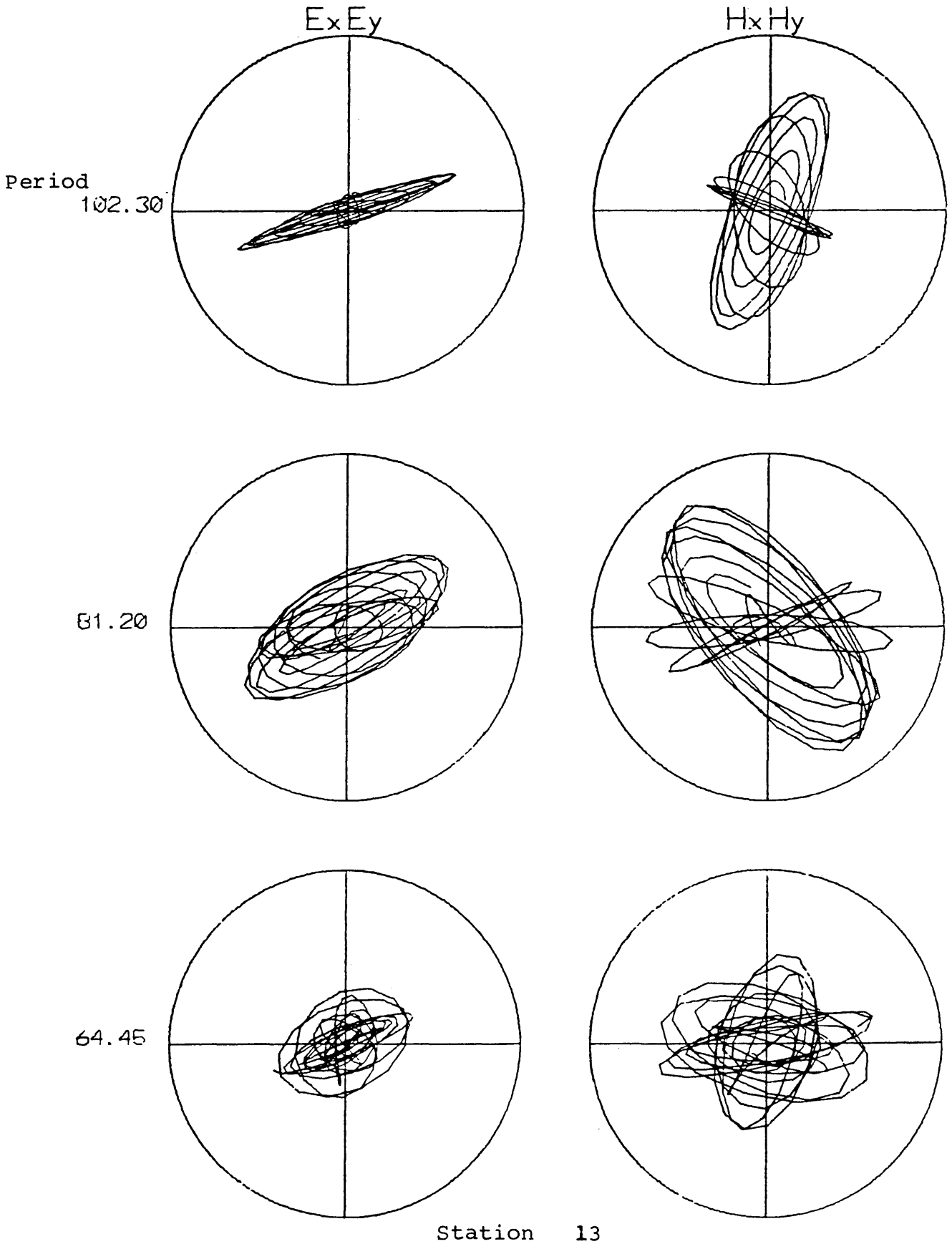

Station 13

BL1501

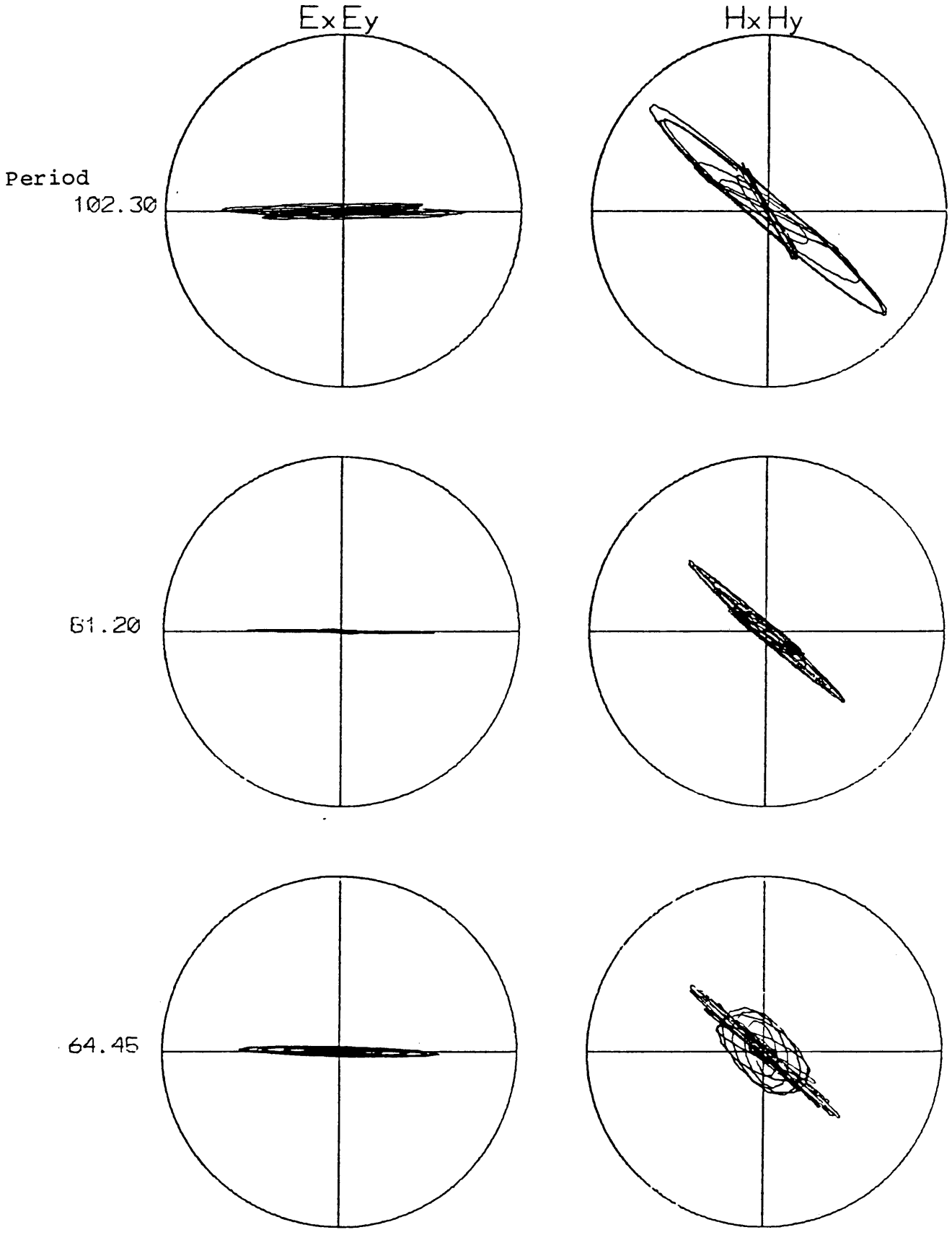

Station 15

BL1600

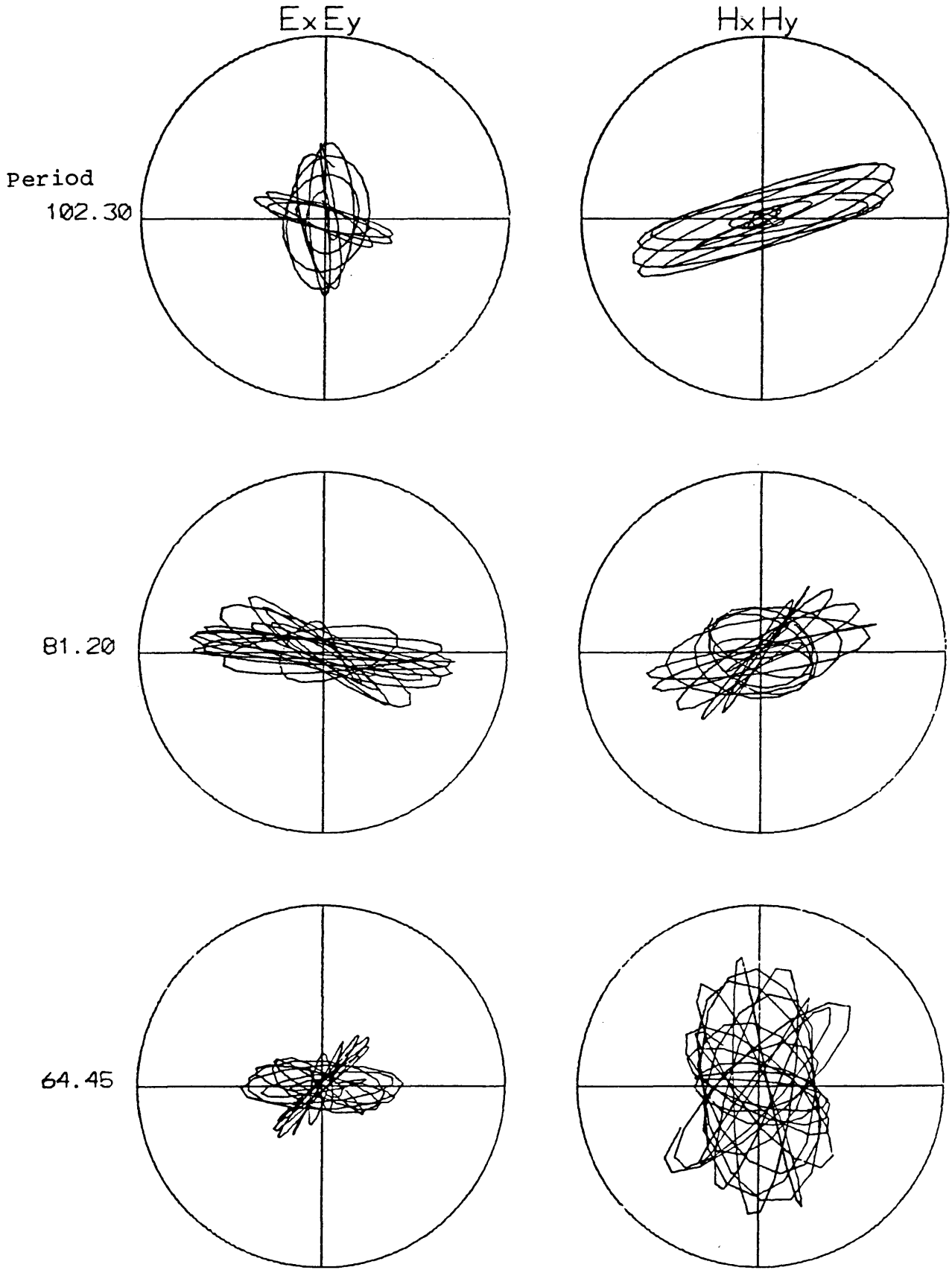

Station 16

BL1802

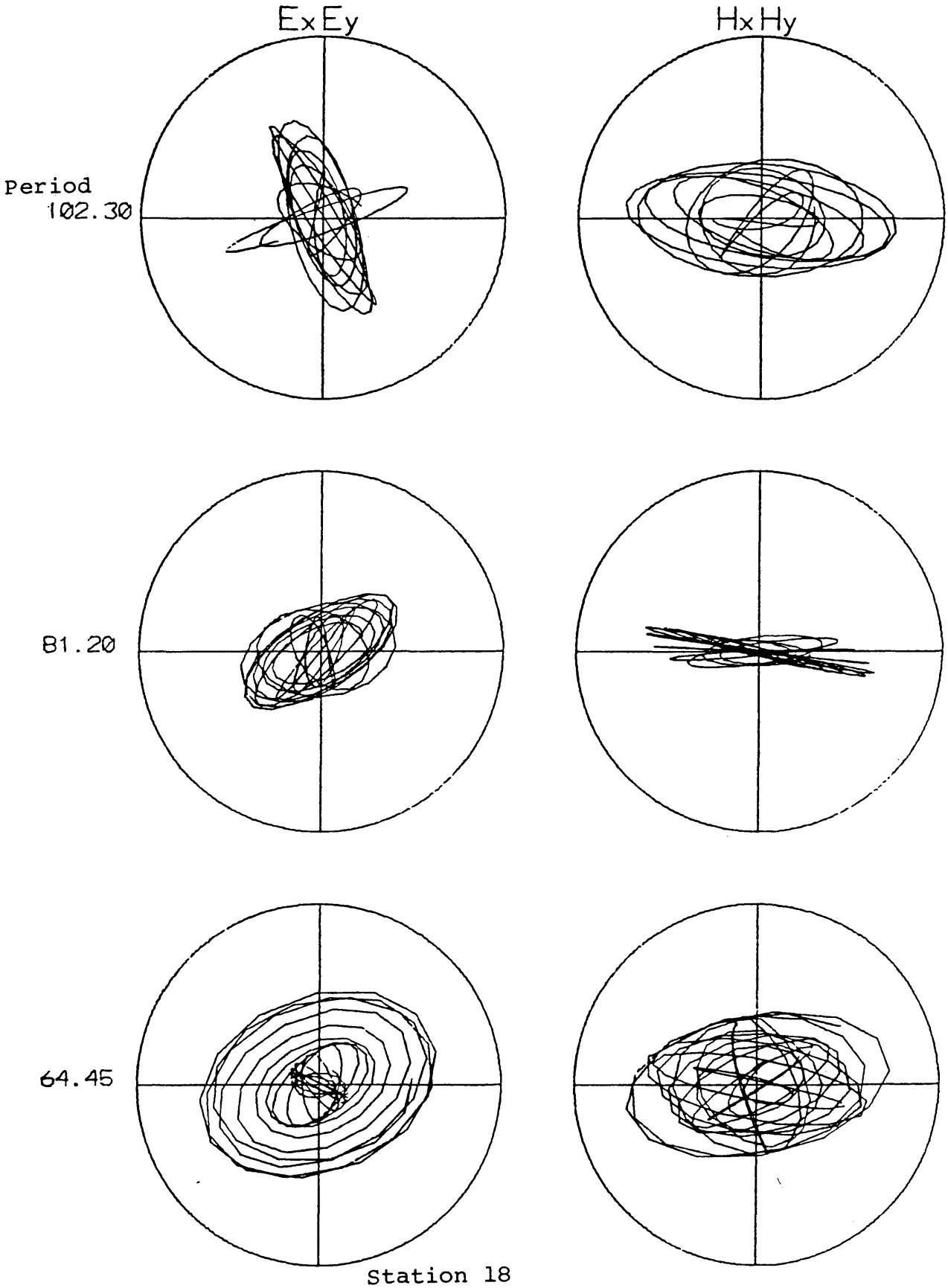

BL1900

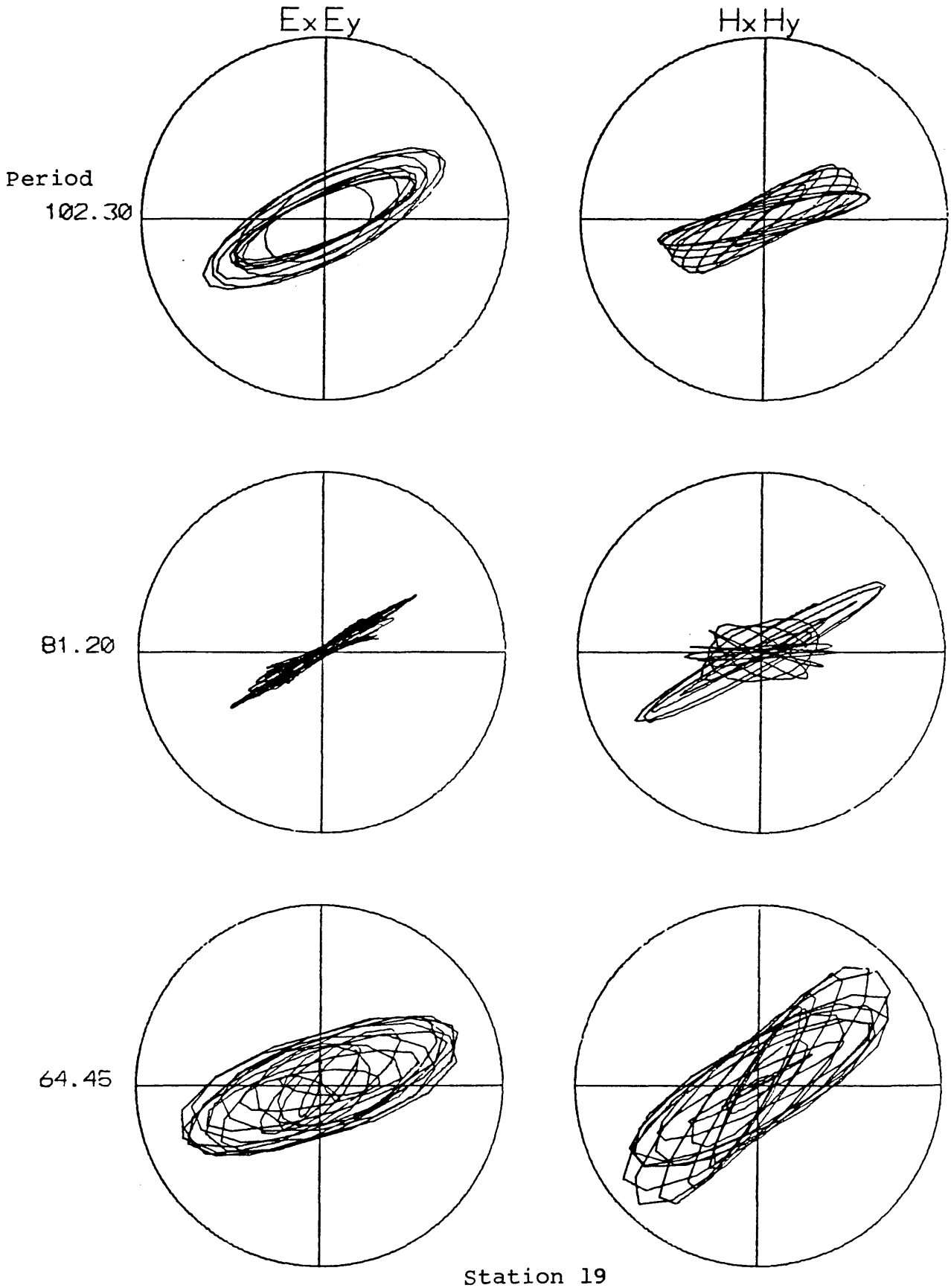

Station 19

APPENDIX C

```
C               PROGRAM TAKE2 PRECONDITIONS MT DATA AND PERFORMS AN
C       FFT ON IT.
C
C       XN = THE FUNCTION TO BE OPERATED ON
C       THE PROGRAM ONLY OPERATES ON ONE COMPONENT OF THE
C       DATA AT A TIME.
C
C       THE E FIELD DATA MUST BE IN MV PER KM AND THE
C       H FIELD DATA MUST BE IN GAMMAS.
C
C       THE DATA IS READ IN BY THE FUNCTION IN AND FORMATS
C       CAN BE MODIFIED TO SUIT THE USER IN THE FUNCTION.
C
C       THE PROGRAM USES AN IMSL LIBRARY PROGRAM TO PERFORM THE
C       FFT SO THE PROGRAM MUST BE LOADED WITH  ,LIB:IMSL
C       FOLLOWING THE PROGRAM NAME
C
C       THE FILTER IS A MODIFICATION OF THE PROGRAM BUT2
C       WRITTEN BY JAN FATTI
        DOUBLE PRECISION FILIN,FILOUT
        DIMENSION XN(2048),ID(6)
C*********************************
C       READ IN DATA
C*********************************
C
2000    WRITE(4,3)
3       FORMAT(1X,'NAME OF FILE ',$)
        READ(4,4) FILIN
4       FORMAT(A10)
        IF (FILIN.EQ.'EXIT') STOP
        OPEN(UNIT=1,ACCESS='SEQIN',MODE='BINARY',FILE=FILIN)
        READ(1) ID
        READ(1) K,AZH,DELTA T,NCOMP
        TYPE 99,K
        JIN=1
99      FORMAT(I)
C
C***************************
C   PREPARE OUTPUT FILE:
C***************************
        WRITE(4,222)
222     FORMAT(1X,'WHAT IS THE OUTPUT FILE NAME???   ',$)
        READ(4,4) FILOUT
        OPEN(UNIT=2,MODE='BINARY',PROTECTION=109,FILE=FILOUT)
        DIV=ALOG(2.)
        NUM=ALOG(FLOAT(K))/DIV
        ANUM=NUM
        NUM=2**(ANUM+1)
        TYPE 33, ID,NUM,K,DELTAT
33      FORMAT(1X,6A5,/2I,F)
        WRITE(2) ID,NUM,K,DELTAT
C*****************************************************************************
C       SUBTRACT INITIAL VALUE FROM DATA
C*************************************************************
C
        DO 20 KK=1,4
        Z=IN(XN,K,JIN)
        XN1=XN(1)
        DO 2 I=1,K
        XN(I)=XN(I)-XN1
```

```
2       CONTINUE
C*************************************************************************
C       REMOVE DRIFT FROM DATA
C*************************************************************************
C
        YMAX=XN(K)
        DO 12 I=1,K
        A=XN(I)
        RI=I
        XN(I)=A-YMAX/K*RI
12      CONTINUE
C*************************************************************************
C       BANDPASS FILTER DATA
C*************************************************************
C
        SAMINT=1.
        F1=5./FLOAT(K)
        F2=.25
        ORDER=2.
        CALL SMOOTH(XN,K)
        CALL BUT2 (ORDER,SAMINT,F1,F2,XN,K)
        CALL FFT(XN,K,NUM)
20      CONTINUE
C
C*************************************
C   WRITE OUT THE FILTERED OUTPUT:
C*************************************
        CLOSE(UNIT=2)
        GO TO 2000
        STOP
        END

        SUBROUTINE BUT2 (ORDER,SAMINT,F1,F2,PIN,NUMSAM)
       DIMENSION FMT(12), FIN(2000), FINS(2200), OUTS(2200),
     1             C(5), COEFF(5,7), FN(3), D(4), PIN(2000)
        EQUIVALENCE (FIN(1),FINS(5))
        DO 22 J=1,NUMSAM
22      FIN(J)=PIN(J)
       DATA MAXDAT/2000/, IN/1/, IOUT/2/
       IORDER = ORDER + .01
C
C*********************************************
C   CALCULATE THE BUTTERWORTH COEFFICIENTS:
C*********************************************
        JORDER=IORDER/2
       DO 100 IFRAC= 1,JORDER
        IFROC=IFRAC
       CALL KOEFF (IORDER,IFROC,F1,F2,SAMINT,C)
       COEFF(IFRAC,1) = 1./C(1)
       COEFF(IFRAC,2) =-2./C(1)
       COEFF(IFRAC,3) = 1./C(1)
       COEFF(IFRAC,4) = C(2)/C(1)
       COEFF(IFRAC,5) = C(3)/C(1)
       COEFF(IFRAC,6) = C(4)/C(1)
 100   COEFF(IFRAC,7) = C(5)/C(1)
C
C
C*********************************************************************
C   SET FIRST 4 INPUT & OUTPUT SAMPLES (IN ARRAYS FINS & OUTS)
C    EQUAL TO ZERO, & SET LAST 196 SAMPLES IN FINS TO ZERO:
```

```
C*********************************************************************
      DO 200 J = 1,4
      FINS(J) = 0.
 200  OUTS(J) = 0.
      DO 220 J = (NUMSAM+5),(NUMSAM+200)
 220  FINS(J) = 0.
C
C
C
      DO 500 IFRAC = 1,IORDER/2
      IF (IFRAC.EQ.1) GO TO 280
C
C*******************************
C   SET INPUT = PREVIOUS OUTPUT:
C*******************************
      DO 250 K = 5,(NUMSAM+200)
 250  FINS(K) = OUTS(K)
C
C*******************************
C   CHOOSE THE APPROPRIATE COEFFICIENTS:
C*******************************
 280  DO 300 L=1,3
 300  FN(L) = COEFF(IFRAC,L)
      DO 330 L = 1,4
 330  D(L) = COEFF(IFRAC,(L+3))
C
C*********************************************************************
C   FILTER ARRAY FINS RECURSIVELY WITH ONE POLYNOMIAL FRACTION TO
C    GET ARRAY OUTS:
C*********************************************************************
      DO 400 ISAM = 5,(NUMSAM+200)
      FNUMIN = FN(1)*FINS(ISAM)+FN(2)*FINS(ISAM-2) + FN(3)*FINS(ISAM-4)
      DENOUT = 0.
      DO 360 J = 1,4
      AA = D(J)*OUTS(ISAM-J)
 360  DENOUT = DENOUT+AA
 400  OUTS(ISAM) = FNUMIN - DENOUT
 500  CONTINUE
C
C
C
C*********************************************
C   REVERSE ARRAY OUTS AND PUT IT INTO ARRAY FIN:
C*********************************************
      DO 550 ISAM = 1,(NUMSAM+196)
 550  FIN(ISAM) = OUTS(NUMSAM+201-ISAM)
C
C
C
C*****************************************************
C   SET THE FIRST 4 INPUT & OUTPUT SAMPLES EQUAL TO ZERO:
C*****************************************************
      DO 570 J = 1,4
      FINS(J) = 0.
 570  OUTS(J) = 0.
C
C
C
      DO 1000 IFRAC = 1,IORDER/2
      IF (IFRAC.EQ.1) GO TO 600
```

```
C
C*******************************
C   SET INPUT = PREVIOUS OUTPUT:
C*******************************
       DO 580 K = 5,(NUMSAM+200)
 580   FINS(K) = OUTS(K)
C
C************************************
C   CHOOSE THE APPROPRIATE COEFFICIENTS:
C************************************
 600   DO 620 L = 1,3
 620   FN(L) = COEFF(IFRAC,L)
       DO 640 L = 1,4
 640   D(L) = COEFF(IFRAC,L+3)
C
C*****************************************************************
C   FILTER ARRAY FINS (WHICH IS THE OUTPUT OF PREVIOUS FILTER,
C    REVERSED) RECURSIVELY WITH ONE POLYNOMIAL FRACTION TO GET
C    ARRAY OUTS:
C*****************************************************************
       DO 800 ISAM = 5,(NUMSAM+200)
       FNUMIN = FN(1)*FINS(ISAM) + FN(2)*FINS(ISAM-2)+FN(3)*FINS(ISAM-4)
       DENOUT = 0.
       DO 700 J = 1,4
       AA = D(J)*OUTS(ISAM-J)
 700   DENOUT = DENOUT+AA
 800   OUTS(ISAM) = FNUMIN - DENOUT
 1000  CONTINUE
C
C
C*****************************************************************
C   REVERSE ARRAY OUTS AND PUT IT INTO ARRAY PIN.   THE FILTERED
C    TIME SERIES IS THEN THE RIGHT WAY ROUND  (IN ARRAY PIN):
C*****************************************************************
       DO 1100 ISAM = 1,NUMSAM
 1100  PIN(ISAM) = OUTS(NUMSAM+201-ISAM)
C
C
        RETURN
       END

        SUBROUTINE KOEFF (N,M,F1,F2,DELT,C)
C*****************************************************************
C
C   THIS SUBROUTINE CALCULATES THE 5 BUTTERWORTH DENOMINATER
C   COEFFICIENTS.   A CORRECTION IS MADE FOR THE ERROR INTRODUCED
C   BY THE BILINEAR TRANSFORMATION.
C
C
C   DEFINITION OF ARGUMENTS:
C       N    = ORDER OF BUTTERWORTH FILTER  (MUST BE EVEN)  - INPUT
C       M    = POLYNOMIAL FRACTION #  - INPUT
C       F1   = LOWER CUTOFF FREQ., IN HZ.  - INPUT
C       F2   = UPPER CUTOFF FREQ., IN HZ.  - INPUT
C       DELT = SAMPLE INTERVAL, IN SEC.  - INPUT
C       C    = ARRAY CONTAINING THE 5 COEFFICIENTS  - OUTPUT
C
C
C                       JORGE PARRA
C                       APRIL, 1972
```

```
C
C***********************************************************************
C
      DIMENSION C(5)
      PI=3.1415927
      F2A=SIN(PI*F2*DELT)/COS(PI*F2*DELT)
      F2A=F2A/(PI*DELT)
      F1A=SIN(PI*F1*DELT)/COS(PI*F1*DELT)
      F1A=F1A/(PI*DELT)
      W0=2.*PI*SQRT(F1A*F2A)
      WC=2.*PI*(F2A-F1A)
      Q=W0/WC
      DEL=WC*DELT
      U=PI/(2.*N)
      K=N+2*M-1
      B21=-2.*COS(U*K)
      X=2./DEL
      Y=X*X
      Z=X*B21
      U=2.*Q*Q+1.
      V=B21*Q*Q/X
      W1=Q**4
      W=W1/Y
      C(5)=Y-Z+U-V+W
      C(4)=-4.*Y+2.*Z-2.*V+4.*W
      C(3)=6.*Y-2.*U+6.*W
      C(2)=-4.*Y-2.*Z+2.*V+4.*W
      C(1)=Y+Z+U+V+W
      RETURN
      END

C/\/\/\/\/\/\/\/\/\/\/\/\/\/\/\/\/\/\/\/\/\/\/\/\/\/\/\/\/\/\/\/\/\/\/\/

C     THIS SUBROUTINE SMOOTHES OUT THE EFFECT OF  TRUNCATION

C     IT FITS A  COSINE SHIFTED UP BY ONE TO THE DATA IN ORDER TO
C             SMOOTH OUT THE TRUNCATION EFFECTS.

C\/\/\/\/\/\/\/\/\/\/\/\/\/\/\/\/\/\/\/\/\/\/\/\/\/\/\/\/\/\/\/\/\/\/\/\

      SUBROUTINE SMOOTH(PHEE,K)
      DIMENSION PHEE(K)
      XINCR=2.*3.14159/FLOAT(K+1)
      DO 20 I=1,K
      XINC=-3.14159+XINCR*FLOAT(I)
      FACTOR=(COS(XINC)+1.)/2.
      PHEE(I)=FACTOR*PHEE(I)
20    CONTINUE
      RETURN
      END
      SUBROUTINE FFT(XN,K,NUM)
      COMPLEX GAMN
      DIMENSION XN(K),IWK(100)
      DIV=ALOG(2.)
      NUM=ALOG(FLOAT(K))/DIV
      ANUM=NUM
      NUM=2**(ANUM+1)
      NZER=(NUM-K)
      DO 10 J=1,NZER
      XN(K+J)=0.
```

```
10      CONTINUE
        CALL FFTR(XN,GAMN,NUM,IWK)
        WRITE(2) XN
        RETURN
        END
        FUNCTION IN(X,N,JIN)
        DIMENSION X(N)
        READ(JIN) X
        IN=K
        RETURN
        END
```

```
C       PROGRAM COEFF CALCULATES COEFFICIENTS
C       FOR A RECURSIVE BUTTERWORTH FILTER.
C
C       THE FILTER PROGRAM IS CALLED 3FREQ
        DIMENSION C(5)
        OPEN(UNIT=1,MODE='BINARY',FILE='COEFF.DAT')
        TYPE 10
10      FORMAT(' INPUT SAMPLING RATE '$)
        ACCEPT 11,DELT
11      FORMAT(2F)
        TYPE 20
20      FORMAT(' INPUT HIGH,LOW FREQ. ')
        ACCEPT 11,HIGH,XLOW
        TYPE 30
30      FORMAT(' INPUT NO. OF FREQS. WANTED '$)
        ACCEPT 31,NUM
31      FORMAT(I)
        XINC=(ALOG10(HIGH)-ALOG10(XLOW))/(FLOAT(NUM))
        WRITE (1) NUM
        DO 1 J=1,NUM
        CFREQ=10**(ALOG10(HIGH)-XINC*(FLOAT(J)))
        F2=CFREQ+CFREQ/10.
        F1=CFREQ-CFREQ/10.
        CALL KOEFF(2,1,F1,F2,DELT,C)
        CFREQ=1./CFREQ
        WRITE(1) CFREQ,C
1       CONTINUE
        CLOSE(UNIT=1)
        STOP
        END
        SUBROUTINE KOEFF (N,M,F1,F2,DELT,C)
C*****************************************************************
C
C   THIS SUBROUTINE CALCULATES THE 5 BUTTERWORTH DENOMINATER
C   COEFFICIENTS.   A CORRECTION IS MADE FOR THE ERROR INTRODUCED
C   BY THE BILINEAR TRANSFORMATION.
C
C
C   DEFINITION OF ARGUMENTS:
C       N    = ORDER OF BUTTERWORTH FILTER  (MUST BE EVEN)  - INPUT
C       M    = POLYNOMIAL FRACTION #  - INPUT
C       F1   = LOWER CUTOFF FREQ., IN HZ.  - INPUT
C       F2   = UPPER CUTOFF FREQ., IN HZ.  - INPUT
C       DELT = SAMPLE INTERVAL, IN SEC.  - INPUT
C       C    = ARRAY CONTAINING THE 5 COEFFICIENTS  - OUTPUT
C
C
C                       JORGE PARRA
C                       APRIL, 1972
C
C*****************************************************************
C
        DIMENSION C(5)
        PI=3.1415927
        F2A=SIN(PI*F2*DELT)/COS(PI*F2*DELT)
        F2A=F2A/(PI*DELT)
        F1A=SIN(PI*F1*DELT)/COS(PI*F1*DELT)
        F1A=F1A/(PI*DELT)
        W0=2.*PI*SQRT(F1A*F2A)
        WC=2.*PI*(F2A-F1A)
```

```
Q=W0/WC
DEL=WC*DELT
U=PI/(2.*N)
K=N+2*M-1
B21=-2.*COS(U*K)
X=2./DEL
Y=X*X
Z=X*B21
U=2.*Q*Q+1.
V=B21*Q*Q/X
W1=Q**4
W=W1/Y
C(5)=Y-Z+U-V+W
C(4)=-4.*Y+2.*Z-2.*V+4.*W
C(3)=6.*Y-2.*U+6.*W
C(2)=-4.*Y-2.*Z+2.*V+4.*W
C(1)=Y+Z+U+V+W
RETURN
END
```

```
C       PROGRAM 3FREQ  FILTERS A SET OF MT DATA WITH A NARROW
CC      BANDPASS BUTTERWORTH FILTER.
C       THE FILTER IS A MODIFICATION OF THE PROGRAM BUT2
C       WRITTEN BY JAN FATTI
C
C       THE FIELDS ARE READ IN IN THE FUNCTION IN AND THE FORMAT
C       THE DATA IS TO BE READ IN  SHOULD BE MODIFIED THERE
        DOUBLE PRECISION FILIN,FILOUT
        DIMENSION XN(2048),ID(6)
C*********************************
C       READ IN DATA
C*********************************
C
2000    WRITE(4,3)
3       FORMAT(1X,'NAME OF FILE ',$)
        READ(4,4) FILIN
4       FORMAT(A10)
        IF (FILIN.EQ.'EXIT') STOP
        OPEN(UNIT=1,ACCESS='SEQIN',MODE='BINARY',FILE=FILIN)
        READ(1) ID
        READ(1) K,AZH,DELTA T,NCOMP
        TYPE 22, AZH,DELTA T,NCOMP
22      FORMAT(2F,I)
C
C*************************************************************************
C       SUBTRACT INITIAL VALUE FROM DATA
C*************************************************************
C
        DO 2001 IQ=1,4
        Z=IN(XN,K)
        XN1=XN(1)
        DO 2 I=1,K
        XN(I)=XN(I)-XN1
2       CONTINUE
C*************************************************************************
C       REMOVE DRIFT FROM DATA
C*************************************************************************
C
        YMAX=XN(K)
        DO 12 I=1,K
        A=XN(I)
        RI=I
        XN(I)=A-YMAX/K*RI
12      CONTINUE
C*************************************************************************
C       BANDPASS FILTER DATA
C*************************************************************
C
        CALL BUT2 (XN,K,DELTA T)
2001    CONTINUE
        CLOSE(UNIT=1)
        STOP
        END

        SUBROUTINE BUT2 (PIN,NUMSAM,DELTAV)
      DIMENSION FMT(12), FIN(2000), FINS(2200), OUTS(2200),
     1            C(5), COEFF(7), FN(3), D(4), PIN(2000)
        EQUIVALENCE (FIN(1),FINS(5))
        OPEN(UNIT=3,MODE='BINARY',FILE='3F.DAT')
        READ(3) NUM
```

```
        TYPE 4,NUM
4       FORMAT(I)
        IOUT=11
        DO 1000 JJ=1,NUM
        DO 22 J=1,NUMSAM
22      FIN(J)=PIN(J)
C
C***********************************************
C   CALCULATE THE BUTTERWORTH COEFFICIENTS:
C***********************************************
        READ(3) CFREQ,C
       COEFF(1) = 1./C(1)
       COEFF(2) =-2./C(1)
       COEFF(3) = 1./C(1)
       COEFF(4) = C(2)/C(1)
       COEFF(5) = C(3)/C(1)
       COEFF(6) = C(4)/C(1)
 100   COEFF(7) = C(5)/C(1)
C
C
C*************************************************************************
C   SET FIRST 4 INPUT & OUTPUT SAMPLES (IN ARRAYS FINS & OUTS)
C    EQUAL TO ZERO, & SET LAST 196 SAMPLES IN FINS TO ZERO:
C*************************************************************************
       DO 200 J = 1,4
       FINS(J) = 0.
 200   OUTS(J) = 0.
       DO 220 J = (NUMSAM+5),(NUMSAM+200)
 220   FINS(J) = 0.
C
C
C
C
C*******************************
C   SET INPUT = PREVIOUS OUTPUT:
C*******************************
C
280     DO 300 L=1,3
300     FN(L)=COEFF(L)
       DO 330 L = 1,4
 330   D(L) = COEFF(L+3)
C
C*************************************************************************
C   FILTER ARRAY FINS RECURSIVELY WITH ONE POLYNOMIAL FRACTION TO
C    GET ARRAY OUTS:
C*************************************************************************
       DO 400 ISAM = 5,(NUMSAM+200)
       FNUMIN = FN(1)*FINS(ISAM)+FN(2)*FINS(ISAM-2) + FN(3)*FINS(ISAM-4)
       DENOUT = 0.
       DO 360 J = 1,4
       AA = D(J)*OUTS(ISAM-J)
 360   DENOUT = DENOUT+AA
 400   OUTS(ISAM) = FNUMIN - DENOUT
C
C
C
C*********************************************
C   REVERSE ARRAY OUTS AND PUT IT INTO ARRAY FIN:
C*********************************************
       DO 550 ISAM = 1,(NUMSAM+196)
```

```
 550    FIN(ISAM) = OUTS(NUMSAM+201-ISAM)
C
C
C
C*************************************************************
C    SET THE FIRST 4 INPUT & OUTPUT SAMPLES EQUAL TO ZERO:
C*************************************************************
       DO 570 J = 1,4
       FINS(J) = 0.
 570   OUTS(J) = 0.
C
C
C
C************************************
C    CHOOSE THE APPROPRIATE COEFFICIENTS:
C************************************
 600   DO 620 L = 1,3
 620   FN(L) = COEFF(L)
       DO 640 L = 1,4
 640   D(L) = COEFF(L+3)
C
C*****************************************************************
C    FILTER ARRAY FINS (WHICH IS THE OUTPUT OF PREVIOUS FILTER,
C     REVERSED) RECURSIVELY WITH ONE POLYNOMIAL FRACTION TO GET
C     ARRAY OUTS:
C*****************************************************************
       DO 800 ISAM = 5,(NUMSAM+200)
       FNUMIN = FN(1)*FINS(ISAM) + FN(2)*FINS(ISAM-2)+FN(3)*FINS(ISAM-4)
       DENOUT = 0.
       DO 700 J = 1,4
       AA = D(J)*OUTS(ISAM-J)
 700   DENOUT = DENOUT+AA
 800   OUTS(ISAM) = FNUMIN - DENOUT
C
C
C*****************************************************************
C    REVERSE ARRAY OUTS AND PUT IT INTO ARRAY PIN.   THE FILTERED
C     TIME SERIES IS THEN THE RIGHT WAY ROUND  (IN ARRAY PIN):
C*****************************************************************
       DO 1100 ISAM = 1,NUMSAM
1100    FIN(ISAM) = OUTS(NUMSAM+201-ISAM)
        Q=OUT(FIN,NUMSAM,CFREQ,IOUT,DELTAV)
1000    CONTINUE
        CLOSE(UNIT=3)
        RETURN
       END
        FUNCTION OUT(X,N,CFREQ,IOUT,DELTAV)
        DIMENSION X(N)
        WRITE(IOUT) N,CFREQ,DELTAV
        WRITE(IOUT) X
        OUT=10.
        IOUT=IOUT+1
        RETURN
        END
        FUNCTION IN(X,N)
        DIMENSION X(N)
        READ(1) X
        IN=K
        RETURN
        END
```

```
C       IMPEDE CALCULATES  APPARENT RESISTIVITY VALUES FOR
C       MT SOUNDINGS.
C
C       THE PROGRAM TAKES INPUT FROM THE FOURIER TRANSFORM
C       PROGRAM TAKE2
C
C       QE1,QE2 = THE COMPLEX FOURIER TRANSFORM
C       OF THE PERPENDICULAR E FIELDS.
C
C       QH1,QH2 = THE COMPLEX FOURIER TRANSFORM OF THE
C       PERPENDICULAR H FIELDS.
C
        PROGRAM IMPEDE
        IMPLICIT COMPLEX(Q,C)
        DOUBLE PRECISION FILIN,FILOUT
        DIMENSION QE1(1024),QE2(1024),QH1(1024),QH2(1024)
        DIMENSION ID(6),IFREQ(50)
        DATA SQ2/1.4142136/
        AMP(Q1)=SQRT(REAL(Q1)*REAL(Q1)+AIMAG(Q1)*AIMAG(Q1))
        PHAZ(Q1)=ATAN2(AIMAG(Q1),REAL(Q1))
C       READ IN DATA
2000    WRITE(4,3)
3       FORMAT(1X,'NAME OF FILE ',$)
        READ(4,4) FILIN
4       FORMAT(A10)
        IF (FILIN.EQ.'EXIT') STOP
        OPEN(UNIT=1,ACCESS='SEQIN',MODE='BINARY',FILE=FILIN)
        READ(1) ID,NUM,K,DELTAT
        TYPE 99,K
        JIN=1
99      FORMAT(I)
C
        Z=IN(QE1,QE2,QH1,QH2,NUM)
C***************************
C   PREPARE OUTPUT FILE:
C***************************
        WRITE(4,222)
222     FORMAT(1X,'WHAT IS THE OUTPUT FILE NAME???   ',$)
        READ(4,4) FILOUT
        OPEN(UNIT=2,MODE='BINARY',PROTECTION=109,FILE=FILOUT)
C       MAXIMUM NUMBER TO SUBTRACT FROM 1
C       FOR CHECKING COHERENCE ESTIMATES
        ACOH=.30
        FREQLO=K/10.
        IST=NUM/FREQLO
        IFIN=NUM/5.
        DEC=ALOG10(FLOAT(IFIN)/FLOAT(IST))
        IDEC=10.*DEC
        WRITE(2) ID,IDEC
        WRITE(3,11) ID
11      FORMAT(////,1X,6A5,/)
        XINC=(ALOG10(FLOAT(IFIN))-ALOG10(FLOAT(IST)))/
        1FLOAT(IDEC)
        DO 10 J=0,IDEC
        IFREQ(J)=10**(ALOG10(FLOAT(IFIN))-XINC*J)
10      CONTINUE
        KOUNT=0
C       DETERMINE CROSS AND AUTO POWER SPECTRA
        DO 20 J=1,IDEC-1
        QAE1=(0.,0.)
```

```
      QAE2=(0.,0.)
      QAH1=(0.,0.)
      QAH2=(0.,0.)
      QX12=(0.,0.)
      QX21=(0.,0.)
      QE11=(0.,0.)
      QE22=(0.,0.)
      QH11=(0.,0.)
      QH22=(0.,0.)
      QX11=(0.,0.)
      QX22=(0.,0.)
      DO 30 L=IFREQ(J+1),IFREQ(J-1)
      QAE1=QE1(L)+QAE1
      QAE2=QE2(L)+QAE2
      QAH1=QH1(L)+QAH1
      QAH2=QH2(L)+QAH2
      QX12=QE1(L)*CONJG(QH2(L))+QX12
      QX21=QE2(L)*CONJG(QH1(L))+QX21
      QE11=QE1(L)*CONJG(QE1(L))+QE11
      QE22=QE2(L)*CONJG(QE2(L))+QE22
      QH11=QH1(L)*CONJG(QH1(L))+QH11
      QH22=QH2(L)*CONJG(QH2(L))+QH22
      QX11=QE1(L)*CONJG(QH1(L))+QX11
      QX22=QE2(L)*CONJG(QH2(L))+QX22
30    CONTINUE
C     CALCULATE COMPLEX IMPEDANCES
      FREQ=NUM/FLOAT(IFREQ(J))*DELTAT
      QZ12=QX12/QH22
      QZ11=QX11/QH11
      QZ21=QX21/QH11
      QZ22=QX22/QH22
      QP12=QZ12*QAH2
      QP21=QZ21*QAH1
C     CHECK COHERENCIES
      AC12=AMP(QX12)/SQRT(AMP(QE11)*AMP(QH22))
      AC21=AMP(QX21)/SQRT(AMP(QE22)*AMP(QH11))
      TYPE 51,AC12,AC21
51    FORMAT(4F/2F)
      QZIMP1=QZ12*QZ12
      IF(ABS(1.-AC12).GT.ACOH) QZIMP1=(0.,0.)
      QZIMP2=QZ21*QZ21
      IF(ABS(1.-AC21).GT.ACOH) QZIMP2=(0.,0.)
      IF(QZIMP1.EQ.(0.,0.).AND.QZIMP2.EQ.(0.,0.)) GO TO 20
C     CALCULATE APPARENT RESISTIVITIES
      ZX=.2*FREQ*AMP(QZIMP1)
      ZY=.2*FREQ*AMP(QZIMP2)
      P12=PHAZ(QZ12)
      P21=PHAZ(QZ21)
C     OUTPUT RESULTS
      WRITE(2) FREQ,ZX,ZY,P12,P21
      WRITE(3,5) FREQ,ZX,AC12,ZY,AC21,P12,P21
5     FORMAT(7F)
      KOUNT=KOUNT+1
20    CONTINUE
      TYPE 1,KOUNT
1     FORMAT(I)
      CLOSE(UNIT=1)
      CLOSE(UNIT=2)
      GO TO 2000
      STOP
```

```
      END
C     FUNCTION TO ARRAY READ DATA IN FORMATLESS BINARY FILES
      FUNCTION IN(A,B,C,D,N)
      DIMENSION A(N),B(N),C(N),D(N)
      READ(1) A
      READ(1) B
      READ(1) C
      READ(1) D
      IN=NNUM
      RETURN
      END
```